UNIVERSIDADE FEDERAL DE SANTA CATARINA
PROGRAMA DE PÓS-GRADUAÇÃO EM
ENGENHARIA MECÂNICA

EQUAÇÃO DE BOLTZMANN EM REDE PARA ESCOAMENTOS TÉRMICOS

Tese submetida à
UNIVERSIDADE FEDERAL DE SANTA CATARINA
para a obtenção do grau de
DOUTOR EM ENGENHARIA MECÂNICA

LUIZ ADOLFO HEGELE JÚNIOR

Florianópolis, Maio de 2010.

Aos meus pais;

à Vó Aurora.

AGRADECIMENTOS

A Paulo Cesar Philippi pela amizade e orientação nessa jornada de tantos anos, pelo exemplo, e também ao Luís Orlando; por compartilharem sua visão do mundo.

Aos membros da banca, pela leitura atenta e pelas sugestões.

Aos amigos e colegas do LMPT Paulo Cesar Facin, Rodrigo Surmas, Eduardo "Passarinho" de Carli, Alexandre Dutra Alves, Eduardo Mayer, Carlos Enrique Pico Ortiz,. Daniel Carelli, Antonio Vinícius Gomes Teixeira, Guilherme Eller Haverroth, Diogo Nardelli Siebert, Fabiano Gilberto Wolf, Julian, Vicente, Ivan Georg.

Aos professores António Fabio Carvalho da Silva, Walter Bazzo, Eduardo Fancello, Celso Peres Fernandes, José Antonio Bellini da Cunha Neto, Saulo Güths, Vicente de Paulo Nicolau.

Aos amigos Guilherme Maran, Viviane Zanol, e a toda a Família Maran - Dr. Carlos, Dona Marta, Mariana, Bianca - por esses anos todos de amizade; Bernardo Walmott Borges, Felipe Reinoldo Schramm, Raquel Helena Zanatta Schramm, Renata Haverroth, Ricardo "Tanaka" Senne, Jesiel Sales, Carlos José Borges, Fernanda, André, Juninho, Zé, Minêro, Linhares, Virginia Yunes, Ângela, Matheus "Capacete" "Veranópolis" Lodetti, Demian, Marília, Sílvia, Preta, Yuri, Pedro “Vivente”.

Aos colegas da Petrobras, especialmente ao Ricardo Ruy, e também aos já “amigos de infância” Joãozinho e Mellão.

A minha família, especialmente meus pais e irmãos, e também a tia Guísela.

Ao CNPq, pelo suporte financeiro.

TABLE OF CONTENTS

LIST OF SYMBOLS

a	scaling factor
$a_{r_n}^{(n)}$	Coefficient of the tensor Hermite polynomial of order n
c_p	specific heat at constant pressure
c_v	specific heat at constant volume
c_s	sound speed
$\vec{c}$	lattice velocity
D	dimension of the Euclidean space
e	internal energy
f	particle distribution function
$f^{(eq)}$	equilibrium particle distribution function
f_i	discrete particle distribution function in a given direction i
$H_{r_n}^{(n)}$	tensor hermite polynomial of order n
k	thermal conductivity
k_B	Boltzmann constant
Kn	Knudsen number
ℓ	mean free path
L	characteristic lenght
m	mass of a given molecule
n	particle density
P	pressure
q_α	heat flux vector
t	time
t_c	characteristic time
t^*	dimensionless time
T	temperature
T_0	reference temperature
$\vec{u}$	velocity

$\vec{u}^*$ lattice velocity

$\vec{u}_0$ dimensionless velocity

$\vec{U}$ peculiar velocity

$\vec{x}$ spatial coordinate

Greek letters

α_T thermal diffusivity

$\delta_{\alpha\beta}$ Kronecker delta

θ temperature deviation

λ second viscosity coefficient

μ viscosity

ν kinematic viscosity

$\vec{\xi}$ molecular velocity

$\overline{\xi}$ average molecular velocity

$\vec{\xi}_0$ dimensionless molecular velocity

$\Pi_{\alpha\beta}$ momentum flux tensor

ρ density

τ relaxation time

τ_c collisional time

$\tau_{\alpha\beta}$ stress tensor

Ω collision operator

LIST OF FIGURES

RESUMO

Para que se possa simular as equações macroscópicas totalmente compressíveis partindo da equação de Boltzmann é necessário muito cuidado no processo de discretização do espaço de velocidades. Deste modo, a conexão física existente entre a equação de Boltzmann em rede (lattice-Boltzmann equation) e a sua similar no contínuo deve ser levada em consideração, e para tal um procedimento é formalmente derivado. A discretização do espaço de velocidades é feita através de um processo de quadratura, onde a norma dos polinômios de Hermite do espaço de Hilbert contínuo é igualada à norma do espaço discreto de velocidades O método, chamado de quadratura com abscissas prescritas, permite que se fixem os pólos de integração, podendo deste modo ter-se o processo de propagação exata, característica importante dos métodos que resolvem a equação de Boltzmann em rede. Utilizando a quadratura com abscissas prescritas, redes tradicionais do método são derivadas, tais como D1Q3, D2Q7, D2Q9, D3Q15, D3Q19 e D3Q27, e também redes de ordens mais altas para uma, duas e três dimensões. Ao invés de usar a técnica de ajuste dos coeficientes polinomiais para a expansão da distribuição de equilíbrio, a distribuição de Maxwell-Boltzmann é aproximada para uma dada ordem. Uma análise de estabilidade linear é então feita e mostra a melhor performance do método proposto frente a outros métodos.

Palavras chave: equação de Boltzmann em rede (lattice-Boltzmann equation), quadratura

ABSTRACT

In order to simulate the fully compressible thermohydrodynamical flows using the Boltzmann equation, much of the attention has to be paid in the process of the discretization of the velocity space. Hence, the physical connection between the lattice-Boltzmann equation and its continuous counterpart is taken into account and a procedure is formally derived. The velocity discretization is performed through a quadrature process, where the discrete norm of the tensor Hermite polynomials of the given order of approximation is made equal to the continuous norm of the Hermite polynomials in the Hilbert space. The method, named prescribed abscissas quadrature, allows one to locate the poles of integration leading to exact streaming schemes, an important attribute of the lattice-Boltzmann method. Using this prescribed abscissas quadrature, conventional lattice-Boltzmann models, such as D1Q3, D2Q7, D2Q9, D3Q15, D3Q19 and D3Q27 are obtained, and also lattices of higher orders for one, two and three dimensions. Instead of using a posteriori techniques to match coefficients in an expanded equilibrium distribution function, the Maxwellian distribution function is approximated according to a chosen order. A linear stability analysis is applied and shows the better performance of the proposed method when confronted to other methods.

Keywords: Lattice-Boltzmann method, discrete Boltzmann equation, quadrature problem

1. INTRODUCTION

The problem of solving the hydrodynamic macroscopic equations is of great importance in industry and academy. The set of partial differential equations which governs the flow is complicated to solve, and only a few analytical solutions for simple cases are known for the complete set of the Navier-Stokes-Fourier equations.

In this context, the computational fluid dynamics is used as an alternative method complementing experimental and analytical techniques. With the increasing capacity of computer processing, the process of solving the flow governing equations is fast enough to be done even in the fast pace of the industry, finding solutions for daily problems.

An alternative way to computational fluid dynamics is the lattice-Boltzmann method (LBM). Historically, the method was derived from the lattice gas automata (Frisch et al. 1986), but its obvious relationship to the Boltzmann equation was always used as an inspiration. Only in 1997, He & Luo, and also Abe, made a formal connection between the continuous and the lattice-Boltzmann equation.

The first of a series of models to simulate flows were proposed by Hardy et al. (1973, 1976). The model is composed by a lattice in which particles can hop from one node to another following strict rules. The state of the lattice can be described by boolean variables, since in each direction only one particle is allowed. The density, for example, will be the sum of the particles in a given node, and the momentum will be the weighted sum of the density in each direction.

The evolution of the model can be divided into two steps: collision and propagation. In the collision step, the particles in one particular node can change their velocities, inasmuch as the density and momentum of the node are preserved. In the following step – the propagation – the particles hop from one node to the other following their own velocity vector.

However, due to the lack of velocities and isotropy – they have used only four velocities in two dimensions – the Hardy et al. model was not able to simulate full hydrodynamic conditions, as obtained from the macroscopic equations.

In the beginning of the 1980's, Stephen Wolfram suggested the use of cellular automata to simulate fluids (Wolfram 1983, 1984), but it was only in 1986, when Frisch et al., and also Wolfram, almost at the same time, came up with a hexagonal lattice with

six directions per node, latter known as FHP lattice, that the model was able to simulate real flows. The isotropy of the lattice was the fundamental piece for the sucess of the model. Several models were proposed in sequence, for two and three dimensions (d'Humières et al., 1986; d'Humières & Lallemand, 1987), mainly differing in the collision process, For the three dimensional model, the projection of a 4D lattice was used. These models were also used to complex phenomena, such as phase transition (Appert, 1994), flow of immiscible fluids (Rothman & Keller, 1988; Chen et al., 1991), and also used to calculate intrinsic and relative permeabilities in reservoir rocks (Ferréol & Rothman, 1994; Santos et al., 2000).

For boundary conditions, the bounce back (Ziegler, 1993) and the halfway bounce back (Cornubert et al., 1991) were used in order to retrieve null velocity at the wall, simply reflecting the distributions after the collision with the wall.

Despite all the efforts and good agreement with the theory, the cellular automata had many problems, namely: lack of galilean invariance, pressure-velocity dependency and noise. In order to avoid the noise interference, McNamara & Zanetti (1988) made an ensemble average on the collision operator. Although the noise was reduced, the pressure dependence on the velocity persisted. Higuera & Jimenez (1989) linearized the collision operator, but many calculations need to be done in order to perform the collision process.

The critical step in developing the method was taken in 1992, when Qian et al. and Chen et al. proposed the BGK (Bathnagar, Gross & Krook, 1954) collision operator, retrieving the incompressible Navier-Stokes equations, without the galilean invariance and with an isothermal equation of state. Nevertheless, third order velocity non-physical terms in the macroscopic equations still continue (Qian & Orszag, 1993) affecting the flow when the Mach number increases.

The lattice-Boltzmann-BGK became very popular in two and three dimensions, and it was used in a great range of applications, from single phase flow to complex phenomena (Shan & Chen, 1994, 1995; Shan & Doolen, 1995; Chen & Doolen, 1998), such as flows of miscible and immiscible fluids (Facin et al., 2003; Santos et al. 2003).

The connection between the continuous Boltzmann equation and the lattice-Boltzmann equation came in 1997, with He & Luo and Abe. From that moment on, many resources taken from the computational fluid dynamics and other numerical methods were applied to the LBE (Succi, 2001).

For thermal flows, many attemps have been made in the lattice Boltzmann context without sucess due to, mainly, stability issues. Only in the recent years the causes of these instabilities were made clear, and the focus of the present work is to provide the detailed derivation of lattice-Boltzmann models able to simulate the fully compressible thermohydrodynamical flows.

This work is organized as follows: in Chapter 2, the departure from the Boltzmann equation to the lattice-Boltzmann equation is reviewed, considering only the spatial and temporal discretization, leading to the macroscopic equations through the Chapman-Enskog expansion. In Chapter 3, some lattice-Boltzmann models for athermal and thermal flows are discussed. In Chapter 4, the connection between the Boltzmann and the lattice-Boltzmann equation is obtained formally through the use of the prescribed abcissas method for the velocity discretization. Lattices for one, two and three dimensions are derived, given a degree of accuracy to the Maxwellian distribution. Hexagonal lattices in two dimensions are derived, and a simple rectangular lattice is also shown. Some models developed after the prescribed abscissas method are discussed. In Chapter 5, aditional discussions and conclusions are presented.

2. FROM THE CONTINUOUS TO THE LATTICE-BOLTZMANN EQUATION

2.1 Basic Kinetic Theory

The function $f(\vec{x},\vec{c},t)d\vec{x}d\vec{c}$ is defined as the expected number of molecules, with mass *m*, of a gas at time *t* within the volume $d\vec{x}$ around $\vec{x}$ with molecular velocity between $\vec{c}$ and $\vec{c}+d\vec{c}$. The macroscopic state of this gas – density ρ, macroscopic velocity $\vec{u}$ and internal energy *e* – is given by the moments of the distribution function in the velocity space $\vec{\xi}$ as,

$$n(\vec{x},t)=\int f(\vec{x},\vec{\xi},t)d\vec{\xi}\,, \tag{2.1.1}$$

$$\rho(\vec{x},t)=\int mf(\vec{x},\vec{\xi},t)d\vec{\xi}\,, \tag{2.1.2}$$

$$\rho(\vec{x},t)\vec{u}(\vec{x},t)=\int m\vec{\xi}\,f(\vec{x},\vec{\xi},t)d\vec{\xi}\,, \tag{2.1.3}$$

$$\rho(\vec{x},t)e(\vec{x},t)=\frac{1}{2}\int m(\vec{\xi}-\vec{u})^2\,f(\vec{x},\vec{\xi},t)d\vec{\xi}\,. \tag{2.1.4}$$

The internal energy is related to the temperature through the thermal equation of state, which for an ideal gas which presents solely kinetic energy of translational motion is given by:

$$e=\frac{D}{2}\frac{k_BT}{m}, \tag{2.1.5}$$

where k_B the Boltzmann Constant and *D* is the spatial dimension.

Higher order moments of the distribution function, namely, the stress tensor $\tau_{\alpha\beta}$ and the heat flux q_α, are defined in the following way:

$$\tau_{\alpha\beta}(\vec{x},t)=\int mU_\alpha U_\beta f(\vec{x},\vec{\xi},t)d\vec{\xi}\,, \tag{2.1.6}$$

$$q_\alpha(\vec{x},t)=\frac{1}{2}\int mU^2U_\alpha f(\vec{x},\vec{\xi},t)d\vec{\xi}\,. \tag{2.1.7}$$

where $\vec{U}$ is the peculiar velocity $\vec{\xi}-\vec{u}$ and $U=\left|\vec{U}\right|$.

2.1.1 Boltzmann Equation

The Boltzmann equation is a closed balance for the particle distribution $f\left(\vec{x},\vec{\xi},t\right)$. These molecules, subject to an external force $\vec{F}$, within a phase space element $d\vec{x}d\vec{\xi}$ around $\vec{x},\vec{\xi}$, at time *t* will be after a time *dt*, within $d\vec{x}'d\vec{\xi}'$ around $\vec{x}+\vec{\xi}dt,\vec{\xi}+\frac{\vec{F}}{m}dt$. The effect of the collision between molecules is modelled by the the collision term $\left(\frac{\partial f}{\partial t}\right)_{col} d\vec{x}d\vec{\xi}dt$, which is the rate of change of the distribution due *only* to collisions. After expanding the particle balance in Taylor series, and taking into account only first order terms in *dt*, one obtains:

$$\left(\frac{\partial}{\partial t}+\vec{\xi}\cdot\vec{\nabla}_{\vec{x}}+\frac{\vec{F}}{m}\cdot\vec{\nabla}_{\vec{\xi}}\right)f=\left(\frac{\partial f}{\partial t}\right)_{col}, \tag{2.1.8}$$

where the collision term in the right-hand side is yet to be closed.

Boltzmann determined the collision term under the following assuptions:

- only binary collisions are considered;
- during the collision process, the effect of the external force are not taken into account;
- the motion of the two molecules is uncorrelated (molecular chaos or *Stosszahlansatz*).

The resulting equation is the Boltzmann equation (Cercignani, 1990)

$$\left(\frac{\partial}{\partial t}+\vec{\xi}\cdot\vec{\nabla}_{\vec{x}}+\frac{\vec{F}}{m}\cdot\vec{\nabla}_{\vec{\xi}}\right)f=\int\left(f'f_1'-ff_1\right)\left|\vec{\xi}-\vec{\xi}_1\right|\sigma d\Omega d\vec{\xi}_1, \tag{2.1.9}$$

where the prime refers to post-collisional distributions, σ is the collisional cross section which relates incoming particles with the particles beamed in the direction of the solid angle *d*Ω.

2.1.2 Conservation laws

It can be shown that, for a given conserved quantity $\chi\left(\vec{x},\vec{\xi}\right)$, the following relation is valid (Cercignani, 1990):

$$\int \chi\left(\vec{x},\vec{\xi}\right)\left(\frac{\partial f}{\partial t}\right)_{col} d\vec{\xi} = 0\,. \tag{2.1.10}$$

This equation is the same as

$$\int \chi\left(\vec{x},\vec{\xi}\right)\left(\frac{\partial}{\partial t} + \vec{\xi}\cdot\vec{\nabla}_{\vec{x}} + \frac{\vec{F}}{m}\cdot\vec{\nabla}_{\vec{\xi}}\right) f\left(\vec{x},\vec{\xi},t\right) d\vec{\xi} = 0\,. \tag{2.1.11}$$

Replacing χ by m, $m\vec{\xi}$ and $\frac{1}{2}m\left(\vec{\xi}-\vec{u}\right)^2$, one obtains:

$$\partial_t \rho + \partial_\alpha \rho u_\alpha = 0\,, \tag{2.1.12}$$

$$\partial_t \rho u_\alpha + \partial_\beta(\rho u_\alpha u_\beta + \tau_{\alpha\beta}) = \rho F_\alpha\,, \tag{2.1.13}$$

$$\partial_t \rho e + \partial_\alpha(\rho e u_\alpha + q_\alpha) + \tau_{\alpha\beta}\partial_\alpha u_\beta = \rho F_\alpha u_\alpha\,. \tag{2.1.14}$$

These are the mass, momentum and thermal energy balance equations, respectively. In these equations, the final form of the stress tensor $\tau_{\alpha\beta}$ and the heat flux q_α is yet to be closed by a formal expansion – the Chapman-Enskog method - in terms of observable quantities: the transport coefficients and gradients of the velocity and temperature. For the closure of the transport equations and the terms $\tau_{\alpha\beta}$ and q_α, given an interparticle potencial, several cases are solved in Chapman and Cowling (1970).

2.1.3 Equilibrium solution of the Boltzmann equation

In equilibrium, the total effect of the collisions are null. Then, one can write:

$$\left(\frac{\partial f}{\partial t}\right)_{col} = 0\,. \tag{2.1.15}$$

This leads to the so-called detailed balance condition:

$$ff_1 = f'\,f_1'\,, \tag{2.1.16}$$

or, equivalently, to:

$$\ln f + \ln f_1 = \ln f' + \ln f_1'\,. \tag{2.1.17}$$

Thus, the quantity ln f is a collisional invariant, i.e., a property which does not vary during the collision step. In this case, ln f must be a linear combination of the collisional invariants: mass, momentum and kinetic energy. In this way:

$$\ln f = A + B_\alpha \xi_\alpha + E\xi^2\,, \tag{2.1.18}$$

where the constants A, B_α and E can be determined by the Eqs. (2.1.1), (2.1.3) and (2.1.4), leading to the Maxwell-Boltzmann distribution:

$$f^{MB}\left(\vec{x},\vec{\xi},t\right)=n\left(\frac{m}{2\pi k_B T}\right)^{\frac{D}{2}} e^{\left(-m\frac{(\vec{\xi}-\vec{u})^2}{2k_B T}\right)}. \tag{2.1.19}$$

2.2 Time and space discretization

The Boltzmann equation is, as said before, a closed equation for the particle distribution function in the space of $2D+1$ variables, namely, spatial dimension, particle velocity and time. The Boltzmann equation can be written for discrete velocities, without external forces, as[1]

$$\partial_t f_i+\xi_{i\alpha}\partial_\alpha f_i=\Omega_i, \tag{2.2.1}$$

where

$$f_i\left(\vec{x},t\right)=f\left(\vec{x},\vec{\xi}_i,t\right), \tag{2.2.2}$$

since the variables are independent.

Now, one can apply an upwind first order Euler finite difference scheme in time to obtain:

$$\partial_t f_i=\frac{f_i\left(\vec{x},t+\Delta t\right)-f_i\left(\vec{x},t\right)}{\Delta t}+O\left(\Delta t\right). \tag{2.2.3}$$

For the advection term, one uses the upwind scheme resulting in the *i* direction

$$\xi_{i\alpha}\partial_\alpha f_i=\vec{\xi}_i\frac{f_i\left(\vec{x}+\Delta\vec{x}_i,t+\Delta t\right)-f_i\left(\vec{x},t+\Delta t\right)}{\Delta x_i}+O\left(\xi_i\Delta x_i\right), \tag{2.2.4}$$

where $\Delta\vec{x}_i$ is the lattice spatial discretization in the *i* direction.

In order to obtain the collision-propagation scheme, the following relation is usually adopted:

$$\vec{\xi}_i=\frac{\Delta\vec{x}_i}{\Delta t}. \tag{2.2.5}$$

Collecting the equations and neglecting second order terms in time, one obtains the lattice-Boltzmann equation:

$$f_i\left(\vec{x}+\xi_i\Delta t,t+\Delta t\right)=f_i\left(\vec{x},t\right)+\Omega_i\Delta t. \tag{2.2.6}$$

[1] The summation convention is applied only to spatial indexes.

2.3 Chapman-Enskog expansion

For the Chapman-Enkog expansion, one starts from the lattice-Boltzmann equation without external forces in the form

$$f_i\left(\vec{x}+\xi_i\Delta t, t+\Delta t\right) = f_i\left(\vec{x},t\right)+\Omega_i\Delta t\,. \tag{2.3.1}$$

Proceding with a Taylor expansion in the left hand side of the Eq. (2.3.1|), one obtain:

$$\begin{aligned} f_i\left(\vec{x}+\xi_i\Delta t, t+\Delta t\right) = {} & f_i\left(\vec{x},t\right)+\Delta t\left(\partial_t+\xi_{i\alpha}\partial_\alpha\right) f_i\left(\vec{x},t\right)+ \\ & \frac{\Delta t^2}{2}\left(\partial_t\partial_t+2\xi_{i\alpha}\partial_\alpha\partial_t+\xi_{i\alpha}\xi_{i\beta}\partial_\alpha\partial_\beta\right) f_i\left(\vec{x},t\right) \end{aligned}\,, \tag{2.3.2}$$

where third order terms and beyond in Δt are not taken into account. Then, the Taylor expanded lattice-Boltzmann equation reads:

$$\left(\partial_t+\xi_{i\alpha}\partial_\alpha\right) f_i+\frac{\Delta t}{2}\left(\partial_t\partial_t+2\xi_{i\alpha}\partial_\alpha\partial_t+\xi_{i\alpha}\xi_{i\beta}\partial_\alpha\partial_\beta\right) f_i=\Omega_i\,. \tag{2.3.3}$$

In order to proceed with the Chapman-Enskog expansion, one have to perform a scale analysis. Defining the dimensionless variables,

$$\vec{x}^{\,*}=\frac{\vec{x}}{L}, \tag{2.3.4}$$

$$t^*=\frac{t}{t_c}, \tag{2.3.5}$$

$$\xi_{i\alpha}^*=\frac{\xi_{i\alpha}}{\overline{\xi}}, \tag{2.3.6}$$

$$\Omega_i^*=\Omega_i\tau_c, \tag{2.3.7}$$

where L, t_c, $\overline{\xi}$ and τ_c are characteristics macroscopic lenght, macroscopic time, average molecular velocity and time between collisions (i.e., the collisional time), respectively. The average molecular velocity can be approximated by

$$\overline{\xi}\approx\frac{\ell}{\tau_c}, \tag{2.3.8}$$

where ℓ is the mean free path of molecules.

Substituting these variables into Eq. (2.3.3), one will find two dimensionless quantities. The first is the Knudsen number, defined by

$$Kn = \frac{\ell}{L}, \tag{2.3.9}$$

which gives the level of rarefection in the system. The second is a relation between microscopic and macroscopic time scales:

$$\frac{\tau_c}{t_c}, \tag{2.3.10}$$

which will be assumed to have the same order as the Knudsen number. Also, it is assumed that Δt has the same order of τ_c.

With these assumptions, one obtains:

$$\left(\partial_{t^*} + \xi_{i\alpha^*}\partial_{\alpha^*}\right) f_i + Kn\frac{\Delta t}{2}\left(\partial_{t^*}\partial_{t^*} + 2\xi_{i\alpha^*}\partial_{\alpha^*}\partial_t + \xi_{i\alpha^*}\xi_{i\beta^*}\partial_{\alpha^*}\partial_{\beta^*}\right) f_i = \frac{\Omega_i}{Kn}. \tag{2.3.11}$$

For the following derivation, it will be used the Bhatnagar-Gross-Krook (BGK, 1954) collision operator:

$$\Omega_i = \frac{f_i^{eq} - f_i}{\tau}, \tag{2.3.12}$$

where τ is the relaxation time.

In order to complete the expansion, one has to separate the particle distribution scales in Knudsen orders. Denoting $\varepsilon = Kn$, one obtains

$$f_i = f_i^{(0)} + \varepsilon f_i^{(1)} + \varepsilon^2 f_i^{(2)} + \ldots, \tag{2.3.13}$$

and for the temporal derivative,

$$\partial_t = \partial_0 + \varepsilon\partial_1 + \varepsilon^2\partial_2 + \ldots. \tag{2.3.14}$$

The method consists in collecting terms of the same order in Knudsen, and then solving the next order with the known result from the previous order. Returning to the original equation, at zero order in the Knudsen number, one obtains

$$f_i^{(0)} = f_i^{eq}, \tag{2.3.15}$$

which means that at zero order the distribution function is the maxwellian. Hence, the first result to be used is the maxwellian itself, which will be used to find $f^{(1)}$, or the moments of $f^{(1)}$, and so on, if one wants to do so.

For the first and second order, the following two equations are obtained:

$$\partial_0 f_i^{(0)} + \xi_{i\alpha}\partial_\alpha f_i^{(0)} = -\frac{f_i^{(1)}}{\tau}, \tag{2.3.16}$$

$$\partial_1 f_i^{(0)} + \left(\partial_0 + \xi_{i\alpha}\partial_\alpha\right)\left(1 - \frac{\Delta t}{2\tau}\right) f_i^{(1)} = -\frac{f_i^{(2)}}{\tau}. \tag{2.3.17}$$

According to the Chapman-Enskog expansion, one has to restore the hydrodynamic variables to their equilibrium values, namely, density, momentum and energy. For the sake of simplicity, without losing generality, from now on, $m = 1$ will be used. Hence,

$$\rho = \sum_i f_i^{(0)}, \tag{2.3.18}$$

$$\rho u_\alpha = \sum_i f_i^{(0)} \xi_{i\alpha}, \tag{2.3.19}$$

$$\rho e = \frac{1}{2}\sum_i f_i^{(0)} \left(\vec{\xi}_i - \vec{u}\right)^2, \tag{2.3.20}$$

and for superior orders in Knudsen, one has

$$\sum_i f_i^{(l)} = 0, \tag{2.3.21}$$

$$\sum_i f_i^{(l)} \xi_{i\alpha} = 0, \tag{2.3.22}$$

$$\frac{1}{2}\sum_i f_i^{(l)} \left(\vec{\xi}_i - \vec{u}\right)^2 = 0, \tag{2.3.23}$$

for $l \geq 1$.

To obtain the Euler equations, one just have to multiply Eq. (2.3.16) by the respective hydrodynamical moment and sum up over the index *i*. From now on, the summation will be substituted by the integration of the maxwellian distribution. This leads to

$$\partial_0 \rho + \partial_\alpha \rho u_\alpha = 0, \tag{2.3.24}$$

for mass conservation, and

$$\partial_0 \rho u_\alpha + \partial_\beta \Pi_{\alpha\beta}^{(0)} = 0, \tag{2.3.25}$$

for momentum, where

$$\Pi_{\alpha\beta}^{(0)} = P\delta_{\alpha\beta} + \rho u_\alpha u_\beta \tag{2.3.26}$$

is the momentum flux tensor, where *P* is the thermodynamic pressure for ideal gases:

$$P = nk_B T, \tag{2.3.27}$$

and $\delta_{\alpha\beta}$ is the Kronecker's delta.

In order to obtain the internal energy balance equation, one has to multiply the Eq. (2.3.16) by $\frac{1}{2}\xi_i^2$, sum up over the index and subtract the part due to the average kinetic energy, that is obtained multiplying scalarly Eq. (2.3.25) by u_α. Then one obtains:

$$\partial_0 \rho e + \partial_\alpha \left(\rho e u_\alpha \right) + P \partial_\alpha u_\alpha = 0 . \tag{2.3.28}$$

The next order of approximation of the transport equations is obtained multiplying Eq. (2.3.17) by the hydrodynamic moments and look for the moments of $f^{(1)}$ in the preceding equation, eq. (2.3.16).

For the density:

$$\partial_1 \rho = 0 , \tag{2.3.29}$$

and for first and second orders in Knudsen

$$\partial_t \rho + \partial_\alpha \rho u_\alpha = 0 , \tag{2.3.30}$$

for the momentum,

$$\partial_1 \rho u_\alpha + \left(1 - \frac{\Delta t}{2\tau} \right) \partial_\beta \Pi^{(1)}_{\alpha\beta} = 0 . \tag{2.3.31}$$

To obtain the first order momentum flux tensor, one use eq. (2.3.16):

$$\Pi^{(1)}_{\alpha\beta} = -\tau \left(\partial_0 \Pi^{(0)}_{\alpha\beta} + \partial_\gamma Q^{(0)}_{\alpha\beta\gamma} \right), \tag{2.3.32}$$

where

$$Q^{(0)}_{\alpha\beta\gamma} = \sum_i f_i^{(0)} \xi_{i\alpha} \xi_{i\beta} \xi_{i\gamma} . \tag{2.3.33}$$

After some calculation, it follows that:

$$\partial_0 \Pi^{(0)}_{\alpha\beta} + \partial_\gamma Q^{(0)}_{\alpha\beta\gamma} = P \left[\partial_\alpha u_\beta + \partial_\beta u_\alpha - \frac{2}{D} \delta_{\alpha\beta} \partial_\gamma u_\gamma \right]. \tag{2.3.34}$$

Summing the first and second orders for the momentum equation,

$$\partial_t \rho u_\alpha + \partial_\beta \left(\rho u_\alpha u_\beta \right) = -\partial_\alpha P + \partial_\beta \left[\mu \left(\partial_\alpha u_\beta + \partial_\beta u_\alpha - \frac{2}{D} \delta_{\alpha\beta} \partial_\gamma u_\gamma \right) \right], \tag{2.3.35}$$

which is the momentum equation with viscous terms and the viscosity coefficient given by

$$\mu = P \left(\tau - \frac{\Delta t}{2} \right) \tag{2.3.36}$$

and the second viscosity coefficient is

$$\lambda = -\frac{2}{D} P\left(\tau - \frac{\Delta t}{2}\right). \tag{2.3.37}$$

Note that in one dimension, the viscous term is zero, and the Euler equation is retrieved.

It is important to note that there is an analytical error $\left(1 - \frac{\Delta t}{2\tau}\right)$ which is embodied into the viscous stress tensor becoming part of the viscosity coefficient.

For the energy equation, the process is repeated, multiplying eq. (2.3.17) by the total energy and subtracting the part due to kinetic energy, obtained from eq. (2.3.31):

$$\partial_1(\rho e) + \left(1 - \frac{\Delta t}{2\tau}\right)\left(\partial_\alpha q_\alpha^{(1)} + \Pi_{\alpha\beta}^{(1)} \partial_\alpha u_\beta\right) = 0, \tag{2.3.38}$$

where $q_\alpha^{(1)}$ is defined as follows

$$q_\alpha^{(1)} = \frac{1}{2}\sum_i f_i^{(1)}\left(\xi_{i\beta} - u_\beta\right)\left(\xi_{i\beta} - u_\beta\right)\left(\xi_{i\alpha} - u_\alpha\right). \tag{2.3.39}$$

To obtain $q_\alpha^{(1)}$, from eq. (2.3.17), one will need to retrieve moments until the fourth-order, namely

$$\sum_i f_i^{(0)} \xi_i^2 \xi_{i\beta} \xi_{i\alpha}\,. \tag{2.3.40}$$

After a lenghty calculation, one obtain

$$\partial_t \rho e + \partial_\alpha\left(\rho e u_\alpha\right) = -\partial_\alpha q_\alpha - P\partial_\alpha u_\alpha + \lambda\left(\partial_\alpha u_\alpha\right)^2 + \mu\left(\partial_\gamma u_\beta + \partial_\beta u_\gamma\right)\partial_\beta u_\gamma, \tag{2.3.41}$$

with

$$q_\alpha = -\frac{D+2}{2}\frac{Pk_B}{m}\left(\tau - \frac{\Delta t}{2}\right)\partial_\alpha T\,. \tag{2.3.42}$$

The thermal conductivity from the model, then, is

$$k = \frac{D+2}{2}\frac{Pk_B}{m}\left(\tau - \frac{\Delta t}{2}\right). \tag{2.3.43}$$

From the ideal gas equation of state, one can obtain the specific heat at constant pressure:

$$c_p = \frac{D+2}{2}\frac{k_B}{m}, \tag{2.3.44}$$

and the thermal diffusivity is obtained straightforward

$$\alpha_T = \frac{k}{\rho c_p} = \frac{P}{\rho}\left(\tau - \frac{\Delta t}{2}\right). \tag{2.3.45}$$

The Prandtl number for the lattice Boltzmann BGK collision model is 1, differently from the value in the continuous kinetic theory, $\frac{2}{3}$, for the same collision model.

These are the full compressible equations for thermohydrodynamical flows. The same set of equations have also been obtained, in a similar manner, by Y. Chen et al, in 1994.

The sound speed is obtained from its thermodynamical definition:

$$c_s = \left(\frac{\partial P}{\partial \rho} \right)_s^{\frac{1}{2}} = \left(\frac{c_p}{c_v} \frac{k_B T}{m} \right)^{\frac{1}{2}}, \tag{2.3.46}$$

where c_v is the specific heat at constant volume ($c_v = \frac{D}{2}\frac{k_B}{m}$ for ideal gases).

For athermal models, to retrieve the incompressible Navier-Stokes equations, a second order model will be sufficient inasmuch the Mach number is kept small, because third order errors are still in the equation. For the Navier-Stokes equations without third order errors, one have to keep all third order terms in the equilibrium distribution.

Another comment that has to be made is about the sound speed. In athermal incompressible fluids,

$$c_p = c_v = c\,, \tag{2.3.47}$$

and the sound speed will be

$$c_s = \left(\frac{\partial P}{\partial \rho} \right)_s^{\frac{1}{2}} = \left(\frac{k_B T_0}{m} \right)^{\frac{1}{2}}, \tag{2.3.48}$$

where T_0 is a reference (lattice) temperature.

For thermal models, one has to retrieve moments until the incomplete fourth-order given in Eq. (2.3.40) and the sound speed is

$$c_s = \left(\frac{D+2}{D} \frac{k_B T}{m} \right)^{\frac{1}{2}}. \tag{2.3.49}$$

It is also possible to simulate thermal flows with third order models, inasmuch is the Mach number is kept low (Siebert, 2007).

For other collision models, the same procedure described above must be applied in order to know the order of the equilibrium distribution that must be recovered.

3. LATTICE BOLTZMANN MODELS FOR ATHERMAL AND THERMAL FLOWS

In this chapter, a brief review of some lattice Boltzmann models is given, starting with the popular lattice BGK, and then the thermal ones.

3.1 Lattice Boltzmann BGK (1992)

The lattice Boltzmann with the celebrated BGK collision operator was proposed by Qian et al. (1992) and Chen et al. (1992), with the following evolution equation,

$$f_i\left(\vec{x}^* + \vec{c}_i, t+1\right) - f_i\left(\vec{x}^*, t\right) = -\frac{1}{\tau}\left(f_i - f_i^{eq}\right), \tag{3.1.1}$$

where the equilibrium distribution function was derived as:

$$f_i^{eq}\left(\rho, \vec{u}^*\right) = \rho w_i\left(1 + a^2 u_\alpha^* c_{i,\alpha} - \frac{a^2}{2}u^{*2} + \frac{a^4}{2}u_\alpha^* u_\beta^* c_{i,\alpha} c_{i,\beta}\right), \tag{3.1.2}$$

$a = \sqrt{3}$, for the D2Q9, D3Q14, D3Q19 and D3Q27 lattices. This model allows to simulate an incompressible isothermal fluid flow for low Mach numbers, and became very popular because of its simplicity. Several modifications of these models were suggested (e.g., He & Luo, 1997b) and it was also the framework for various models for complex flows (Shan & Chen, 1993; Giraud et al, 1997, 1998).

3.2 Lallemand & Luo (2000)

Lallemand & Luo were the first to realize that the decomposition of the maxwellian function in its moments is a powerful method, using that to improve stability. The method *per se* was first employed by d'Humières in 1992 for thermal models, using a lattice with only nine degrees of freedom, without sucess.

Lallemand and Luo used the method for athermal flows in this way:

$$\hat{f}_j^{'} = \hat{f}_j + \hat{\Lambda}\left(\hat{f}_j - \hat{f}_j^{(eq)}\right) \tag{3.2.1}$$

where $\hat{f}_j$ stands for the moments of the distribution funcion, the prime indicates that is a post-collisional moment, and the matrix $\hat{\Lambda}$ is a diagonal matrix, where the diagonal elements are the relaxation coefficients for the various moments. It is assumed that the moments of equilibrium $\hat{f}_j^{(eq)}$ are the maxwellian moments – until the second order – of the vector *j*. The moments are then reversed to the velocity space through the linear mapping:

$$f_i = M_{ij}^{-1} \hat{f}_j , \tag{3.2.2}$$

where *M* is the matrix constituted by the eigenvectors of the collision operator Λ.

Therefore, the evolution equation can be represented as follows:

$$f_i\left(\vec{x}+\vec{c}_i, t+1\right) = f_i\left(\vec{x}, t\right) + \Lambda_{ij} f_j^{(neq)}\left(\vec{x}, t\right), \tag{3.2.3}$$

where $f_j^{(neq)} = f_j - f_j^{(eq)}$. Nevertheless, for pratical purposes, the collision process is executed in the moment space, and the advection is executed in the velocity space

For the D2Q9 model, the matrix M reads:

$$M = \begin{bmatrix} 1 & 1 & 1 & 1 & 1 & 1 & 1 & 1 & 1 \\ -4 & -1 & -1 & -1 & -1 & 2 & 2 & 2 & 2 \\ 4 & -2 & -2 & -2 & -2 & 1 & 1 & 1 & 1 \\ 0 & 1 & 0 & -1 & 0 & 1 & -1 & -1 & 1 \\ 0 & -2 & 0 & 2 & 0 & 1 & -1 & -1 & 1 \\ 0 & 0 & 1 & 0 & -1 & 1 & 1 & -1 & -1 \\ 0 & 0 & -2 & 0 & 2 & 1 & 1 & -1 & -1 \\ 0 & 1 & -1 & 1 & -1 & 0 & 0 & 0 & 0 \\ 0 & 0 & 0 & 0 & 0 & 1 & -1 & 1 & -1 \end{bmatrix}, \tag{3.2.4}$$

where the vectors which form the matrix are given in terms of the velocity vectors obtained by a Gram-Schmidt procedure:

$$m_i^{(0)} = \left\|c_i\right\|^0 , \tag{3.2.5}$$

$$m_i^{(1)} = 4\left\|c_i\right\|^0 - 3\left\|c_i\right\|^2 , \tag{3.2.6}$$

$$m_i^{(2)} = \frac{9}{2}\left\|c_i\right\|^4 - \frac{21}{2}\left\|c_i\right\|^2 + 4\left\|c_i\right\|^0 , \tag{3.2.7}$$

$$m_i^{(3)} = c_{ix} , \tag{3.2.8}$$

$$m_i^{(4)} = c_{ix}(3\left\|c_i\right\|^2 - 5\left\|c_i\right\|^0) , \tag{3.2.9}$$

$$m_i^{(5)} = c_{iy} , \tag{3.2.10}$$

$$m_i^{(6)} = c_{iy}(3\|c_i\|^2 - 5\|c_i\|^0), \tag{3.2.11}$$

$$m_i^{(7)} = c_{ix}^2 - c_{iy}^2, \tag{3.2.12}$$

$$m_i^{(8)} = c_{ix}c_{iy}. \tag{3.2.13}$$

These vectors are chosen to be the eigenvectors of the collision matrix Λ, and the eigenvalues of the collision matrix are the inverse of the relaxation time of the moment related to the eigenvector. For isotropy reasons, four parameters are allowed to be set independently, respecting the stability limits.

The authors found out optimal relations for the relaxation parameters, in order to improve stability. This will also be discussed later in Chapter 5.

3.3 Alexander et al. (1993)

Alexander et al. (1993) were the first to try to solve the full compressible Navier-Stokes-Fourier equations with the use of the lattice-Boltzmann method. They have used a BGK collision operator, and a hexagonal lattice with thirteen velocities, and a polynomial equilibrium distribution function of the type

$$f_i^{(eq)} = A_i + B_i c_{i\alpha}u_\alpha + C_i\left(c_{i\alpha}u_\alpha\right)^2 + D_i u^2 + E_i\left(c_{i\alpha}u_\alpha\right)^3 + F_i\left(c_{i\alpha}u_\alpha\right)u^2 \tag{3.3.1}$$

in order to fullfil the hydrodynamical constraints. The constants of the equilibrium distribution are derived in order to maintain moments until $c_i^2 c_{i\alpha}$.

The model is weak in a critical point: the lattice behind (the D2Q13H) does not have the property of the linear independence of the vectors even for complete third order. In two dimensions, ten moments are admitted, but only nine of them are independent. So, as a consequence, no fourth-order terms are allowed in the equilibrium distribution, and the macroscopic equations have third and fourth order spurious terms. This explains the instability that this model is subjected to. Nonetheless, the authors obtain computationally the transport coefficients, such as the viscosity, thermal conductivity and sound speed, which confirm the theoretical predictions from the Chapman-Enskog expansion.

3.4 Chen et al. (1994)

Chen et al. (1994) also proposed a lattice-Boltzmann model for thermal flows based on matching the coefficients of a general equilibrium distribution function, but now they carry the expansion until incomplete fourth-order moments, i.e., $c_i^2 c_{i\alpha} c_{i\beta}$. As the number of adjustable coefficients is larger than the number of constraints, they have the freedom to choose the "best" coefficients. At the present time this is known to be not totally true, because of the inherent isotropy properties of a given lattice (Philippi et al., 2006).

This model does not show deviation terms in the macroscopic equations, as the one of Alexander et al. Nonetheless, there is no equilibrium state which give all positive distributions. This is a non-physical behavior, because contradicts the probabilistic interpretation of the distribution function, and also has been shown recently (Servan-Camas & Tsai, 2009) that negative distributions may cause numerical instabilities in the simulations. Despite this, the model represents well the benchmark Sod's shock tube problem and theoretical predictions for transport coefficients give accurate results compared with simulations.

3.5 He et al. (1998)

He, Chen and Doolen use two distribution functions in order to simulate thermohydrodynamics: the usual one, using the BGK operator for the hydrodynamical fields, and derive another evolution equation for the temperature field, using a second distribution function for that. The complete set of equations for thermohydrodynamics are recovered, but the calculation is not local, which turns this model into a very computationally expensive one.

3.6 Lallemand & Luo (2003)

Lallemand & Luo (2003) continue with the d'Humières' multiple-relaxation times approach, this time applied to thermal models. In this way, in order to mimic thermohydrodynamical behavior, the energy conservation must also be satisfied. Because the authors were not using suitable lattices – only velocity vectors in the main and diagonal axis are employed, they have to use another numerical method to solve the

temperature field, whilst the lattice-Boltzmann method was used to solve the hydrodynamic fields. This makes the temperature and the hydrodynamic fields (velocity and pressure) decoupled, and the full thermohydrodynamical equations are not recovered.

4. PRESCRIBED ABSCISSAS QUADRATURE

4.1 Development of the method

Very few attempts have been made in order to formally connect the Boltzmann equation to the lattice-Boltzmann equation, although the main concepts used in lattice-Boltzmann models are derived from the kinetic theory . He and Luo (1997) formally derived some already known lattices (D2Q7, D2Q9, D3Q15, D3Q19 and D3Q27) using Gauss-Radau and Gauss-Hermite quadratures. However, this kind of quadrature can only generate regular lattices with the use of only the first neighborhood. If one wants to have additional orders in the equilibrium distribution function, one has to go further in the neighbourhood, and another kind of quadrature has to be used.

The goal is to represent moments like (Philippi et al. 2006; Shan et al. 2006):

$$\left\langle \varphi_{r_p}^{(p)} \right\rangle^{eq} = \int \varphi_{r_p}^{(p)}\left(\vec{\xi}\right) f^{eq}\left(\vec{x},\vec{\xi},t\right) d\vec{\xi}\,, \tag{4.1.1}$$

where the monomial φ_{r_p} is defined as

$$\varphi_{r_p} = \xi_{\alpha_1}\xi_{\alpha_2}\ldots\xi_{\alpha_p}\,,\quad r_p = \alpha_1\alpha_2\ldots\alpha_p\,, \tag{4.1.2}$$

in order to retrieve moments demanded by the Chapman-Enskog expansion. The moments of equilibrium are only functions of the density, velocity and temperature.

The quadrature reads

$$\left\langle \varphi_{r_p}^{(p)} \right\rangle^{eq} = \sum_i W_i f_i^{eq}\left(\vec{x},\vec{\xi},t\right)\varphi_{r_p}^{(p)}\left(\vec{\xi}_i\right), \tag{4.1.3}$$

where W_i are the still undetermined weights .

The continuous equilibrium distribution function can be written as

$$f^{eq}\left(\vec{x},\vec{\xi},t\right) = \rho\left[\frac{m}{2\pi k_B T_0\left(\theta+1\right)}\right]^{D/2} e^{-\frac{1}{2}\frac{\left(\vec{\xi}_0-\vec{u}_0\right)^2}{\theta+1}}, \tag{4.1.4}$$

where

$$\vec{u}_0 = \sqrt{\frac{m}{k_B T_0}}\vec{u}\,, \tag{4.1.5}$$

$$\vec{\xi}_0 = \sqrt{\frac{m}{k_B T_0}}\vec{\xi}\,, \tag{4.1.6}$$

are the nondimensional macroscopic velocity and molecular velocity, respectively, and

$$\theta = \frac{T}{T_0} - 1, \tag{4.1.7}$$

is the deviaton to the reference temperature. It is also convenient to define

$$e_0 = \frac{m}{k_B T_0} e, \tag{4.1.8}$$

as the nondimensional internal energy.

Such expansion has to be done in this way to take away the unphysical dependence of molecular velocity on the temperature. If one does not proceed in this way, the lattice speed will be dependent on the temperature, leading to deformed grid for simulations (Philippi et al., 2006).

Now, one can use the expansion of the equilibrium distribution in terms of tensor Hermite polynomials, obtaining:

$$f^{eq}\left(\vec{x},\vec{\xi},t\right) = \left[\frac{m}{2\pi k_B T_0}\right]^{D/2} e^{-\frac{\xi_0^2}{2}} \sum_{n=0}^{\infty} \frac{1}{n!} a_{r_n}^{eq,(n)}\left(\vec{x},\vec{\xi}_0,t\right) H_{r_n}^{(n)}\left(\vec{\xi}_0\right), \tag{4.1.9}$$

where $H_{r_n}^{(n)}$ is the n-th order Hermite polynomial tensor (on r_n).

A few coments must be provided about the nature of the tensor Hermite polynomials. The tensor Hermite polynomials are defined as the following (Grad, 1949):

$$H_{r_n}^{(n)}\left(\vec{\xi}_0\right) = \frac{(-1)^n}{\omega\left(\vec{\xi}_0\right)} \nabla_{r_n}^{(n)} \omega\left(\vec{\xi}_0\right), \tag{4.1.10}$$

where

$$\omega\left(\vec{\xi}_0\right) = \frac{e^{-\xi_0^2}}{\left(2\pi\right)^{\frac{D}{2}}} \tag{4.1.11}$$

is the weighting function and

$$\nabla_{r_n}^{(n)} = \partial_{\alpha_1}\partial_{\alpha_2}\ldots\partial_{\alpha_n} \tag{4.1.12}$$

is the generalized nabla operator. These tensor polynomials obey an orthogonal relation in the $L^2 - space$:

$$\int \omega\left(\vec{\xi}_0\right) H_{p_n}^{(n)}\left(\vec{\xi}_0\right) H_{q_m}^{(m)}\left(\vec{\xi}_0\right) d\vec{\xi}_0 = \delta_{p_n q_m}\left(n_{\alpha_1}!\, n_{\alpha_2}!\ldots n_{\alpha_D}!\right), \tag{4.1.13}$$

where $\delta_{p_n q_m}$ is 1 if p_n is a permutation of q_m (and zero otherwise), and the factorials refer to the number of times that a given coordinate appears in p_n (or q_m).

The first four tensor Hermite polynomials are given as follows:

$$H^{(0)}\left(\vec{\xi}_0\right)=1, \tag{4.1.14}$$

$$H_{\alpha}^{(1)}\left(\vec{\xi}_0\right)=\xi_{0,\alpha}, \tag{4.1.15}$$

$$H_{\alpha\beta}^{(2)}\left(\vec{\xi}_0\right)=\xi_{0,\alpha}\xi_{0,\beta}-\delta_{\alpha\beta}, \tag{4.1.16}$$

$$H_{\alpha\beta\gamma}^{(3)}\left(\vec{\xi}_0\right)=\xi_{0,\alpha}\xi_{0,\beta}\xi_{0,\gamma}-\left(\xi_{0,\alpha}\delta_{\beta\gamma}+\xi_{0,\beta}\delta_{\alpha\gamma}+\xi_{0,\gamma}\delta_{\alpha\beta}\right). \tag{4.1.17}$$

Now, one can expand the equilibrium distribution function as

$$f^{eq}\left(\vec{x},\vec{\xi},t\right)=\left[\frac{m}{2\pi k_B T_0}\right]^{D/2}\omega\left(\vec{\xi}_0\right)\sum_{n=0}^{\infty}\frac{1}{n!}a_{r_n}^{eq,(n)}\left(\vec{x},t\right)H_{r_n}^{(n)}\left(\vec{\xi}_0\right), \tag{4.1.18}$$

and the coefficients $a_{r_n}^{eq,(n)}\left(\rho,\vec{u}_0,\theta\right)$ are given by

$$a_{r_n}^{eq,(n)}\left(\vec{x},t\right)=\left(\frac{k_B T_0}{m}\right)^{\frac{D}{2}}\int f^{eq}\left(\vec{x},\vec{\xi},t\right)H_{r_n}^{(n)}\left(\vec{\xi}_0\right)d\vec{\xi}_0, \tag{4.1.19}$$

The first four coefficients of the tensor Hermite polynomial expansions are given below:

$$a^{eq,(0)}\left(\vec{x},t\right)=\rho, \tag{4.1.20}$$

$$a_{\alpha}^{eq,(1)}\left(\vec{x},t\right)=\rho u_{0,\alpha}, \tag{4.1.21}$$

$$a_{\alpha\beta}^{eq,(2)}\left(\vec{x},t\right)=\rho\left(u_{0,\alpha}u_{0,\beta}-\theta\delta_{\alpha\beta}\right), \tag{4.1.22}$$

$$a_{\alpha\beta\gamma}^{eq,(3)}\left(\vec{x},t\right)=\rho\left[u_{0,\alpha}u_{0,\beta}u_{0,\gamma}-\theta\left(u_{0,\alpha}\delta_{\beta\gamma}+u_{0,\beta}\delta_{\alpha\gamma}+u_{0,\gamma}\delta_{\alpha\beta}\right)\right]. \tag{4.1.23}$$

In fact, not only the equilibrium distribution function can be expanded by the tensor Hermite polynomial formula, but every square integrable function, without any influence in the higher orders terms of this function. The particle distribution itself is the best example for this purpose. It can be expanded as a function of the conserved moments – the equilibrium moments, i.e., density, velocity and temperature – and the non-conserved quantities – the kinetic moments, as the stress tensor, the heat flux and so on. Take, for example, eq . (4.1.18), where the coefficients $a_{r_n}^{(n)}$ are given by conserved and non-conserved moments. Now, for the sake of discretization, one can truncate the distribution in a given order *N:*

$$f^{N}\left(\vec{x},\vec{\xi},t\right)=\left[\frac{m}{2\pi k_B T_0}\right]^{D/2}\omega\left(\vec{\xi}_0\right)\sum_{n=0}^{N}\frac{1}{n!}a_{r_n}^{(n)}\left(\vec{x},t\right)H_{r_n}^{(n)}\left(\vec{\xi}_0\right) \tag{4.1.24}$$

where

$$a_{r_n}^{N,(n)}=a_{r_n}^{(n)} \tag{4.1.25}$$

when $n \leq N$. This is a very important conclusion, since one can represent exactly the moments til up a given order *N*. Indeed, any vector can be represented by

$$\varphi_{r_n}\left(\vec{\xi}_0\right) = \sum_{m=0}^{n} b_{r_m}^{(m)} H_{r_m}^{(m)}\left(\vec{\xi}_0\right) \tag{4.1.26}$$

Now, calculating a moment represented by the tensor Hermite polynomial in continous space, one has

$$\int f^{eq,(N)}\left(\vec{x},\vec{\xi},t\right) H_{r_n}^{(n)}\left(\vec{\xi}\right) d\vec{\xi} = \frac{1}{\left(2\pi\right)^{\frac{D}{2}}} \sum_{\ell=0}^{n} a_{r_\ell}^{eq,(\ell)} \int e^{-\frac{\xi_0^2}{2}} H_{r_\ell}^{(\ell)}\left(\vec{\xi}_0\right) H_{r_n}^{(n)}\left(\vec{\xi}_0\right) d\vec{\xi}_0 \,. \tag{4.1.27}$$

And for the discrete space,

$$\sum_i W_i f^{eq}\left(\vec{x},\vec{\xi}_i,t\right) H_{r_n}^{(n)}\left(\vec{\xi}_i\right) = \sum_{\ell=0}^{n} a_{r_\ell}^{eq,(\ell)} \sum_i w_i H_{r_\ell}^{(\ell)}\left(\vec{\xi}_{0,i}\right) H_{r_n}^{(n)}\left(\vec{\xi}_{0,i}\right), \tag{4.1.28}$$

where

$$w_i = W_i \left(\frac{m}{2\pi k_B T_0}\right)^{\frac{D}{2}} e^{-\frac{\xi_{0,i}^2}{2}} \tag{4.1.29}$$

Since the moments $a_{r_\ell}^{eq,(\ell)}$ are independents moments, the above equations must hold for every moment. Hence,

$$\frac{1}{\left(2\pi\right)^{\frac{D}{2}}} \int e^{-\frac{\xi_0^2}{2}} H_{r_\ell}^{(\ell)}\left(\vec{\xi}_0\right) H_{r_n}^{(n)}\left(\vec{\xi}_0\right) d\vec{\xi}_0 = \sum_i w_i H_{r_\ell}^{(\ell)}\left(\vec{\xi}_{0,i}\right) H_{r_n}^{(n)}\left(\vec{\xi}_{0,i}\right) \tag{4.1.30}$$

The tensor Hermite polynomials are orthogonal in continuous space, and then the induced norm of the discrete space will also be orthogonal. In this way,

$$\frac{1}{\left(2\pi\right)^{\frac{D}{2}}} \int e^{-\frac{\xi_0^2}{2}} \left[H_{r_n}^{(n)}\left(\vec{\xi}_0\right)\right]^2 d\vec{\xi}_0 = \sum_i w_i \left[H_{r_n}^{(n)}\left(\vec{\xi}_{0,i}\right)\right]^2 . \tag{4.1.31}$$

Philippi et al. (2006) proved that when the induced norm of the discrete tensor Hermite polynomial is made equal to the continuous norm of the corresponding tensor Hermite polynomial, the orthogonality of the discrete Hermite polynomial is verified for Bravais lattices, the inner product in the discrete space defined as:

$$\left\langle g,h\right\rangle = \sum_i w_i g_i\left(\vec{\xi}_{0,i}\right) h_i\left(\vec{\xi}_{0,i}\right). \tag{4.1.32}$$

Shan et al. (2006) also found a set of equations like the Eq. (4.1.31):

$$\sum_i w_i H_{r_n}^{(n)}\left(\vec{\xi}_{0,i}\right) = 1, \text{ if } n = 1 \tag{4.1.33}$$

and

$$\sum_i w_i H_{r_n}^{(n)}\left(\vec{\xi}_{0,i}\right) = 0 \text{ otherwise.} \tag{4.1.34}$$

The sets of equations found by Philippi et al. (2006) and Shan et al. (2006) are completely equivalent.

As observed before, the main goal of the method is to obtain the moments of the distribution, and not the distribution itself. Then, the following simplification is commonly used:

$$f_i^{eq}\left(\vec{x},t\right) = W_i f^{eq}\left(\vec{x},\xi_i,t\right). \tag{4.1.35}$$

To retrieve the macroscopic equations, one has to scale the macroscopic velocity and the molecular velocity in this way:

$$\vec{\xi}_{0,i} = a\vec{c}_i, \tag{4.1.36}$$

and

$$\vec{u}_0 = a\vec{u}^*. \tag{4.1.37}$$

where a is the scaling factor. It is also convenient to write

$$e_0 = a^2 e^*. \tag{4.1.38}$$

Now, one can obtain the relation between e^* and θ:

$$\theta = a^2 e^* - 1. \tag{4.1.39}$$

For the molecular velocity, for the sake of discretization, it is convenient to associate a spatial and a temporal scale. In this way:

$$\vec{\xi}_i = \frac{h}{\Delta t}\vec{c}_i, \tag{4.1.40}$$

where, commonly in lattice Boltzmann models, h is the spatial scale:

$$h = \Delta x = \Delta y = \Delta z. \tag{4.1.41}$$

Then, the relation between lattice and physical scales is:

$$\frac{h}{\Delta t} = a\sqrt{\frac{k_B T_0}{m}}. \tag{4.1.42}$$

Returning to the velocity discretization, the poles $\vec{c}_i$ can be chosen freely. In order to obtain a lattice-Boltzmann model of order N, one have to determine the set of velocities, the respective weight of this set, and the scaling factor of the lattice. As the poles can be chosen at will, giving models with exact streaming, leading to collision-propagation type evolution for the model, one can also let the poles to be determined by

the set of equations, obtaining reduced lattices, but without the collision-propagation scheme. Several irregular lattices for different orders are given in Surmas et al. (2009) and Pico (2008).

Now, one can write the equilibrium distribution for the lattice-Boltzmann models. Below, as an example, the full third-order equilibrium distribution is given as:

$$f_i^{eq,3}\left(\vec{x},t\right)=w_i\left\{1+a^2\left(\vec{u}^*\cdot\vec{c}_i\right)+\frac{1}{2}\left[a^4\left(\vec{u}^*\cdot\vec{c}_i\right)^2-a^2\vec{u}^{*2}+\theta\left(a^2c_i^2-D\right)\right]+\right.$$
$$\left.\frac{a^2}{6}\left(\vec{u}^*\cdot\vec{c}_i\right)\left[a^4\left(\vec{u}^*\cdot\vec{c}_i\right)^2-3a^2\vec{u}^{*2}+3\theta\left(a^2c_i^2-D-2\right)\right]\right\}. \qquad (4.1.43)$$

The set of equations given in Eq. (4.1.31) can be simplified in order to find suitable lattices for lattice-Boltzmann models. One can see that, for orders higher than 0, one will have the norms of the tensor Hermite polynomials to be restored, and in the equation will also appear lower order tensor Hermite polynomials, which already have their norm preserved (induction), and the odd order tensor will vanish in the summation and integration. With this in mind, then one only has to obey not the polynomial norm preservation, but only the monomial norm preservation:

$$\frac{1}{\left(2\pi\right)^{\frac{D}{2}}}\int e^{-\frac{\xi_0^2}{2}}\left[M_{r_n}^{(n)}\left(\vec{\xi}_0\right)\right]^2 d\vec{\xi}_0=\sum_i w_i\left[M_{r_n}^{(n)}\left(\vec{\xi}_{0,i}\right)\right]^2, \qquad (4.1.44)$$

where the monomial $M_{r_n}^{(n)}$ is defined as

$$M^{(0)}\left(\vec{\xi}_0\right)=1, \qquad (4.1.45)$$

and for $n\geq 1$

$$M_{r_n}^{(n)}\left(\vec{\xi}_0\right)=\prod_{m=1}^{n}\xi_{0,\alpha_m}. \qquad (4.1.46)$$

Strictly speaking, one will have to preserve the norm of tensor Hermite polynomials exclusively if one wants, for example, a model with only higher orders in the polynomials (higher frequencies). However, this will never happen to hydrodynamical models, because in these models the lower moments are precisely the most important modes.

To make calculations simpler to transport to a programming language for simulation, there is an easier way to write down the equilibrium distribution function. Once one has found the scaling factor and the weights for a given lattice, one writes:

$$f_i^{eq,N}\left(\vec{x},t\right)=w_i\rho\sum_{n=0}^{N}A_{r_n}^{(n)}\left(\vec{u}^*,\theta\right)M_{r_n}^{(n)}\left(\vec{\xi}_{0,i}\right). \tag{4.1.47}$$

For a given order *N*, now one just has to find the coefficients $A_{r_n}^{(n)}\left(\vec{u}^*,\theta\right)$, matching the moments of this discrete equilibrium distribution with the moments of the continuous one.

As shown in Chapter 2, to recover the full compressible Navier-Stokes-Fourier equations one has to recover until up the incomplete fourth-order moment

$$\left\langle \xi_0^2\xi_{0,\alpha}\xi_{0,\beta}\right\rangle. \tag{4.1.48}$$

One can apply the Gram-Schmidt procedure in the continuous space in order to orthogonalize these moments, and then recover the norm of these new set of vectors, finally finding a lattice with the weigths and the scaling factor to simulate termo-hydrodynamics. Instead, one can only add this set of equations

$$\frac{1}{\left(2\pi\right)^{\frac{D}{2}}}\int e^{-\frac{\xi_0^2}{2}}\left(\xi_0^2\xi_{0,\alpha}\xi_{0,\beta}\right)^2 d\vec{\xi}_0=\sum_i w_i\left(\xi_{0,i}^2\xi_{0,\alpha,i}\xi_{0,\beta,i}\right)^2, \tag{4.1.49}$$

which gives two equations in 2D and 3D, choose a suitable lattice and then apply the simpler procedure described above.

4.2 Relation to fit polynomial equilibria

In order to retrieve the moments until a given order, one can simply choose a lattice and apply the following polynomial equilibria to the discrete distribution function:

$$f_i^{eq,N}\left(\vec{x},t\right)=\rho\sum_{n=0}^{N}B_{r_n}^{(n)}\left(\vec{u}^*,\theta\right)M_{r_n}^{(n)}\left(\vec{\xi}_{0,i}\right), \tag{4.2.1}$$

One does not have now the weights and the scaling factor. For a given moment of order *p*, one has to retrieve the same moment in discrete and continuous space:

$$\left\langle\varphi^p\right\rangle^{eq}=\int f^{eq,N}\left(\vec{\xi}\right)\varphi^p\left(\vec{\xi}\right)d\vec{\xi}=\sum_i f_i^{eq,N}\left(\vec{\xi}_i\right)\varphi^p\left(\vec{\xi}_i\right), \tag{4.2.2}$$

and then find the respective coefficients $B_{r_n}^{(n)}$. One can find a set of orthogonal vectors in the lattice by the Gram-Schmidt procedure with the following inner product in the discrete space:

$$a*b=\sum_i a_i b_i \ . \tag{4.2.3}$$

Then, now one has a set of "lattice" tensor polynomials, which are not related to the tensor Hermite polynomials, because the lattice polynomials depend on the chosen set of vectors which will constitute the lattice, but which form an orthogonal set. In this way, one can write:

$$f_i^{eq,(N)}=\sum_{\ell=0}^{N} a_{r_\ell}^{eq,(\ell)} L_{r_\ell}^{(\ell)}\left(\vec{\xi}_i\right), \tag{4.2.4}$$

where $L_{r_\ell}^{(\ell)}\left(\vec{\xi}_i\right)$ are the lattice tensor polynomials of order ℓ. Since this polynomials are orthogonal in discrete space, one can write the coefficients as:

$$a_{r_\ell}^{eq,(\ell)}=\frac{\int f^{eq,(N)} L_{r_\ell}^{(\ell)}\left(\vec{\xi}\right) d\vec{\xi}}{\sum_{m=0}^{N}\left[L_{r_m}^{(m)}\left(\vec{\xi}_i\right)\right]^2}. \tag{4.2.5}$$

One can equally depart from the continuous equilibrium distribution and write

$$f^{eq,(N)}\left(\vec{x},\vec{\xi}_0,t\right)=\left[\frac{m}{2\pi k_B T_0}\right]^{D/2} e^{-\frac{\xi_0^2}{2}}\sum_{n=0}^{N}\frac{1}{n!}a_{r_n}^{eq,(n)}\left(\vec{x},\vec{\xi}_0,t\right)L_{r_n}^{(n)}\left(\vec{\xi}_0\right), \tag{4.2.6}$$

but now the tensor polynomials $L_{r_n}^{(n)}$ are not orthogonal in the continuous space. Calculating the moments until the order *N*, a closed system of equations for the coefficients $a_{r_n}^{(n)}$ will be obtained and the solution will be that given in Eq. (4.46), and also

$$\frac{1}{(2\pi)^{\frac{D}{2}}}\int e^{-\frac{\xi_0^2}{2}}\left[L_{r_n}^{(n)}\left(\vec{\xi}_0\right)\right]^2 d\vec{\xi}_0=\sum_i w_i\left[L_{r_n}^{(n)}\left(\vec{\xi}_{0,i}\right)\right]^2. \tag{4.2.7}$$

which is not generally true for $n\geq 3$.

The conclusion is that this equilibrium distribution, given by Eq. (4.2.4) lost the connection with its continuous conterpart, f^{eq}, although leading to correct macroscopic equations because correct moments can be retrieved. In Chapter 5, some insights on this question are given in terms of linear stability analysis.

4.3 Application to lattices

4.3.1 - 1D lattices

For second order, the D1V3 lattice is obtained.

D1V3		
Velocity	Symmetries	Weight
0	1	$\frac{2}{3}$
± 1	2	$\frac{1}{6}$
$a = \sqrt{3}$		

For third order, two possible solutions in one dimension with five velocities – D1V5 – are obtained:

D1V5a		
Velocity	Symmetries	Weight
0	1	$\frac{4}{45}\left(4-\sqrt{10}\right) \cong 0.0744642$
± 1	2	$\frac{3}{80}\left(8+\sqrt{10}\right) \cong 0.418585$
± 3	2	$\frac{1}{720}\left(16+5\sqrt{10}\right) \cong 0.0441825$
$a = \sqrt{\frac{1}{3}\left(5-\sqrt{10}\right)} \cong 0.783958$		

D1V5b		
Velocity	Symmetries	Weight
0	1	$\frac{4}{45}\left(4+\sqrt{10}\right) \cong 0.636647$
± 1	2	$\frac{3}{80}\left(8-\sqrt{10}\right) \cong 0.181415$

± 3	2	$\frac{1}{720}\left(16-5\sqrt{10}\right) \cong 0.000261961$
a = $\sqrt{\frac{1}{3}\left(5+\sqrt{10}\right)} \cong 1.64947$		

For thermal models, the following solution with seven velocities is given:

D1V7		
Velocity	Symmetries	Weight
0	1	0.476669886589207442331764996408
± 1	2	0.233914737826824713372866771883
± 2	2	0.026938189344825451680983762681 8
± 3	2	0.000812129533746113780266967231658
a = 1.196979770393074358972388463 85		

4.3.2 - 2D lattices

For the second order, the D2Q9 lattice is the minimal square lattice which preserves the norm of the Hermite polynomials. The set of equations obtained from the norm preservation, until the second order, is the following:

$$w_0 + 4w_1 + 4w_2 = 1, \tag{4.3.1}$$

$$2a^2\left(w_1 + 2w_2\right) = 1, \tag{4.3.2}$$

$$2a^4\left(w_1 + 2w_2\right) = 3, \tag{4.3.3}$$

$$4a^4 w_2 = 1. \tag{4.3.4}$$

resulting in the well known outcome:

$$w_0 = \frac{4}{9},\ w_1 = \frac{1}{9},\ w_2 = \frac{1}{36},\ a = \sqrt{3}. \tag{4.3.5}$$

One surprising result, for the D2Q9 lattice, is that it can also recover two third order moments ($\xi_\alpha^{\,2}\xi_\beta,\ \alpha \neq \beta$) and also one fourth order moment ($\xi_x^{\,2}\xi_y^{\,2}$), completing its total nine degrees of freedom: one zero order moment (mass), two first order moments

(momentum) and three second order moments (related to the stress tensor) are the other six moments. This result will be used later for improving the stability of the method.
In the search for third order models, the next choice would be the D2Q13 lattice.

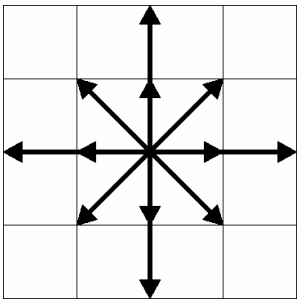

Fig.4.1. D2Q13 lattice

However, one does not obtain any result for the third order with this lattice, except that the scaling factor *a* is now free for second order models, because now there is another speed in the lattice. The following set of equations for the weights is then obtained:

$$w_0 = \frac{32a^4 - 20a^2 + 5}{32a^4}, \tag{4.3.6}$$

$$w_1 = \frac{8a^2 - 3}{48a^4}, \tag{4.3.7}$$

$$w_2 = \frac{1}{64a^4}, \tag{4.3.8}$$

$$w_3 = \frac{3 - 4a^2}{384a^4}. \tag{4.3.9}$$

The weights are non-negative for values of the scaling factor between the interval $\left[\sqrt{\frac{3}{2}}, \sqrt{3}\right]$, ranging from a rotated and enlongated version of the D2Q9 lattice (for $a = \sqrt{\frac{3}{2}}$), which can be seen in the Fig. 4.2, and the D2Q9 lattice itself (for $a = \sqrt{3}$).

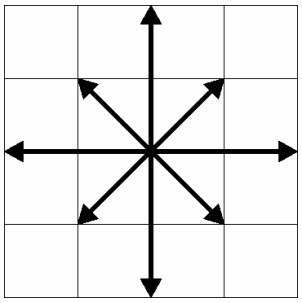

Fig.4.2. Rotated D2Q9 lattice

Between these two values, for example, the scaling factor can be set in order to improve stability, but this remains as an open question.

Continuing the quest for third order models, our next choice would be the square D2Q17, but also no results were found for this lattice. As now for the third order problem there are six equations, a lattice with six unknowns would be the best (or minimal) choice, and a square lattice with seventeen velocities fullfil this constraint. Two lattices with seventeen velocities were found, the D2V17*a* and D2V17*b*. For finding the D2V17*a* lattice, the lattice D2Q21 was used in order to see what parameters can be taken out, because now there are more unknowns than equations (seven unknowns and six equations).

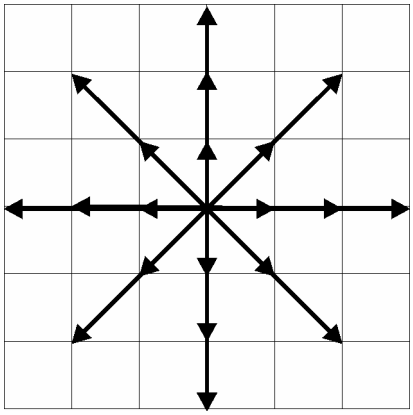

Fig.4.3. D2Q21 lattice

The free parameter is the scaling factor, set to a value where a given weight will be null. For that, the lower bound value of the scaling factor would lead to the D2Q21 lattice without the zero velocity, or the D2V20 lattice, while the upper bound value for the scaling factor would lead to the D2V17*a* lattice (Philippi et al, 2006).

Surmas et al. (2007) used this degree of freedom, in the scaling factor, to generate a model with reduced compressibility, adjusting the equilibrium distribution to

a van der Waals equation of state (without the long range term), obtaining good results in several benchmark cases.

To find the D2V17*b* lattice (Pico, 2008), one has to recover that the D1V5 lattice is the lattice used to third order models in one dimension. Using the product formulae, one can find the D2V17*b* lattice and verify that the D1V5 is precisely the projection in one dimension of the D2V17*b* lattice.

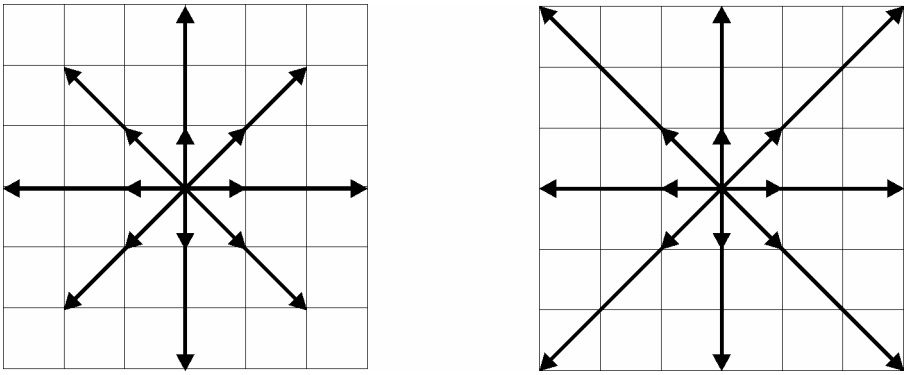

Fig. 4.4. D2V17 *a* and *b* lattices

In the next, the complete set of parameter for the D2V17 lattices are given.

D2V17*a*		
Velocity	Symmetries	Weight
(0,0)	1	0.402005146909112625941664392459
$(\pm 1,0)$	4	0.116154866497781543874035456626
$(\pm 1,\pm 1)$	4	0.033006353622986913949753825914 7
$(\pm 2,\pm 2)$	4	0.000079078602165918131237133240 5482
$(\pm 3,0)$	4	0.000258414549787467559557486104050
a = 1.643430608797954146822654167 4		

D2V17*b*		
Velocity	Symmetries	Weight
(0,0)	1	0.406671058564575223071626794184
$(\pm 1,0)$	4	0.114736659610102759919933612666
$(\pm 1,\pm 1)$	4	0.033338964066791507565053939708 9

$(\pm 3,0)$	4	0.00025126267064870996642603666124 6
$(\pm 3, \pm 3)$	4	$5.34901131321678067971241787436\times10^{-6}$
a = 1.64947240657615319927567150 60		

For thermal lattices, one needs lattices which preserve $\left\langle c^2 c_\alpha c_\beta \right\rangle$, and then one has to go again to higher lattices. It is very important to notice that one does not need full fourth-order lattices for thermal models, because that would require five moments more (three equations more), instead of only three moments with $\left\langle c^2 c_\alpha c_\beta \right\rangle$ (two equations more) in two dimensions. This has great consequences on the models, because square lattices with vectors only in the main axes and in the diagonal ones have the interesting property:

$$c_{ix}{}^3 c_{iy} = c_{iy}{}^3 c_{ix} . \tag{4.3.10}$$

This equality can be seen more clearly if one writes the above equation in the following way:

$$c_{ix}{}^2 (c_{ix} c_{iy}) = c_{iy}{}^2 (c_{ix} c_{iy}) . \tag{4.3.11}$$

The $c_{ix} c_{iy}$ factor selects non-null terms only in positions in the diagonal and, for diagonal vectors, in the so-called DQ-lattices, $c_{ix}{}^2 = c_{iy}{}^2$. One cannot write an equilibrium distribution function expanded in monomials with linearly dependent vectors.

There is another reason why such a thing cannot be done: the vectors $c_{ix}{}^3 c_{iy}$ (also $c_{iy}{}^3 c_{ix}$) and $c_{ix}{}^2 c_{iy}{}^2$ have the same norm in discrete space, but not in the Hilbert space. With that, the system of equations will be impossible. So, for complete fourth-order models one has to look for lattices with vectors like (a,b), $a \neq b$ in order to obtain complete fourth-order models.

For lattices with only moments until $\left\langle c^2 c_\alpha c_\beta \right\rangle$, one has to obey eight equations, and then one can go to the so called D2Q29 lattice (Fig. 4.5), with nine unknowns (eight weights plus the scaling factor), and than tune the free parameter (the scaling factor) in order to obtain smaller lattices.

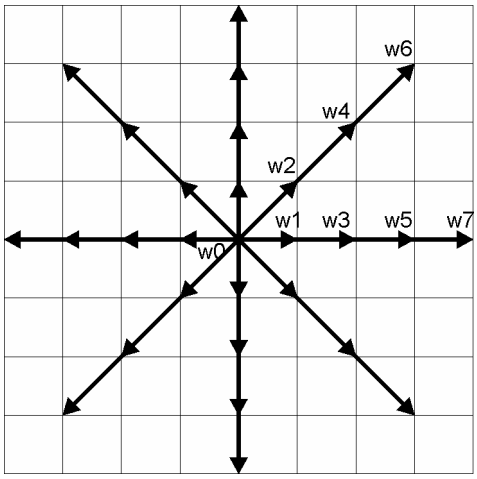

Fig. 4.5. D2Q29 lattice

In this case, it is obtained a solution, and when the scaling factor is properly adjusted, two lattices with twenty-five velocities are achieved, namely, D2V25(w_1) and D2V25(w_6). The weight in parenthesis means that it is made null in the aforementioned lattice. The complete solution for both lattices is found in the Appendix A.

For complete fourth-order models, as explained before, now one has to use velocity vectors of the type (a,b), $a \neq b$. As one has only one more equation to solve, departing from the D2V25 lattices, a solution would be achieved only adding one more set of speeds. This is accomplished with the D2V33 lattice (Fig. 4.6), which is a D2V25(w_6) plus the vector (4,2) and its symmetries.

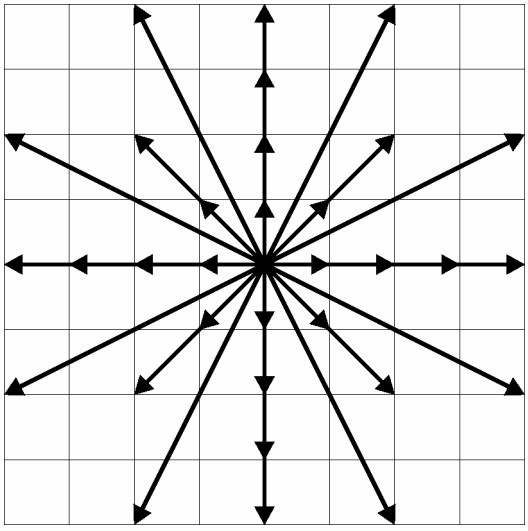

Fig. 4.6. D2V33 lattice

Velocity	Symmetries	Weight
(0,0)	1	0.21023106314221377744802257 4103
$(\pm 1,0)$	4	0.00344286611503926824136459992303
$(\pm 1,\pm 1)$	4	0.08665763189913955076509937 38682
$(\pm 2,0)$	4	0.06351135379975099003724532 43513
$(\pm 2,\pm 2)$	4	0.02839854273049944219891810 92785
$(\pm 3,0)$	4	0.01054087602611832727243329 88426
$(\pm 4,\pm 0)$	8	0.00227850463434393566210689760079
$(\pm 4,\pm 2)$	8	0.00130622950477752073041337630489
a = 0.77079903623126709388093065559		

Another interesting feature of this lattice is that one of the branches of the rotated (4,2) vector does not necessarily has to be used, resulting in two lattices with twenty-nine velocities (Fig. 4.7). This slight modification results in a doubled weight – in relation with the D2V33 lattice – for the (4,2) vectors that still are in the lattice. It is important to notice that these lattices also obey all the norm equations until the fourth-order (fourth-order included).

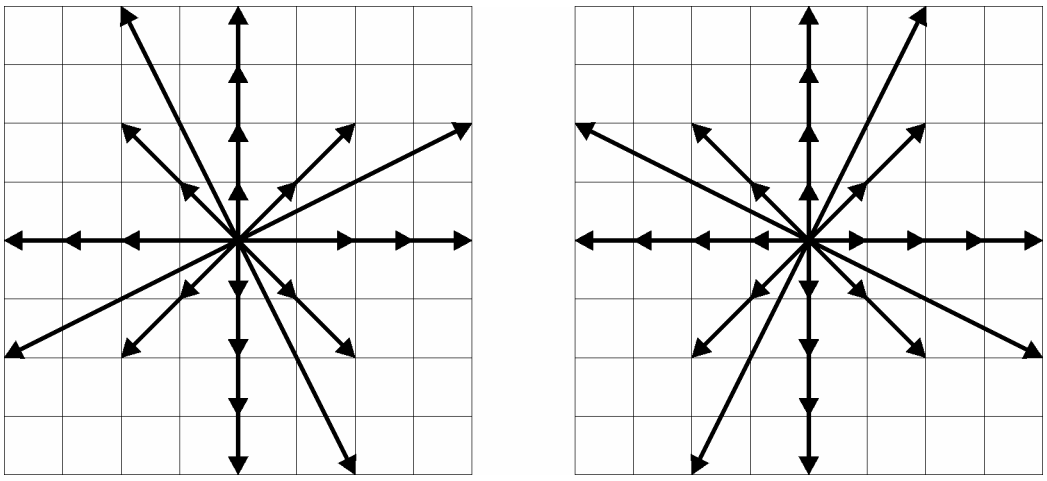

Fig. 4.7. D2V29 *l* (left) and *r* (right) lattices

Another variation for the fourth-order lattice is the D2V37 lattice (Fig. 4.8), which first appeared in the paper of Philippi et. al (2006), and now used by some other authors (Shan and Chen, 2007; Sbragaglia et. al, 2009; Colosqui, 2010). This lattice is more

compact than the D2V33, in the sense that its maximum velocity is three, instead of four, lattice sites per time step.

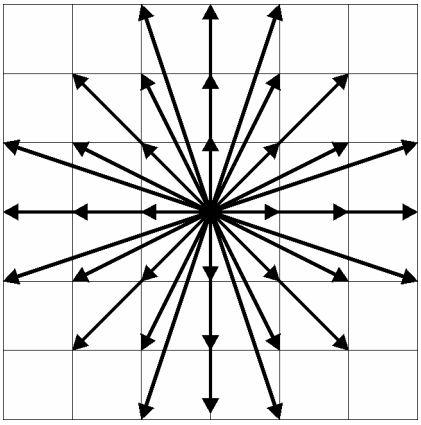

Fig. 4.8. D2V37 lattice

The weights and the scaling factor for the D2V37 lattice are:

Velocity	Symmetries	Weight
(0,0)	1	0.23315066913235250228650670406 7
$(\pm 1,0)$	4	0.10730609154221900241246428718 3
$(\pm 1,\pm 1)$	4	0.05766785988879488203006921539 33
$(\pm 2,0)$	4	0.01420821615845075026469894234 41
$(\pm 2,\pm 1)$	8	0.00535304900051377523273150166 219
$(\pm 2,\pm 2)$	4	0.00101193759267357547541090850 664
$(\pm 3,0)$	4	0.00024530102775771734546591664 3268
$(\pm 3,\pm 1)$	8	0.00028341425299419821740052529 4195
a = 1.19697977039307435897238846385		

Four more lattices can be obtained pruning the D2V37 lattice: one only has to subtract one of the two branches of $(\pm 2,\pm 1)$ and $(\pm 3,\pm 1)$, and there are four ways to perform this task. All these four lattices recover the polynomial norm of the Hermite functions. As an example, in Fig. 4.9 it is shown the D2V29 *lr* lattice obtained with the subtraction of the right branch of the vectors set $(\pm 2,\pm 1)$ and the subtraction of the left branch of the set $(\pm 3,\pm 1)$.

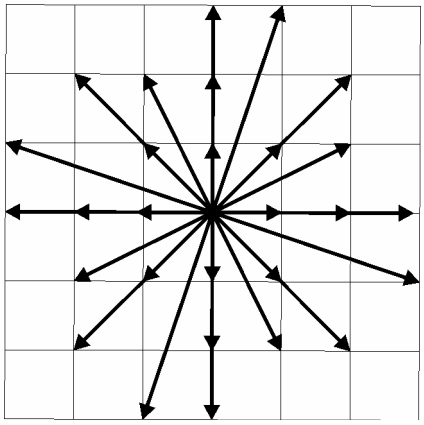

Fig. 4.9. D2V29 *lr* lattice

Results for fifth and sixth order lattices are shown in the Appendix A. It is important to note that, to the author's knowledge, the fifth order lattice in literature has fifty-three velocity vectors - D2V53 (Philippi et al, 2007; Surmas et al. 2009), and the sixth order lattice has eighy-one vectors (Philippi et al, 2007). In this work, it is presented a fifth order lattice with forty-five velocity vectors (D2V45) and a sixth order lattice with seventy-seven velocity vectors (D2V77).

4.3.3 - 3D lattices

For second order lattices in three dimensions, one departs from the simplest possible arrangement of the nearest velocities. One finds the following result for the weights, where w_3 is the weight related to the set $(\pm 1, \pm 1, \pm 1)$.

Velocity	Symmetries	Weight
(0,0,0)	1	$\frac{1}{3} - 8w_3$
$(\pm 1,0,0)$	6	$\frac{1}{18} + 4w_3$
$(\pm 1, \pm 1,0)$	12	$\frac{1}{36} - 2w_3$
a = $\sqrt{3}$		

If one sets $w_3 = 0$, $w_3 = \frac{1}{72}$, and $w_3 = \frac{1}{216}$ one obtains the D3Q19, D3Q15 and D3Q27 lattices, respectively, extensively used in the literature. In fact, any value between the interval $\left[0, \frac{1}{72}\right]$ can be used for w_3, and nothing can be said about which lattice is the best, because the error of approximation is the same.

The resulting lattice for third order 3D lattices, D3V39.

Velocity	Symmetries	Weight
(0,0,0)	1	$\frac{1}{12}$
$(\pm 1,0,0)$	6	$\frac{1}{12}$
$(\pm 1,\pm 1,\ \pm 1)$	8	$\frac{1}{27}$
$(\pm 2,0,0)$	6	$\frac{2}{135}$
$(\pm 2,\pm 2,0)$	12	$\frac{1}{432}$
$(\pm 3,\ 0,0)$	6	$\frac{1}{1620}$
$a = \sqrt{\frac{3}{2}}$		

For incomplete fourth order models, two lattices with fifty-nine velocities were found:

a)

Velocity	Symmetries	Weight
(0,0,0)	1	0.095878916237752832729094450 2319
$(\pm 1,0,0)$	6	0.073104708212914839109417455 6584
$(\pm 1,\ \pm 1,0)$	12	0.003465889710933800440249684 82340

$(\pm 1, \pm 1, \pm 1)$	8	0.036610808204451537873743770620 7
$(\pm 2,0,0)$	6	0.015923523223205955321354273428 2
$(\pm 2, \pm 2,0)$	12	0.002524808451050943939087549285 73
$(\pm 3, 0,0)$	6	0.000765879439346839706093878513082
$(\pm 2, \pm 2, \pm 2)$	8	0.000072696866251515863464366236825 1
$(\pm 4, 0,0)$	6	0
a = 1.202885123310261711239887502 35		

b)

Velocity	Symmetries	Weight
(0,0,0)	1	0.177196885566026225541728262120
$(\pm 1,0,0)$	6	0
$(\pm 1, \pm 1,0)$	12	0.029333545000359415200686719039 5
$(\pm 1, \pm 1, \pm 1)$	8	0.028992275460468759372674648221 1
$(\pm 2,0,0)$	6	0.024609227537606918116599023410 5
$(\pm 2, \pm 2,0)$	12	0.005746168846479715388192079614 46
$(\pm 3, 0,0)$	6	0.002019086321064313556395262570 61
$(\pm 2, \pm 2, \pm 2)$	8	0.001098122067707758447477661021 41
$(\pm 4, 0,0)$	6	0.000225580815744112465423660701025
a = 1.039155346051997071898004640 34		

Full fourth order lattices are given in the Appendix A.

4.4 Rectangular Lattices

Sometimes, in computational fluid dynamics, one wants to simulate systems with geometries such that rectangular lattices are more suitable for simulation than square lattices. In order to do that, one can try lattices in the way pictured in Fig. 4.10, where r is defined as the aspect ratio $r = \frac{\Delta x}{\Delta y}$.

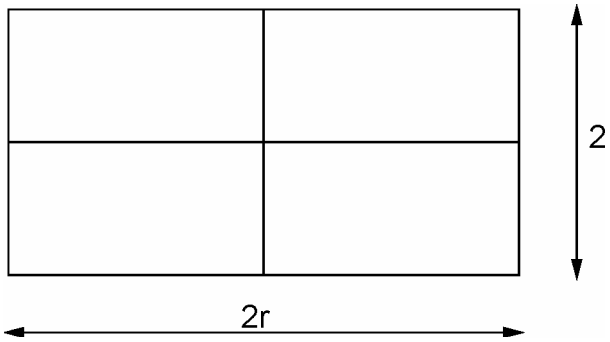

Fig. 4.10. Rectangular lattice

Bouzidi et al. (2001) also presents a scheme like this using an MRT model. The authors use the MRT model in order to avoid anisotropic transport coefficients, so in their model they can tune several modes independently, and the macroscopic equations are recovered with isotropic transport coefficients – sound speed and viscosity. Using BGK approximation, one does not have the freedom to tune the moments independently, and the price to pay for that is the increase in the number of lattice speeds. This is due to the number of equations that one have to obey, because now $\langle c_x \rangle$ will be diferent from $\langle c_y \rangle$, for aspect ratio $r \neq 1$. So, for second order, instead of four equations, one now has six equations. This is partially equilibrated by the fact that now new weights are added into the set of variables.

Order	Number of equations	Total number of equations
0	1 (1)	1
1	2 (c_x, c_y)	3
2	3 ($c_x, c_x c_y, c_y$)	6

Such an analysis can also be carried on for high order models, and also for 3D lattices, but for this example, i.e., for second order models in two dimensions, there are analytical results that can illustrate in a good manner the method that is proposed without losing generality.

Trying to solve the equation for the second order with nine velocities – the rectangular D2Q9 lattice – one does not find any solution. For this problem, the system

has six equations and five unknowns (four weights and the scaling factor). Then, one have to go one lattice further, the D2Q13 rectangular lattice – D2Q13R (Fig. 4.11).

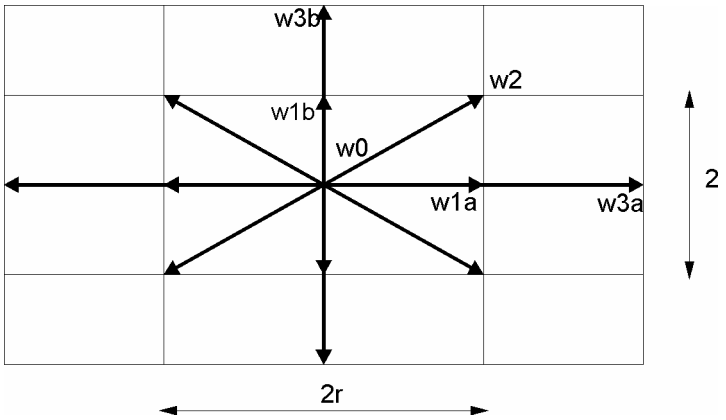

Fig.4.11. D2Q13R

For this lattice, one obtains the following solutions for the weights:

Velocity	Weight
(0, 0)	$w_0 = \frac{3+4r^2-20a^2r^2+3r^4-20a^2r^4+64a^4r^4}{64a^4r^4}$
$(\pm r, 0)$	$w_{1a} = \frac{16a^2r^2-3r^2-3}{96a^4r^4}$
$(0, \pm 1)$,	$w_{1b} = \frac{16a^2r^2-3r^2-3}{96a^4r^2}$
$(\pm r, \pm 1)$	$w_2 = \frac{1}{64a^4r^2}$
$(\pm 2r, 0)$	$w_{3a} = \frac{3-4a^2r^2}{384a^4r^4}$
$(0, \pm 2)$	$w_{3b} = \frac{3-4a^2}{384a^4}$

Clearly, if $r = 1$, one returns to the equations for the D2Q13 lattice already presented. In this model, there are two free parameters: the aspect ratio and the scaling factor. In order to obtain positive weights, the scaling factor has to obey:

$$\frac{1}{2}\sqrt{3\left(\frac{1}{r^2}+1\right)} < a < \frac{1}{r}\sqrt{3}\,, \tag{4.4.1}$$

and

$$a < \sqrt{3}\,. \tag{4.4.2}$$

From this two equations follows that:

$$\frac{1}{\sqrt{3}} < r < \sqrt{3}\,. \tag{4.4.3}$$

A result of the type $1/b < r < b$, $b > 1$, were expected because of the problem symmetry. It is interesting to note that the weight related to the direction $(0, \pm 2)$ is independent from the aspect ratio r. This might suggest that one can obtain a consistent model with less speeds than that it is proposed – for example, a D2Q11 lattice, but many trials were made in this direction without success.

As an example, the following model is obtained with an aspect ratio $r = 1.5$ and scaling factor $a = \sqrt[4]{\frac{13}{9}} \cong 1.096289$. This value of a was chosen as the geometric mean between the lower and the upper bounds for the positivity of the weights.

Velocity	Weight
(0, 0)	0.427174148043850615046478318041
$(\pm r, 0)$	0.024311198322324054230374103758 7
$(0, \pm 1)$,	0.054700196225229122018341733457 0
$(\pm r, \pm 1)$	0.076923076923076923076923076923 1
$(\pm 2r, 0)$	0.001685678309982951738806746720 21
$(0, \pm 2)$	0.051869699274384718335392103197 4

4.5 Hexagonal Lattices

In the case of hexagonal lattices the number of equations to be solved is equal to the number of variables, in a desired order to be achieved (Mayer, 2008). This property can be seen in the Fig 4.12.:

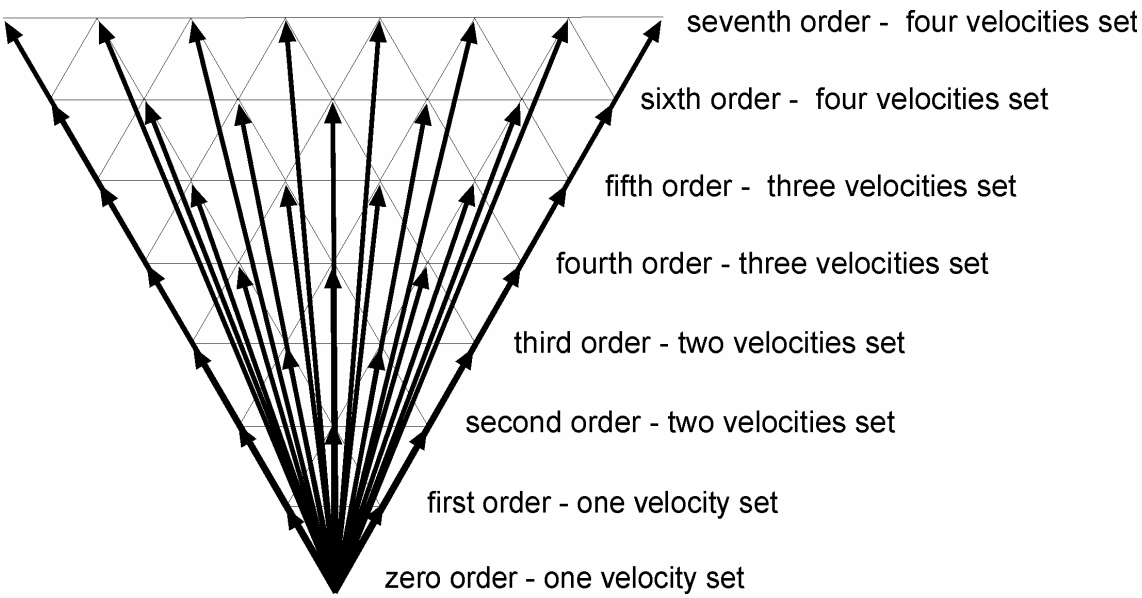

Fig. 4.12. Hexagonal hierachy

The lattice is formed with six rotations filling all the space and also adding slower velocities.

The equations for the second order moment,

$$\sum_i w_i \left(c_{ix} c_{ix}\right)^2 = \left\langle {c_x}^2, {c_x}^2 \right\rangle, \tag{4.5.1}$$

$$\sum_i w_i \left(c_{ix} c_{iy}\right)^2 = \left\langle {c_x}^2, {c_y}^2 \right\rangle, \tag{4.5.2}$$

where $\langle a,b \rangle$ stands for the norm of the a and b in the Hilbert space, are **equal** for hexagonal lattices. This statement can be proved writing down the general equation for a basic hexagonal lattice

$$\vec{c}_i = c\left(\cos\left(\theta + i\frac{\pi}{3}\right), \sin\left(\theta + i\frac{\pi}{3}\right)\right), \tag{4.5.3}$$

$i = 0,...,5$; and c is the speed of the lattice, leading to a single equation, instead of two, for the second order:

$$a^4 c^4 w_{b^2} = \frac{1}{3}, \tag{4.5.4}$$

where a stands for the scaling factor of the lattice. This means that the norm preservation for the second order is fulfilled for the various lattices, independing from the lattice orientation. This is also related to a theorem proved by Chen & Shan (2008) regarding also symmetric non-space-filling lattices.

For the various hexagonal lattices they will form the desided one, one only has to sum up the right hand side of the former equation for all the basic hexagonal lattices. For example, applying the norm preservation for the lattice D2V19H (also known as GBL, due to Grosfils, Boon and Lallemand, 1992), the equation for the second order reads as follows,

$$3a^4(w_1 + 9w_3 + 16w_4) = 1, \tag{4.5.5}$$

where w_α such that $\alpha = \|c_i\|^2$, for $i = 0,\ldots,18$. No relations like that were found for higher orders.

The number of equations to be carried on can be resumed in the following table:

Order	Number of equations	Total number of equations
0	1 (1)	1
1	1 (c_α)	2
2	2 ($c_\alpha^2, c_\alpha c_\beta$)	4
3	2 ($c_\alpha^3, c_\alpha{}^2 c_\beta$)	6
4	3 ($c_\alpha^4, c_\alpha{}^3 c_\beta, c_\alpha{}^2 c_\beta{}^2$)	9
5	3 ($c_\alpha^5, c_\alpha{}^4 c_\beta, c_\alpha{}^3 c_\beta{}^2$)	12
6	4 ($c_\alpha^6, c_\alpha{}^5 c_\beta, c_\alpha{}^4 c_\beta{}^2, c_\alpha{}^3 c_\beta{}^3$)	16
7	4 ($c_\alpha^7, c_\alpha{}^6 c_\beta, c_\alpha{}^5 c_\beta{}^2, c_\alpha{}^4 c_\beta{}^3$)	20

The monomial between parathensis is the one with the norm to be preserved. This procedure does not lead to minimal lattices for a given order. Despite not yet proven, this gives a way to look for lattices for higher orders.

The second order lattice is the celebrated FHP lattice, and not the GBL lattice, giving an indication that the hierachy procedure will not provide minimal lattices. The weights are $w_0 = \frac{1}{2}$ for the rest velocity and $w_1 = \frac{1}{12}$ for the non-zero velocity.

For third order models, the GBL lattice will be the natural choise. However, as can be seen in the hierachy, one has to go one level up in the velocity, because no real solutions can be found for the GBL lattice. Then, the lattice for starting the search for third order models is represented in Fig. 4.13:

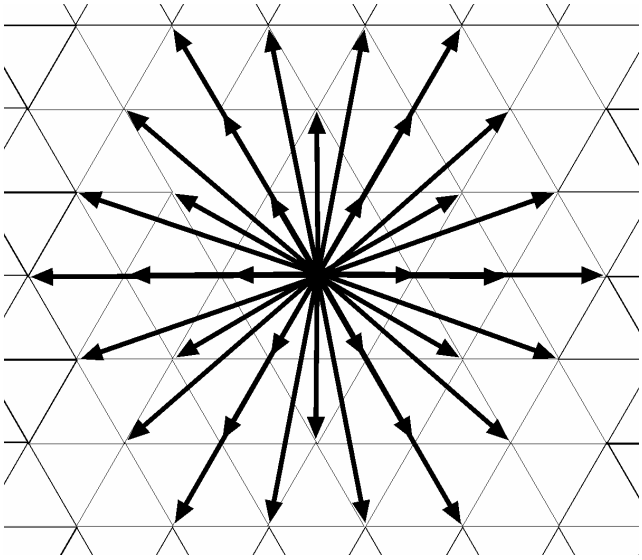

Fig.4.13. Starting lattice for the third order

From this higher lattice, is then derived a pruned lattice with nineteen velocities and its weights given below.

Velocity	Number of symmetries	Weights
(0,0)	1	0.391513907025714534293310384 63
$(1,0)_R$	6	0.095405694150420948329997233861
$(0,\sqrt{3})_R$	6	0.005920257876811155686673018 5412
$(3,0)_R$	6	0.000088396801815473601111350160153
a = 1.710248692777903789163975066 0		

For this lattice, another solution is also possible:

Velocity	Number of symmetries	Weights
(0,0)	1	0.260337944826137317558541467227
$(1,0)_R$	6	0.079594305849579051670002766139
$(0,\sqrt{3})_R$	6	0.042227890271336992461475129 6069
$(3,0)_R$	6	0.001454813074727736275431859716 39
a = 1.232677513908611745793512570 7		

The subscript *R* refers to rotations of the velocity vector to fullfill the space with this lattice.

The result for third-order models is presented in the Fig. 4.14.

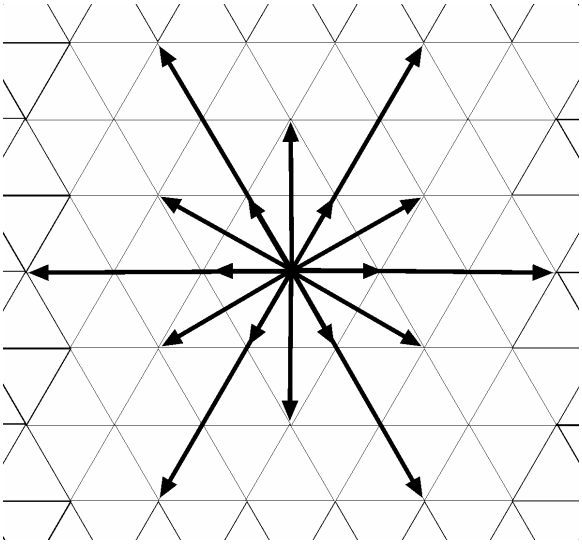

Fig.4.14. D2V19H third order lattice

For fourth-order lattices, the starting point would be, in the hierarchy, one level up than that of the third-order lattices. But, in this case, precisely the starting lattice for third order models is the one which recovers all the equations till up the fourth-order, and the lattice can be seen in Fig. 4.13. The final result for this fourth-order lattice, named D2V37H, is presented in Table II.

Velocity	Number of symmetries	Weights
(0,0)	1	0.26192882117647592351291000204
$(1,0)_R$	6	0.10166658100038346801788752221 5
$(2,0)_R$	6	0.00564842945696859917128146343 66
$(0,\sqrt{3})_R$	6	0.01494024539516952399867089164 36
$(3,0)_R$	6	0.00005552224901369222025851153 3344
$(2,\sqrt{3})_R$	12	0.00035054251785936466987497208 2484
a = 1.38215318530195584190496627 84		

For fifth order models, one can depart again from the hexagonal hierarchy, obtaining the following result (D2V55H):

Velocity	Number of symmetries	Weights
(0,0)	1	0.24099967727866143906697728293 3
$(1,0)_R$	6	0.10088543010228779810636409919 5
$(0,\sqrt{3})_R$	6	0.01731057747415053542720170514 64
$(2,0)_R$	6	0.00711103803974748235271374102 77
$(3,0)_R$	6	0.00009722491296451923383677037 0073
$(2,\sqrt{3})_R$	12	0.00054724839935440014683716068 716
$(4,0)_R$	6	$4.086995367207006271542099281 43\times10^{-7}$
$(4,\sqrt{3})_R$	12	$4.388797469520205429974270590 67\times10^{-7}$
a = 1.325156607128702643436630387 2		

For the sixth order, one can find the following result, a lattice with eighty-five velocities, named D2V85H.

Velocity	Number of symmetries	Weights
(0,0)	1	0.17288953052202360332235871622
$(1,0)_R$	6	0.09235153550409350216982358945
$(0,\sqrt{3})_R$	6	0.02634938567809358325437857342 4
$(2,0)_R$	6	0.01404917380736157896789264682 0
$(2,\sqrt{3})_R$	12	0.00214207215835993587426046154 65
$(3,0)_R$	6	0.00061610719989731878376054138213
$(0,2\sqrt{3})_R$	6	0.00009410129786796477918158329620 8
$(1,2\sqrt{3})_R$	12	0.00004825876551523026003744258474 7
$(4,0)_R$	6	$7.505106239681489209509657755 6\times10^{-6}$
$(4,\sqrt{3})_R$	12	$1.189373923553615783611546747 44\times10^{-6}$
$(3,2\sqrt{3})_R$	12	$4.478619224985842653692888771 49\times10^{-7}$
a = 1.120069335726828620023523048 5		

For the seventh order, the following results are presented (D2V115H).

Velocity	Number of symmetries	Weights
(0,0)	1	0.16075537338884886048864291 77
$(1,0)_R$	6	0.08974232742496675587472924 62
$(0,\sqrt{3})_R$	6	0.02794371286786952254843316 11
$(2,0)_R$	6	0.01558797851139189090571368984
$(2,\sqrt{3})_R$	12	0.00271244212872076254383234402
$(3,0)_R$	6	0.00084536952313302428938897072 6
$(0,2\sqrt{3})_R$	6	0.00014595784264352606407037349 69
$(1,2\sqrt{3})_R$	12	0.00008136607174378374628136460 03
$(4,0)_R$	6	0.00001419641830774179076989793789
$(4,\sqrt{3})_R$	12	$2.624276964406519067061428699 5\times10^{-6}$
$(3,2\sqrt{3})_R$	12	$8.117236632298611247299421880\times10^{-7}$
$(5,0)_R$	6	$6.270006346308609817479371457\times10^{-8}$
$(2,3\sqrt{3})_R$	12	$3.922266770995999096823340900 8\times10^{-9}$
$(5,2\sqrt{3})_R$	12	$1.450049012346706736342867362 3\times10^{-9}$
a = 1.08007903722781536418253427 7		

4.6. Lattice Boltzmann models with multiple speeds

After 2006, several authors proposed lattice-Boltzmann models in order to use the lattices with multiple speeds and exact higher order terms in the equilibrium distribution. Here follows a summary of some works in the field.

4.6.1 Latt & Chopard (2006)

The elegant method proposed by Latt & Chopard and extended to higher orders by Zhang et al. (2006) is based on the projection of the distribution function in the sub-space spanned by tensor Hermite polynomials in a given lattice, with a given order *N* in the equilibrium distribution. In this way, the distribution function will be then expressed in the regularized form, as,

$$\hat{f}_i\left(\vec{x},t\right)=\rho w_i\sum_{n=0}^{N}\frac{1}{n!}a_{r_n}^{(n)}H_{r_n}^{(n)}\left(\vec{\xi}_{0,i}\right) \tag{4.6.1}$$

where

$$a_{r_n}^{(n)}=\sum_i f_i H_{r_n}^{(n)}. \tag{4.6.2}$$

It can readily be seen that

$$a^{(0)}=1, \tag{4.6.3}$$

for mass conservation, and

$$a_\alpha^{(1)}=u_\alpha^*, \tag{4.6.4}$$

for momentum conservation. For energy conserving models, the trace of the second order moment is also conserved. For higher (kinetic) moments, one simply has to evaluate Eq. (4.6.2). Then, the collision process is performed with a given collision operator (e.g., BGK), in the moment space:

$$a_{r_n}^{(n)'}=-\frac{1}{\tau}\left(a_{r_n}^{(n)}-a_{r_n}^{eq,(n)}\right). \tag{4.6.5}$$

The propagation step is made after the regularization procedure, i.e.,

$$f_i\left(\vec{x}+\vec{c}_i\Delta t,t+\Delta t\right)=\rho w_i\sum_{n=0}^{N}\frac{1}{n!}a_{r_n}^{(n)'}H_{r_n}^{(n)}\left(\vec{\xi}_{0,i}\right). \tag{4.6.6}$$

The simplicity of the scheme is remarkable: first, one has to calculate the moments; second, collide the moments in the moment space; third, return to the velocity space according to Eq. (4.6.1) and propagate. With these steps, one removes spurious higher moments from the evolution equation, which affect lower moments and, consequently, lower macroscopic equations, i.e., the hydrodynamics, mainly in stability issues.

Another insteresting feature is that now one needs to store only the lower moments in memory, until the order *N*, and not anymore all the distributions. Memory is not the critical resource – the processing time is, but still this is a positive feature. For example, in the D2V37 lattice, instead 37 floats, one has to keep stored only 15 floats, all the moments until the fourth-order, a reduction of 59,5% in the memory. For the

D2V17, a third order lattice, instead of 17 floats, only 10 are required, a reduction of 41,2%.

4.6.2 Shan & Chen (2007)

Shan and Chen proposed the decoupling of the relaxation part in this way,

$$\Omega_i = -\sum_{n=2}^{N} \frac{1}{\tau_n n!} \left(a_{r_n}^{(n)} - a_{r_n}^{eq,(n)} \right) H_{r_n}^{(n)} \left(\vec{\xi}_{0,i} \right), \tag{4.6.7}$$

where this generalized collision operator turns back to its BGK counterpart if all the τ_n are made equal. For energy conserving models, the zero-th and first order a moments are conserved, while for second order moment only the trace of a is preserved, i.e.,

$$a_{\alpha\alpha}^{(2)} = a_{\alpha\alpha}^{eq,(2)}. \tag{4.6.8}$$

Using a suitable lattice, like D2V25 or higher, the transport coefficients are given as follows:

$$\nu = \frac{P}{\rho} \left(\tau_2 - \frac{\Delta t}{2} \right), \tag{4.6.9}$$

for the kinematic viscosity and

$$\alpha = \frac{P}{\rho} \left(\tau_3 - \frac{\Delta t}{2} \right), \tag{4.6.10}$$

for the thermal diffusivity, giving a Prandtl different from unity if necessary.

4.6.3 Philippi et al. (2007)

Philippi et al. also proposed a model for Prandtl number different from unity in a formal way starting from the kinetic theory.

The distribution function is said to be near equilibrium, i.e.,

$$f = f^{eq} \left(1 + \phi \right), \tag{4.6.11}$$

where ϕ is the departure from equilibrium. The operator is then written as

$$\Omega = f^{eq} \Gamma \left(\phi \right), \tag{4.6.12}$$

where Γ is a linear operator.

One then expands this non-equilibrium part in tensor Hermite polynomials and applies the linear operator, resulting in:

$$\Gamma\left(\phi\right)=\sum_{n=2}^{\infty}b_{r_n}^{(n)}\Gamma\left(H_{r_n}^{(n)}\right), \tag{4.6.13}$$

where $b_{r_n}^{(n)}$ are the resulting non-equilibrium coefficients of the particle distribution. One then applies a diagonalization Gross-Jackson procedure in the linear operator, resulting in

$$\Gamma\left(\phi\right)=-\sum_{n=2}^{N}\lambda_n b_{r_n}^{(n)}H_{r_n}^{(n)}-\gamma_{N+1}\phi, \tag{4.6.14}$$

where λ_n are the eigenvalues related to the moment *n* and the last part of the equation is the absorption term, i.e., all the terms of higher order are condensed into one. If $N=0,1$, then one returns to the BGK collision model. For $N=2$, one obtains the following collision model:

$$\Omega_i=\frac{1}{\tau}\left(f_i^{eq}-f_i\right)-\frac{1}{\tau_2}f_i^{eq}\frac{\tau_{\alpha\beta}}{Pe}\left(c_{i\alpha}-u_\alpha^*\right)\left(c_{i\beta}-u_\beta^*\right). \tag{4.6.15}$$

In this case, the kinematic viscosity is given by:

$$\nu=\frac{P}{\rho}\left(\frac{\tau_2\tau}{\tau_2+2\tau}-\frac{\Delta t}{2}\right), \tag{4.6.16}$$

and the thermal diffusivity is given by:

$$\alpha=\frac{P}{\rho}\left(\tau-\frac{\Delta t}{2}\right), \tag{4.6.17}$$

also giving Prandtl numbers different from unity, if one wishes for.

4.6.4 Sbragaglia et al. (2009)

Until now, no word was given for the lattice-Botlzmann equation with external forces. The problem is still under investigation, because of the great obstacle in performing simulations under gravity: even to recover the continuity equation without error is something difficult.

Very recently, however, Sbragaglia et al. seemed to solve this problem, departing from the Boltzmann equation with a BGK formulation, i.e.,

$$\partial_t f+\xi_\alpha\partial_\alpha f=-\frac{1}{\tau}\left(f-\overline{f}^{eq}\right). \tag{4.6.18}$$

They proved that if one uses the BGK collision operator with a shifted equilibrium, i.e.,

$$\bar{f}^{eq} = f^{eq}\left(\rho, \bar{u}, \bar{\theta}\right), \tag{4.6.19}$$

where

$$\bar{u}_\alpha = u_\alpha + \tau F_\alpha, \tag{4.6.20}$$

and

$$\bar{\theta} = \theta - \frac{\tau^2 F^2}{D}, \tag{4.6.21}$$

one will find the Boltzmann BGK equation with an external field, i.e.,

$$\partial_t f + \xi_\alpha \partial_\alpha f + F_\alpha \partial_{\xi_\alpha} f = -\frac{1}{\tau}\left(f - f^{eq}\right). \tag{4.6.22}$$

This represents a great progress also in the kinetic theory: the authors have used the Boltzmann equation itself, and the BGK equation *per se* is simplified. Regarding the lattice Boltzmann method, now one can simply discretize the equation and use the new scheme. All the work of discretization has been done before, and the authors use a D2V37 lattice to comprove their results. Scagliarini et al. (2010) also used this formulation in order to simulate the Rayleigh-Taylor instability problem, obtaining good agreement with the literature.

The authors also give a light on thermal boundary conditions for multi-speed lattices, a problem until now few explored. Despite some temperature jump in the wall, the results are promising in that direction.

The problem still to be solved is the lattice Boltzmann equation with external forces and tunable Prandtl number, because this formulation only applies to BGK collision operator.

5. LINEAR STABILITY ANALYSIS

In this chapter, a linear stability analysis is performed on several lattice Boltzmann models.

The lattice Boltzmann equation reads,

$$f_i\left(\vec{x}^* + \vec{c}_i, t^* + 1\right) - f_i\left(\vec{x}_i^*, t^*\right) = \Omega_i, \tag{5.1}$$

where $\vec{x}^* = \vec{x}/h$ and $t^* = t/\delta$. In order to perform the linear stability analysis, one has to linearize the lattice Boltzmann equation, because the collision operator has non-linear terms in f_i. For that, it is carried out a Taylor expansion in the collision operator around a chosen equilibrium state $\overline{f} = \left(\overline{f}_0, \overline{f}_1, \ldots, \overline{f}_b\right)$, given by

$$\overline{f}_i = f_i^{eq}(\overline{\rho}, \overline{u}, \overline{e}), \tag{5.2}$$

where $\overline{\rho}, \overline{u}$ and $\overline{e}$ stand for the density, velocity and internal energy in the equilibrium state. The Taylor expansion in the collision operator reads

$$\Omega_i = \Omega_i\left(f_0, f_1, \ldots, f_b\right) = \Omega_i)_{\overline{f}} + \sum_j \left.\frac{\partial \Omega_i}{\partial f_j}\right)_{\overline{f}} \delta f_j, \tag{5.3}$$

where $\delta f_j = f_j - \overline{f}_j$ and terms of second order were dropped off. The term $\Omega_i)_{\overline{f}}$ vanishes because $\overline{f}$ is an equilibrium (maxwellian) distribution. Applying the eq. (5.3) in (5.1), one gets

$$\delta f_i\left(x^* + \vec{c}_i, t^* + 1\right) - \delta f_i\left(\vec{x}_i^*, t^*\right) = \sum_j \left.\frac{\partial \Omega_i}{\partial f_j}\right)_{\overline{f}} \delta f_j. \tag{5.4}$$

In order to do the analysis, one has to perform the discrete Fourier transform to obtain

$$\delta f_i\left(\vec{k}, t^* + 1\right) = e^{-i\vec{c}_i \cdot \vec{k}} \sum_j \left(\delta_{ij} + \left.\frac{\partial \Omega_i}{\partial f_j}\right)_{\overline{f}} \right) \delta f_j\left(\vec{k}, t^*\right). \tag{5.5}$$

The previous equation can also be written as:

$$\delta \vec{f}\left(\vec{k}, t^* + 1\right) = \overline{\overline{L}} \cdot \delta \vec{f}\left(\vec{k}, t^*\right), \tag{5.6}$$

where $\overline{\overline{L}}$ is the second-order tensor:

$$L_{ij} = e^{-i\vec{c}_i \cdot \vec{k}} \left(\delta_{ij} + \frac{\partial \Omega_i}{\partial f_j} \right)_{\bar{f}} \right). \tag{5.7}$$

When one applies *t* times the operator L sequencially over the initial difference distribution $\delta \vec{f}\left(\vec{k},0\right)$, one obtains:

$$\delta \vec{f}\left(\vec{k},t\right) = \bar{\bar{L}}^t \cdot \delta \vec{f}\left(\vec{k},0\right), \tag{5.8}$$

or, written in terms of the eigenvalues z_ℓ and eigenvectors $\vec{z}_\ell$ of the L matrix:

$$\delta \vec{f}\left(\vec{k},t\right) = \sum_\ell b_\ell {z_\ell}^t \vec{z}_\ell, \tag{5.9}$$

where

$$b_\ell = \vec{z}_\ell \cdot \delta \vec{f}\left(\vec{k},0\right). \tag{5.10}$$

Then, now the problem is restricted to an eigenvalue problem. The solution for a large time *t* will converge if the modulus of each of the eigenvalues is less than unity, i.e.,

$$\left\| z_\ell \right\| < 1. \tag{5.11}$$

Now, one has only to compute the eigenvalues of the matrix L for a given set of values $\bar{\rho}, \bar{u}$ and $\bar{e}$ and the wave vector $\vec{k}$. To do that, it is used the BKG collision operator. The range of values of $\vec{k}$ investigated is from 0 to 2π. It was also investigated the relation between the wave vector and the velocity $\bar{u}$, and significant results can be obtained investigating only when $\vec{k}$ and $\bar{u}$ are parallel. Following that, it was also investigated the case where the polar angle (for $\vec{k}$ and $\bar{u}$) gives the worst results in terms of stability, and they can be seen in the Fig. 5.1.

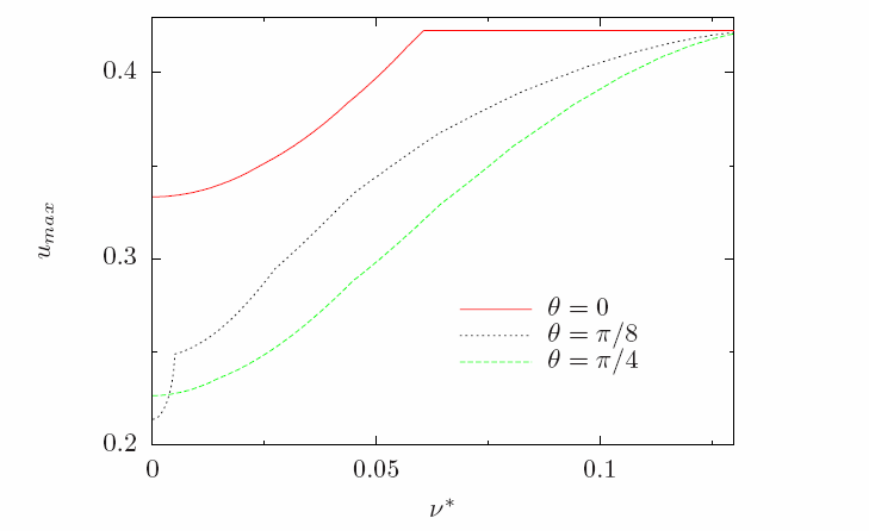

Fig.5.1. Instability polar angle dependence

It is clear that the results of interest are for $\theta = \frac{\pi}{4}$. This preliminary filter of results is very important because of the number of calculations that has to be done in order to obtain the eigenvalues of the matrix *L*.

The first comparison is between athermal models which have their equilibrium distribution discretized til up to second-, third- and fourth-order, namely, D2Q9, D2V17 and D2V37 lattices, respectively. The results are shown in Fig. 5.2 .

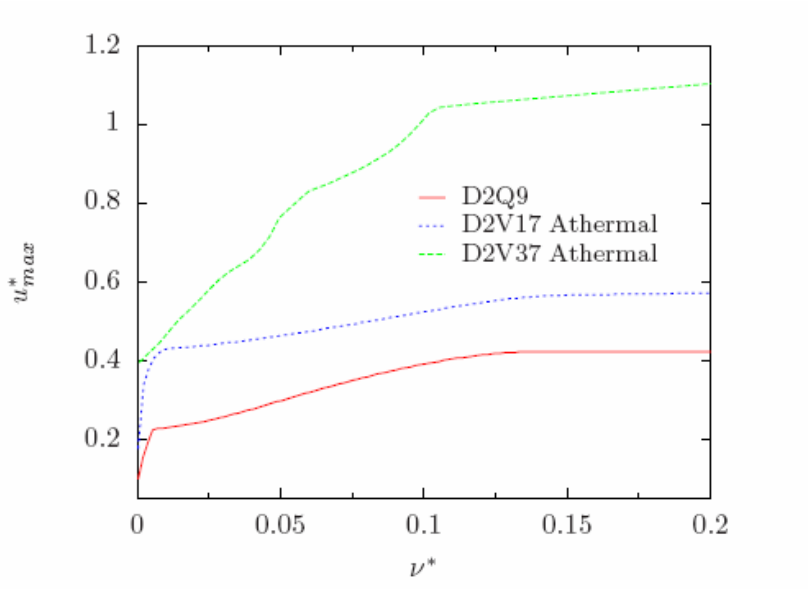

Fig. 5.2. Comparison of the maximum stable velocity for various athermal models

The result is presented for viscosity instead of relaxation time because for the same relaxation time the models have different viscosities, and the viscosity is directly related to the Reynolds number, the most important nondimensional parameter in an athermal flow. The higher order model, D2V37, is far more stable than the two others. This is explained simply because the model has a better representation for the equilibrium distribution. In order to transform the D2V37 in an athermal model, one only has to set the deviation temperature θ in the equilibrium distribution to a null value.

The next comparison is between second-order models for incompressible flows, namely, the standard D2Q9, the MRT-D2Q9 and the D2Q9-3rd with some terms of third order. The standar D2Q9 is the second order model; the MRT-D2Q9 is the model proposed by d'Humières (1992) and adapted to athermal flows by Lallemand and Luo (2000); the D2Q9-3rd is the standard model with second order plus third-order terms in the equilibrium distribution, i.e.,

$$f_i^{eq}(\rho,\vec{u}) = f_i^{eq,2}(\rho,\vec{u}) + \frac{27}{2}\left[u_x^{\,2}u_y c_{iy}\left(c_{ix}^{\,2}-\frac{1}{3}\right)+u_y^{\,2}u_x c_{ix}\left(c_{iy}^{\,2}-\frac{1}{3}\right)\right], \qquad (7.12)$$

The D2Q9-3rd is not a complete third-order model: third order models of the type $c_{i\alpha}^3 = c_{i\alpha}$ could not be added to the equilibrium distribution because of the linear dependence in this lattice.

The results can be seen in the Fig. 5.3.

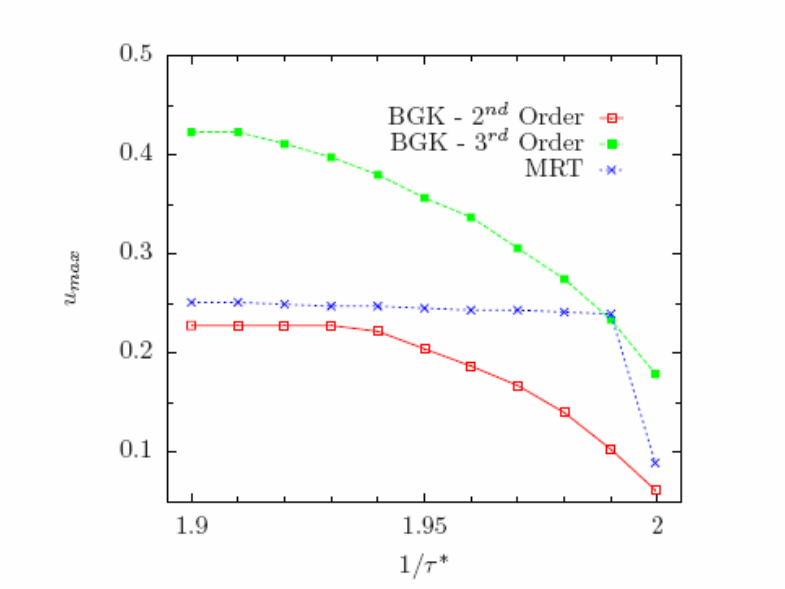

Fig. 5.3. Comparison of various athermal models for the maximum stable velocity

It has to be noticed that now results of the maximum velocity are plotted against the inverse of the relaxation time. The D2Q9-3rd is more stable all over the studied range, and the MRT model is more stable than the standard D2Q9 model.

One possible explanation for this behavior is that only one parameter controls the flow of incompressible fluids, the Reynolds number, and one single parameter is all that one needs to match this parameter: the relaxation time. If one chooses carefully the moments to be retrieved, then one gains in stability without any relations between others relaxation parameters. The D2Q9-3rd, being a more physical model, represents better the reality, and in the real world there is no negative distributions (particles), which is one of the main trigger of instabilities.

For thermal models, four models were compared: Chen et al. (1994), D2V25(w_1), D2V25(w_6) and the D2V37, and models. The results for temperature with zero velocity are shown in Fig. 5.4 and 5.5.

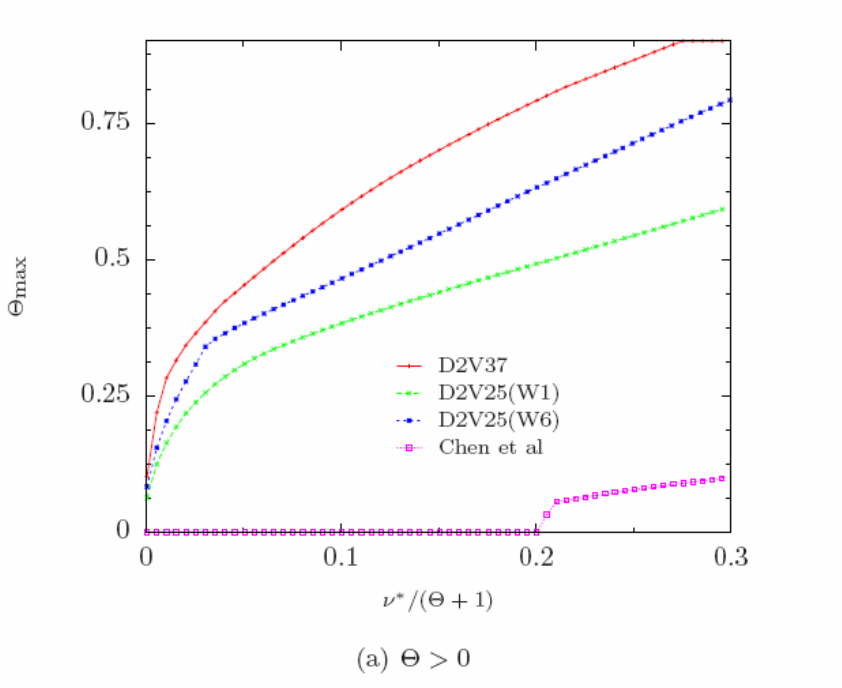

Fig.5.4. Comparison of maximum stable positive deviation temperature for thermal models $(u = 0)$

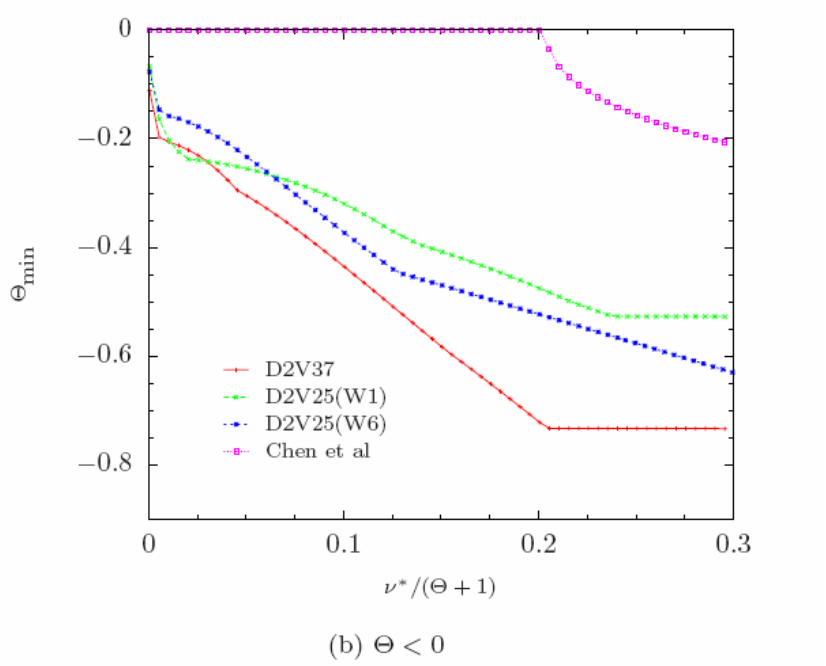

Fig.5.5. Comparison of minimum stable negative deviation temperature for thermal models $(u = 0)$

It can be seen that the model of Chen et al (1994) has no stable window until viscosity reach the value of 0.2, while the other models start the window of stability from the very beginning as the relaxation time departs from 0.5 (and viscosity becomes bigger). It can also be inferred that D2V37 model is more stable than the incomplete fourth-order models, and the model D2V25(w_6) is more stable than the D2V25. (w_1).

For macroscopic velocity higher than zero, the stability window for temperature decreases, as it can be seen in Fig. 5.6 and 5.7, where the velocity used was 0.4. In this range of viscosity, the model of Chen et al. (1994) does not appear in the studied range.

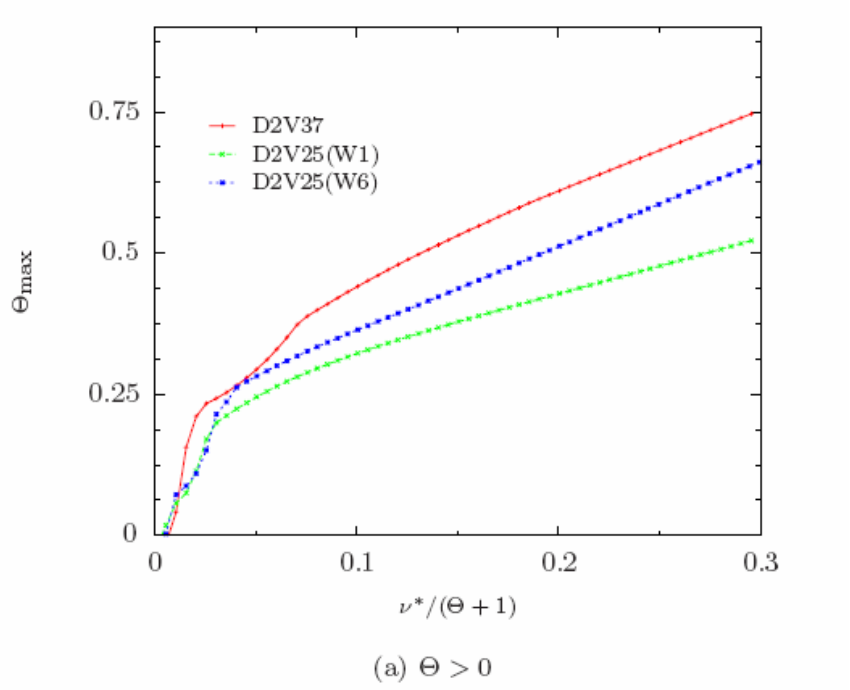

Fig.5.6. Comparison of maximum stable positive deviation temperature for thermal models $(u = 0.4)$

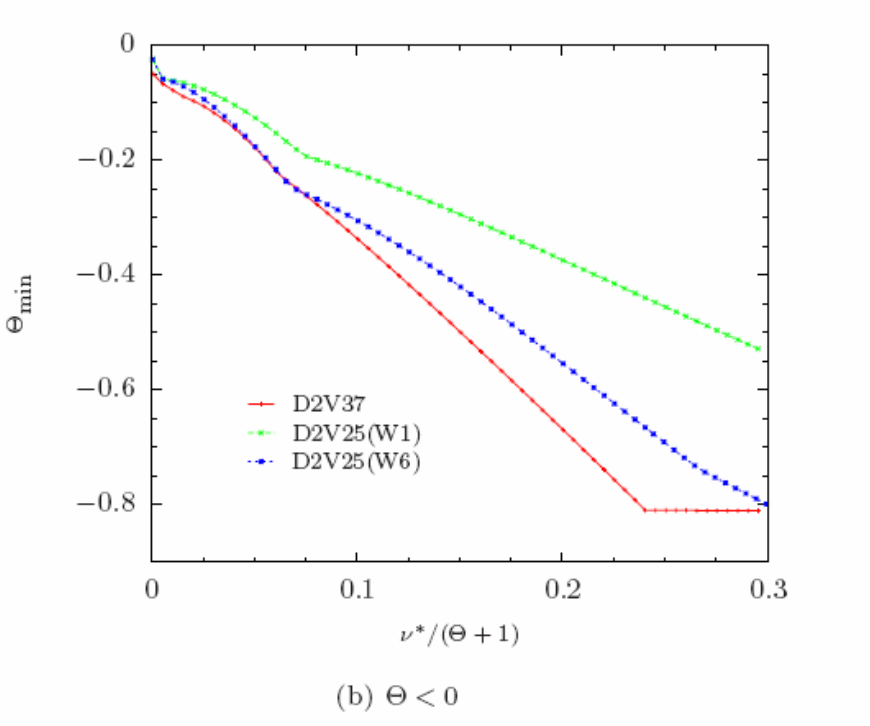

Fig.5.7. Comparison of minimum stable negative deviation temperature for thermal models $(u = 0.4)$

One of the reasons for the model of Chen et al. (1994) to be more unstable is the imposition of moments. The equilibrium distribution is written as an polynomial expansion, an the moments up to $c^2 c_\alpha c_\beta$ are matched adjusting the coefficients of the monomials. The only connection between this distribution and the maxwellian distribution are the moments, and no point-to-point connection is found.

In this way, the following experiment was done: it was used a 37-velocity lattice: fifth- and sixth-order moments were added to the equilibrium distribution funcion using the Gram-Schmidt procedure. This can be done, because these fifth- and sixth-order velocity vectors are linearly independent, so they can span this subspace. In Fig. 5.8 the result is presented.

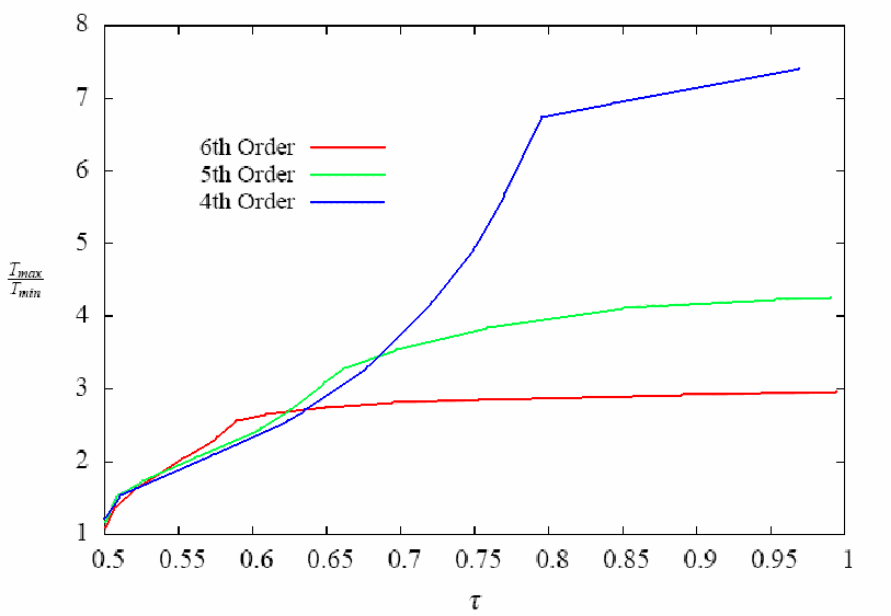

Fig.5.8. Comparison of maximum stable temperature ratio for some models.

As it can be seen, if we add more and more moments, by the Gram-Schmidt procedure, the stability decreases. This happens because the vectors are artificially added, using the Gram-Schimdt procedure in the discrete space, not respecting the norm preservation in the continuous space and this is exactly what is done when using MRT models. Instead, one has to, first, find the suitable lattice, and then use the proper equilibrium distribution function.

6. CONCLUSIONS

In this work it was developed a formal procedure to derive the lattice-Boltzmann equation from its continuous counterpart, the Boltzmann equation. The method is based on the expansion of the Maxwell-Boltzmann distribution, giving a set of relations that the chosen lattice has to meet. The choice of the variables for the equilibrium is very important, leading to a set of velocities independent of temperature, suitable to simulate thermohydrodynamical flows. Through the Chapman-Enskog expansion, it was shown that the lattices can handle the Navier-Stokes-Fourier equations.

Several lattices in one, two and three dimensions were derived, even for hexagonal structures. Rectangular lattices can also be derived, according to the method proposed above.

A stability analysis was performed in order to show the better perfomance of the present method in contrast to former methods.

The simplicity of the collision-propagation scheme, together with the agreement between the macroscopic equations and the equations obtained for the lattice-Boltzmann method make this method a promising tool for complex phenomena, such as thermal immiscible fluids, rheological fluids and phase transitions.

Still, many aspects have to improved in the lattice-Boltzmann framework:

- boundary conditions for multi-speed lattices;
- a theory to find minimal lattices;
- stability analysis and comparisons between models with tunable Prandtl number.

REFERENCES

Abe, T. **Derivation of the lattice Boltzmann method by means of the discrete ordinate method for the Boltzmann equation**. *J. Comput. Phys*. **131**, 241, 1997.

Alexander, F. J.; Chen, S.; Sterling, J. D. **Lattice Boltzmann thermohydrodynam**ics. *Physical Review E* **47**, R2249, 1993.

Appert, C. & Zaleski, S**. Lattice gas with a liquid-gas transition**. *Phys. Rev. Lett*. **64**, 1-4, 1990.

Bhatnagar, P. L.; Gross, E. P.; Krook, M. **A model for collision processes in gases. I: small amplitude processes in charged and neutral one-component system**. *Phys. Rev.* **94** (3), 511, 1954.

Cercignani, C. **Mathematical methods in kinetic theory**. 2nd. ed. New York: *Plenum Press*, 1990.

Chapman, S.; Cowling, T. G. **The mathematical theory of non-uniform gases**.3rd. ed. *Cambridge University Press*, 1970.

Chen H.; Chen, S.; Matthaeus, W. H. **Recovery of the Navier-Stokes equations using a lattice-gas Boltzmann method**. *Physical Review A* **45** (8), R5339-5342, 1992.

Chen H.; Shan, X. **Fundamental conditions for *N*-th order accurate lattice Boltzmann models**. *Physica D* **237**, pages 2003-2008, 2008.

Chen, S.; Doolen, G. D.; Eggert, K. G.; Grunau, D.; Loh, E. **Local lattice-gas model for immiscible fluids**. *Phys. Rev. A,* **43**, 7053-7056, 1991.

Chen, S.; Doolen, G. D. **Lattice Boltzmann method for fluid flows**. *Annu. Rev. Fluid Mech*. **30**, 329-364, 1998.

Chen, Y.; Ohashi, H.; Akiyama, M. **Thermal lattice Bhatnagar-Gross-Krook model without nonlinear deviations in macrodynamic equations**. *Physical Review E **50***, 2776, 1994.

Colosqui, C. E. **High-order hydrodynamics via lattice Boltzmann methods**. *Physical Review E **81***, 026702, 2010.

Cornubert, R.; d'Humières, D.; Levermore, D. A **Knudsen layer theory for lattice gases**. *Physica D **47***, 241-259, 1991.

d'Humières, D.; Lallemand P.; Frisch, U. **Lattice gas models for 3D hydrodynamics**. *Europhys. Lett*. **2**, 291-297, 1986.

d'Humières, D. & Lallemand P. **Numerical Simulations of Hidrodynamics With Lattice Gas Automata in Two Dimensions**. *Complex Sistems* **1**, 599-632, 1987.

d'Humières, D. **Generalized lattice Boltzmann equations**. *Prog. Aeronaut. Astronaut*. **159**, p. 450, 1992.

Facin, P. C.; Santos, L. O. E.; Philippi, P. C. **A non-linear lattice-Boltzmann model for ideal miscible fluids.** *Future Generatioin Computer Systems **20*** (6), 945-949, 2004.

Ferréol, B. & Rothman, D. **Lattice-Boltzmann simulations of flow through Fontainebleau sandstone**. *Transport in Porous Media **20*** (1-2), 3-20, 1994.

Giraud, L.; d'Humières, D.; Lallemand, P. **A lattice boltzmann model for viscoelasticity**. *Int. J. of Mod. Phys. C. **8***, 816, 1997.

Giraud, L.; d'Humières, D.; Lallemand, P. **A lattice boltzmann model for Jeffreys viscoelastic fluid**. *Europhysics Letters **42***, 625, 1998.

Grad, H. **Note on n-dimensional Hermite polynomials**. *Commun. Pure Appl. Maths* **2**, 325, 1949.

Grosfils, P.; Boon, J. P.; Lallemand, P. **Spontaneous fluctuation correlations in thermal lattice-gas automata**. *Phys. Rev. Lett. **68** (7)*, 1077-1080, 1992.

Grad, H. **On the kinetic theory of rarefied gases**. *Commun. Pure Appl. Maths* **2**, 331, 1949.

Gross, E. P.; Jackson, E. A. Kinetic **models and the linearized Boltzmann equation**. *Physics of Fluids* **2**, 432, 1959.

He X.; Luo, L. S. **A priori derivation of the lattice Boltzmann equation**. *Physical Review E* **55**, 6333-36, 1997.

He, X. & Luo, L.-S.. **Theory of the lattice Boltzmann equation: from the Boltzmann equation to the lattice Boltzmann equation**. *Physical Review E **56***, 6811-6817, 1997a.

He, X. & Luo, L.-S.. **Boltzmann equation Model for the Incompressible Navier-Stokes Equation**. *J. of Stat. Phys. **88*** (3/4), 927, 1997b.

He, X.; Chen, S.; Doolen, G. D. **A novel thermal model for the lattice Boltzmann method in incompressible limit**. *Journal of Computational Physics* **146**, 282, 1998.

Higuera, F.; Jimenez, J. **Boltzmann approach to lattice gas simulations**. *Europhysics Letters* **9**, 663, 1989.

Lallemand, P.; Luo, L.-S. **Theory of the lattice Boltzmann method: Dispersion, dissipation, isotropy, galilean invariance, and stability**. *Physical Review E* **61**, 6546, 2000.

Lallemand, P.; Luo, L.-S. **Theory of the lattice Boltzmann method: Acoustic and thermal properties in two and three dimensions**. *Physical Review E* **68**, 36706, 2003.

Latt J.; Chopard, B. **Lattice Boltzmann method with regularized pre-collision distribution functions**. *Mathematics and Computers in Simulation* **72**, 165-168, 2006.

Mayer, Eduardo. *Private communication*, 2008.

Pico, C. E. **Aplicação das Formas Discretas da Equação de Boltzmann à Termo-hidrodinâmica de Misturas.** *Ph.D. Thesis.* Federal University of Santa Catarina, Florianópolis, 2007.

Philippi, P. C.; Hegele, L. A. Jr.; Santos, L. O. E.; Surmas, R. **From the continuous to the lattice Boltzmann equation: The discretization problem and thermal models**. *Physical Review E* **73**, 056702, 2006.

Philippi, P. C.; Hegele, L. A. Jr.; Surmas, R.; Siebert, D. N.; Santos, L. O. E. **From the Boltzmann to the lattice-Boltzmann equation: beyond BGK collision models**. *International Journal of Modern Physics C* **18**, p. 556, 2007.

Qian, Y. H., d'Humieres, D. & Lallemand, P. **Lattice BGK models for Navier–Stokes equation**. *Europhys. Lett*. **17**, 479–484, 1992.

Qian, Y. H. & Orszag, S. **A. Lattice BGK models for the Navier–stokes equation: nonlinear deviation in compressible regimes**. *Europhys. Lett*. **21**, 255–259, 1993.

Rothman, D. H. & Keller, J. M. **Immiscible cellular-automaton fluids.** *Journal of Stat. Phys*. **52** (3-4), 1119-1127, 1988.

Santos, L. O. E.; Philippi, P. C.; Damiani, M. C. **A boolean lattice gas method por predicting intrinsic permeability of porous media**. *Produccion 2000 – Aplicaciones de la ciencia en la ingeniería de petróleo* – Foz do Iguaçu, 2000.

Santos, L. O. E.; Facin, P. C; Philippi, P. C. **Lattice-Boltzmann model based on field mediators for immiscible fluids**. *Phys. Rev. E* **68** (5), 56302, 2003.

Sbragaglia, M.; Benzi, R.; Biferale, L.; Chen, H.; Shan, X.; Succi, S. **Lattice Boltzmann method with self-consistent thermo-hydrodynamic equilibria**. J. Fluid Mech. **628**, 299-309, 2009.

Scagliarini, A.; Biferale, L.; Sbragaglia, M.; Sugiyama K.; Toschi, F. **Lattice Boltzmann Methods for thermal flows: continuum limit and applications to compressible Rayleigh-Taylor systems**. Submitted to *Physics of Fluids*, 2010.

Servan-Camas, B.; Tsai, F. T.-C. **Non-negativity and stability analysis of lattice Boltzmann method for advectoin-diffusion equation**. *J. Comput. Phys.* **228**, 236-256, 2009.

Shan, X.; Chen, H. **Lattice Boltzmann model for simulating flows with multiple phases and components**. *Phys. Rev. E* **47**, 1815–1819, 1993.

Shan, X.; Chen, H. **Simulation of non-ideal gases and liquid–gas phase transitions by lattice Boltzmann equation**. *Phys. Rev. E* **49**, 2941–2948, 1994.

Shan, X.; Doolen, G. D. **Multi-component lattice Boltzmann model with interparticle interaction**. *J. Stat. Phys*. **81**, 379, 1995.

Shan, X.; He, X. **Discretization of the velocity space in solution of the Boltzmann equation**. *Physical Review Letters* **80**, 65, 1998.

Shan, X.; Yuan, X.-F.; Chen, H. **Kinetic theory representation of hydrodynamics: way beyond the Navier-Stokes equation**. *Journal of Fluid Mechanics* **550**, 413, 2006.

Shan, X.; Chen, H. **A General Multiple-Relaxation-Time Boltzmann Collision Model**. *International Journal of Modern Physics C* **18**, 635, 2007.

Siebert, D. **Análise de Formas Discretas da Equação de Boltzmann para problemas térmicos bi-dimensionais**. *Master Dissertation*. Federal University of Santa Catarina, Florianópolis, 2007.

Siebert, D. N.; Hegele, L. A. Jr.; Surmas, R.; Santos, L. O. E.; Philippi, P. C. **Thermal Lattice Boltzmann in two dimensions**. *International Journal of Modern Physics C* **18**, 546, 2007.

Siebert, D. N.; Hegele, L. A. Jr.; Philippi, P. C. **Lattice Boltzmann equation linear stability analysis: Thermal and athermal models**. *Phys. Rev. E* **77**, 26707, 2008.

Sterling, J. D.; Chen, S. **Stability analysis of lattice Boltzmann methods**. *Journal of Computational Physics* **123**, 196-206, 1996.

Succi, S. **The Lattice Boltzmann Equation for Fluid Dynamics and Beyond**. *Oxford University Press*, 2001.

Surmas, R; Pico Ortiz, C. E.; Philippi, P. C. **Simulating thermohydrodynamics by finite difference solutions of the Boltzmann equation**. *Eur. Phys. J. Special Topics* **171**, 81-90, 2009.

Wolfram, S. **Statistical Mechanics of Cellular Automata**. *Reviews of Modern Physics*, **55**, 601-644, 1983.

Wolfram, S. **Cellular Automaton Fluids: Basic Theory**. *J. Stat. Phys* **45**, 471-526, 1986.

Zhang, R.; Shan, X.; Chen, H. **Efficient kinetic method for fluid simulation beyond the Navier-Stokes equation**. *Phys. Rev. E* **74**, 46703, 2006.

Ziegler, D. **Boundary conditions for lattice Boltzmann simulations.** *J. of Stat. Phys.* **71**, 1171-1177, 1993.

APPENDIX A

D2V25 lattice

a)

Velocity	Number of symmetries	Weights
(0,0)	1	0.23905788376748833308837791962 5
$(\pm 1,0)$	4	0.06315899542818160465262511001 19
$(\pm 1,\pm 1)$	4	0.08759457803326792575018724844 46
$(\pm 2,0)$	4	0.03117903098262379095835779619 83
$(\pm 2,\pm 2)$	4	0.00619897383917891598489276594049
$(\pm 3,0)$	4	0.00202012715244465060402382461054
$(\pm 4,0)$	4	0.00008382362243102877781877488801 37
$(\pm 3, \pm 3)$	4	0
a = 1.07560665170067929322785588396		

b)

Velocity	Number of symmetries	Weights
(0,0)	1	0.23518208293564577771920390459 61
$(\pm 1,0)$	4	0
$(\pm 1,\pm 1)$	4	0.10181538342842406716150137382 4
$(\pm 2,0)$	4	0.05921135093563887927827937759 68
$(\pm 2,\pm 2)$	4	0.02004090686644007337442578892 19
$(\pm 3,0)$	4	0.00679520191907580489001573647778
$(\pm 4,0)$	4	0.00219789086982698541955574289210
$(\pm 3, \pm 3)$	4	0.00114374524668274557821221879732
a = 0.83465946021121877831287314483		

D2V45 – Fifth order lattice

This lattice consists of the D2V33 plus the set of vectors $(\pm 4, \pm 4)$, $(\pm 7,0)$ and $(\pm 5, \pm 5)$.

Velocity	Number of symmetries	Weights
(0,0)	1	0.18119501133786848 0725623582766
$(\pm 1,0)$	4	0.00726851851851851851851851852
$(\pm 1, \pm 1)$	4	0.07037037037037037037037037704
$(\pm 2,0)$	4	0.06910030864197530864197530864 20
$(\pm 2, \pm 2)$	4	0.03637566137566137566137566137 57
$(\pm 3,0)$	4	0.01184920634920634920634920634 92
$(\pm 4,0)$	4	0.00446939634439634439634439634440
$(\pm 4, \pm 2)$	8	0.00260416666666666666666666666667
$(\pm 4, \pm 4)$	4	0.00003858024691358024691358024691 36
$(\pm 7,0)$	4	0.00001381731143635905540667445429 35
$(\pm 5, \pm 5)$	4	$7.05467372134038800705467372134 \times 10^{-6}$
$a = \sqrt{2}/2 \cong 0.70710678118654752440084 43$		

D2V77 – Sixth order lattice

Velocity	Number of symmetries	Weights
(0,0)	1	0.15608215343297337331455757683 8
$(\pm 1,0)$	4	0.06146881161589259113459730938 08
$(\pm 1, \pm 1)$	4	0.07497878820202265454142786847 49
$(\pm 2,0)$	4	0.03619792118308647970196250996 35
$(\pm 2, \pm 1)$	8	0.00953602746645247598483838978842
$(\pm 2, \pm 2)$	4	0.00875452639972547506763014310355
$(\pm 3,0)$	4	0.00127217957264136126353038464033
$(\pm 3, \pm 1)$	8	0.00416543006520595675854527269611
$(\pm 4,0)$	4	0.00038554079141081256352732108690 6
$(\pm 4, \pm 1)$	8	0.00003598687685409269098904006857 99
$(\pm 3, \pm 3)$	4	0.00025100968680260940843661710481 9

$(\pm 4, \pm 2)$	8	0.000088778534403651156178042999405 0
$(\pm 5,0)$	4	0.000011349006932882304752413304292 2
$(\pm 5, \pm 2)$	8	$3.319242292155148413716084329 87\times10^{-6}$
$(\pm 6,0)$	4	$2.508128251272075671154578084 67\times10^{-7}$
a = 0.889235292630626530906214274 40		

Fourth order lattice for 3D: D3V107.

Velocity	Symmetries	Weight
(0,0,0)	1	0.075751686096501665271207444317 2
$(\pm 1,0,0)$	6	0.060091280274744707546176537246 9
$(\pm 1, \pm 1,0)$	12	0.003136069066995353128881884716 92
$(\pm 1, \pm 1, \pm 1)$	8	0.036339281207801164731398488197 4
$(\pm 2,0,0)$	6	0.013216933273149235798434015444 2
$(\pm 2, \pm 1,0)$	24	0.004484928511729500107367730651 09
$(\pm 2, \pm 2,0)$	12	0.002487557758083419533391318262 18
$(\pm 3, \pm 1, \pm 1)$	24	0.000607432754970149173093348083 234
$(\pm 2, \pm 2, \pm 2)$	8	0.000464179164402822382615444825 756
$(\pm 4, 0,0)$	6	0.000045192889460987178445574996 3581
a = 1.071820715428848253688563815 58		

In a very recent paper, Shan (2010) showed the existence of a fourth-order lattice with 103 velocites in 3D.

Velocity	Symmetries	Weight
(0,0,0)	1	0.032633351764471159465883667 8817
$(\pm 1,0,0)$	6	0.097656833590334574221368191 0704
$(\pm 1, \pm 1, \pm 1)$	8	0.028097750290257335627002959 7430
$(\pm 2,0,0)$	6	0.001045259560430061466022173 65328
$(\pm 2, \pm 1,0)$	24	0.005705329016894815990853804 06608
$(\pm 2, \pm 2,0)$	12	0.000611939269829747839892853 476436

$(\pm 3, 0,0)$	6	0.00028444325180005520747950579925 5
$(\pm 3, \pm 1, \pm 1)$	24	0.00013069837598519158500894069697 6
$(\pm 2, \pm 2, \pm 2)$	8	0.00015596415937428372299373971461 5
$(\pm 3, \pm 3, \pm 3)$	8	$1.22319450132305818792466112461 \times 10^{-6}$
a = 1.19697977039307435897238846385		

APPENDIX B

The following paper was presented in the 18th International Congress of Mechanical Engineering, held in Ouro Preto, in 2005.

MULTIPLE-RELAXATION-TIME LATTICE-BOLTZMANN MODEL FOR IMMISCIBLE FLUIDS

Luiz Adolfo Hegele Jr.
hegele@lmpt.ufsc.br

Paulo Cesar Philippi
philippi@lmpt.ufsc.br

Luís Orlando Emerich dos Santos
emerich@lmpt.ufsc.br

Universidade Federal de Santa Catarina – UFSC
Laboratório de Meios Porosos e Propriedades Termofísicas – LMPT
Departamento de Engenharia Mecânica – EMC
Campus Universitário – Bairro Trindade – Florianópolis – SC – CEP 88040-900

Abstract. *Classical (macroscopic) modelling of immiscible fluid flow at steady state is treated performing a momentum balance around the transition layer, plus mass and momentum equations and coupling conditions just right at interface. We propose a lattice-Boltzmann based model where the fluid/fluid interface appears from mesoscopic interaction between the fluids themselves through a long-range strength field which intensity is transferred using pseudo-particles called field mediators. These null-mass particles transfer information of the concentration of each fluid to the neighborhood at each time step, allowing the use of this information to create interfacial tension. This lattice Boltzmann model has Galilean invariance and a larger range of viscosities than other models in the lattice Boltzmann framework . Moreover, we use in this model a procedure based on Moment's Method, with a splitted collision operator for mutual and cross collisions, which increases the number of free-paramenters from three to thirteen in two dimensions, which possibly will improve the numerical stability of the model. Quantitative and qualitative numerical simulations are carried out to demonstrate the efficiency of the model.*

Keywords*: immiscible fluids, lattice-Boltzmann methods, moment's method.*

1. Introduction

The Lattice Boltzmann Method (LBM) has been used, in the last decade, in the simulation of the Navier-Stokes equations in the low Mach number limit. Since the pioneer work of Frisch et al. (1986), at that time using lattice gas methods, these models had attracted much attention and were applied in a great variety of problems, including complex flow, such as the modeling of viscoelastic and biologic fluids.

Such kinds of systems describe the dynamics of particles in a regular lattice through a particle distribution function. Each evolution time step δ_t is divided in two main ones: streaming and collision. In the streaming process, at a site $\vec{x}$ and time *t*, the number of particles at direction *i*, $K_i(\vec{x},t)$, hop to the site $\vec{x}+\vec{c}_i\delta_t$, according to the velocity set $\vec{c}_i$, $i=0,1,\ldots,b$. During the collision process, the particles at the same site are stirred towards a prescribed equilibrium distribution function, in a way that quantities such as mass, momentum, chemical species and energy are preserved.

In this work is presented an athermal, bidimensional model for immiscible fluids, in which the collision process is performed in the moment space (d'Humières, 1992), instead in velocity space. Furthermore, we also use the idea of field mediators, proposed by Santos & Philippi (2002), and introduced in the lattice Boltzmann framework by the same authors (Santos et al., 2003).

Gustensen et al. (1991, 1992) are attributed to be the first who introduced immiscible fluids color based models in the frame of the LBM. A more popular two-phase flow model, based on a pseudopotential function, was derived by Shan and Chen (1993). The first tentative to a two-phase thermodynamically consistent model was performed by Swift et al. (1995), but the model that they proposed cannot lead to correct energy transport and it is not Galilean invariant. A detailed comparison between all these models has yet to be done.

This paper is divided as follows. In the next section, the model is explained. Section 3 is used to provide a collection of equilibrium moments in order to correctly retrieve the Navier-Stokes equations. In section 4, results from simulations are compared with theoretical predictions for the model. Section 5 concludes the paper.

2. Model

This LBM is defined in a 2D square lattice, unit length and nine directions for the velocity, called D2Q9. Assuming $\delta_t = 1$, one can define the velocity set as $\vec{c}_0$=(0,0), $\vec{c}_1$=(1,0), $\vec{c}_2$=(0,1), $\vec{c}_3$=(-1,0), $\vec{c}_4$=(0,-1), $\vec{c}_5$=(1,1), $\vec{c}_6$=(-1,1), $\vec{c}_7$=(-1,-1), $\vec{c}_8$=(1,-1), where $\vec{c}_\alpha = (c_{\alpha,x}, c_{\alpha,y})$.

Considering two immiscible fluids *r* and *b*, the long range attraction between the particles is represented through the use of the concept of field mediators at each lattice site. Defining $R_i(\vec{x},t)$ as the *r*-particle distribution function, and in a similar manner $B_i(\vec{x},t)$ for *b*-particles, field mediators for the *k*-phase are created in the following manner

$$M_i^k(\vec{x},t) = \frac{\sum_i K_i}{\sum_i R_i + B_i}, \tag{1}$$

and they are streamed as

$$M_i^k(\vec{x}+\vec{c}_i, t+1) = M_i^k(\vec{x},t). \tag{2}$$

The interference of field mediators in the particle distribution function is described in the following. The evolution of the system of particles is described by the lattice-Boltzmann equation,

$$K_i^{'}(\vec{x},t) - K_i(\vec{x},t) = \sum_j \left[\Lambda_{ij}^k (R_0,\ldots,R_b,B_0,\ldots,B_b)\right], \tag{3}$$

$$K_i(\vec{x}+\vec{c}_i, t+1) = K_i^{'}(\vec{x},t), \tag{4}$$

$K = R, B$, and Λ^k is the collision operator.

The splitted collision operator is proposed in the following manner

$$\sum_j \left[\Lambda_{ij}^k (R_0,\ldots,R_b,B_0,\ldots,B_b)\right] = \sum_j \left[\omega^k \Lambda_{ij}^{kk}(K_0,\ldots,K_b) + \omega^{\bar{k}} \Lambda_{ij}^{rb}(R_0,\ldots,R_b,B_0,\ldots,B_b)\right], \tag{5}$$

where $\omega^k = \rho^k/(\rho^k + \rho^{\bar{k}})$ is the *k*-phase concentration and $\omega^{\bar{k}}$ is the $\bar{k} = b, r$-phase concentration. The first term of the right-hand side of Eq. (5) refers to collisions between particles of same species (e. g., *r*-*r* collisions), while the second term of the r.h.s. refers to cross collisions. This last term is responsible for the phase segregation.

Considering K_i distributions near the equilibrium K_i^{eq}, the collision operator can be linearized, $\Omega : \Re^{b+1} \to \Re^{b+1}$, in the following way

$$\sum_j \left[\omega^k \Lambda_{ij}^{kk}(K_0,\ldots,K_b) + \omega^{\bar{k}} \Lambda_{ij}^{k\bar{k}}(K_0,\ldots,K_b,\bar{K}_0,\ldots,\bar{K}_b)\right] = \sum_j \left[\omega^k \Lambda_{ij}^{kk} K_j^{(neq),kk} + \omega^{\bar{k}} \Lambda_{ij}^{k\bar{k}} K_j^{(neq),k\bar{k}}\right], \tag{6}$$

where $K_j^{(neq),pq} = K_j - K_j^{(eq)}(\rho^p, \vec{u}^q)$, $\bar{k}$ is the other phase of the $k - \bar{k}$ system, and Λ^{pq} is the linearized collision operator.

In this way, the full lattice-Boltzmann equation for this model is

$$K_i(\vec{x}+\vec{c}_i, t+1) = K_i(\vec{x},t) + \sum_j \left[\omega^k \Lambda_{ij}^{kk} K_j^{(neq),kk} + \omega^{\bar{k}} \Lambda_{ij}^{k\bar{k}} K_j^{(neq),k\bar{k}}\right]. \tag{7}$$

The collision process has to preserve the individual mass of species,

$$\sum_i K_i = \sum_i K_i^{(eq)} = \rho^k, \tag{8}$$

and has also to preserve *total* momentum,

$$\sum_i \left(R_i + B_i\right)\vec{c}_i = \sum_i \left(R_i^{(eq)} + B_i^{(eq)}\right)\vec{c}_i = \rho^r \vec{u}^r + \rho^b \vec{u}^b = \rho\vec{u} \cdot \tag{9}$$

The collision operator is defined in such a way that the eigenvalues associated to the eigenvectors of the conserved quantities are set to be zero, and that its eigenvectors form an orthogonal basis for $\Re^{b+1}$. This basis is obtained through a Gram-Schmidt orthogonalization process of the polynomials of $\vec{c}_i$, leading to the D2Q9 result

$$\Psi_{0,i} = \left\|\vec{c}_i\right\|^0, \vec{\Psi}_0 = \left(1,1,1,1,1,1,1,1,1\right), \tag{10}$$

$$\Psi_{1,i} = c_{i,x}, \vec{\Psi}_1 = \left(0,1,0,1,-1,1,-1,-1,1\right), \tag{11}$$

$$\Psi_{2,i} = c_{i,y}, \vec{\Psi}_2 = \left(0,0,1,0,-1,1,1,-1,-1\right), \tag{12}$$

$$\Psi_{3,i} = 3\left\|\vec{c}_i^2\right\| - 4\left\|\vec{c}_i\right\|^0, \vec{\Psi}_3 = \left(-4,-1,-1,-1,-1,2,2,2,2\right), \tag{13}$$

$$\Psi_{4,i} = c_{i,x}^2 - c_{i,y}^2, \vec{\Psi}_4 = \left(0,1,-1,1,-1,0,0,0,0\right), \tag{14}$$

$$\Psi_{5,i} = c_{i,x}c_{i,y}, \vec{\Psi}_5 = \left(0,0,0,0,0,1,-1,-1,1\right), \tag{15}$$

$$\Psi_{6,i} = c_{i,x}\left(3\left\|\vec{c}_i\right\|^2 - 5\left\|\vec{c}_i\right\|^0\right), \vec{\Psi}_6 = \left(0,-2,0,2,0,1,-1,-1,1\right), \tag{16}$$

$$\Psi_{7,i} = c_{i,y}\left(3\left\|\vec{c}_i\right\|^2 - 5\left\|\vec{c}_i\right\|^0\right), \vec{\Psi}_7 = \left(0,0,-2,0,2,1,1,-1,-1\right), \tag{17}$$

$$\Psi_{8,i} = \left(9\left\|\vec{c}_i\right\|^4 - 21\left\|\vec{c}_i\right\|^2 + 8\left\|\vec{c}_i\right\|^0\right)/2, \vec{\Psi}_8 = \left(4,-2,-2,-2,-2,1,1,1,1\right) \cdot \tag{18}$$

Due to the orthogonality of the basis, an expansion of K_i reads

$$K_i = \frac{a_0^k \Psi_{0,i}}{\Psi_0^{\,2}} + \frac{a_1^k \Psi_{1,i}}{\Psi_1^{\,2}} + \ldots + \frac{a_b^k \Psi_{b,i}}{\Psi_b^{\,2}} = \sum_{\theta=0}^{b} \frac{a_\theta^k \Psi_{\theta,i}}{\Psi_\theta^{\,2}} \cdot \tag{19}$$

Applying this formulation to the evolution equation, Eq. (7), it turns out to be an evolution equation for the moments of the equilibrium distribution function. Hence,

$$a_\theta^{k'} - a_\theta^k = \omega_k \lambda_\theta^{kk} a_\theta^{(neq),kk} + \omega_{\bar{k}} \lambda_\theta^{k\bar{k}} a_\theta^{(neq),k\bar{k}}, \tag{20}$$

where λ_θ^{pq} is the eigenvalue from Λ^{pq} associated to Ψ_θ; $a_\theta^{(neq),kk} = a_\theta^{(neq),kk}\left(\rho^k, \vec{u}^k\right)$ and $a_\theta^{(neq),k\bar{k}} = a_\theta^{(neq),k\bar{k}}\left(\rho^k, \vec{\vartheta}^{\bar{k}}\right)$. The first term of the r.h.s. of Eq. (20) is related to the relaxation of the moment a_θ^k towards a prescribed equilibrium, given density and velocity of the component k. The second term considers $r-b$ (i.e. $k-\bar{k}$) collisions, and is related to the relaxation of the moment a_θ^k towards a prescribed equilibrium dependent of density ρ^k and velocity

$$\vec{\vartheta}^{\bar{k}} = \vec{u}^{\bar{k}} \mp A\hat{u}^m, \tag{21}$$

$\bar{k} = r, b$, where A is a free parameter of the model and is related to the interfacial tension. If $A = 0$ the model reduces to a miscible model (Facin et al., 2003). Otherwise, the model mimics two immiscible fluids, where k-particles are taken away from $\bar{k}$-particles by a long-range field. In Eq. (21),

$$\hat{u}^m = \begin{cases} \dfrac{\vec{u}^m}{\left|u^m\right|}, & \text{se } u_m \neq 0\,, \\ 0, & \text{se } u_m = 0\,, \end{cases} \tag{22}$$

where the mediators velocity is given by

$$\vec{u}_m = \sum_i \left(M_i^r - M_i^b\right)\vec{c}_i\,. \tag{23}$$

In this way, the collision process is performed in moment space, and in order to execute the streaming step, one has to find again the new *r* and *b* particle distributions. To do that, one applies Eq. (19).

It is interesting to see that the proposed model reduces to the model of Santos et al. (2003) if $\lambda_3^{kk} = \lambda_4^{kk} = \ldots = \lambda_8^{kk}$, $\lambda_3^{\bar{k}\bar{k}} = \lambda_4^{\bar{k}\bar{k}} = \ldots = \lambda_8^{\bar{k}\bar{k}}$ and $\lambda_3^{k\bar{k}} = \lambda_4^{k\bar{k}} = \ldots = \lambda_8^{k\bar{k}}$, where $\lambda_\theta^{kk} = 1/\tau^k$, $\lambda_\theta^{\bar{k}\bar{k}} = 1/\tau^{\bar{k}}$ and $\lambda_\theta^{k\bar{k}} = 1/\tau^m$.

3. Macroscopic Equations

In order to retrieve the Navier-Stokes equations for incompressible athermal fluids, the equilibrium moments must be chosen as

$$a_0^{(eq),pq} = \rho^p\,, \tag{24}$$

$$a_1^{(eq),pq} = \rho^p u_x^q\,, \tag{25}$$

$$a_2^{(eq),pq} = \rho^p u_y^q\,, \tag{26}$$

$$a_3^{(eq),pq} = -2\rho^p + 3\rho^p u^{q^2}\,, \tag{27}$$

$$a_4^{(eq),pq} = \rho^p (u_x^{q^2} - u_y^{q^2})\,, \tag{28}$$

$$a_5^{(eq),pq} = \rho^p u_x^q u_y^q\,, \tag{29}$$

$$a_6^{(eq),pq} = -\rho^p u_x^q \tag{30}$$

$$a_7^{(eq),pq} = -\rho^p u_y^q \tag{31}$$

$$a_8^{(eq),pq} = \rho^p - 3\rho^p u^{q^2} \tag{32}$$

The macroscopic equations of the LBM are retrieved applying the Chapman-Enskog expansion. Far from the interface for the pure *k*-phase these equations are the continuity equation and the Navier-Stokes equations,

$$\partial_t \rho^k + \partial_\alpha(\rho u_\alpha^k) = 0\,, \tag{33}$$

$$\partial_t \rho^k u_\alpha^k + \partial_\beta(\rho^k u_\alpha^k u_\beta^k) = -\partial_\alpha p^k + \nu^k \partial_\beta\left[\rho(\partial_\alpha u_\beta^k + \partial_\beta u_\alpha^k)\right] + \zeta^k \partial_\alpha(\rho^k \partial_\gamma u_\gamma^k)\,, \tag{34}$$

which first and second viscosity coefficients are related with the collision operator eigenvalues in the following manner:

$$\nu^k = \zeta^k = \frac{1}{3}\left(\frac{1}{\lambda_4^{kk}} - \frac{1}{2}\right) = \frac{1}{3}\left(\frac{1}{\lambda_5^{kk}} - \frac{1}{2}\right). \tag{35}$$

For isotropy reasons, one does $\lambda_4^{kk} = \lambda_5^{kk}$ e $\lambda_6^{kk} = \lambda_7^{kk}$. Far from the interface, pressure p_k is proportional to density, $p_k = {c_s}^2 \rho_k$, where ${c_s}^2 = 1/3$ is the square of the sound speed. In order to conserve momentum, $\lambda_1^{k\bar{k}} = \lambda_2^{k\bar{k}}$.

4. Results

4.1 Interfacial Tension

Santos et al. (2003) used the mechanical definition of interfacial tension in order to deduce an analytical expression, function of the parameters of the model, and in this work the same method will be used to measure interfacial tension. The final expression, after some algebra, reduces to

$$\sigma^{rb} = \frac{{c_s}^2 \rho_0 A}{2\left(2\tau^m - 1\right)} \left\{ \begin{array}{l} \dfrac{1}{\left(\tau^m - \tau^b\right)\left(\tau^m - \tau^r\right)} \left[\left({\tau^m}^2 - \tau^m(\tau^r + \tau^b) + \tau^r \tau^b \right) + 4\tau^m \left(\tau^m \tau^b - 2\tau^r \tau^b + \tau^m \tau^r \right) \right] + \\ 4{\tau^m}^2 \left[\dfrac{\tau^r}{\left(\tau^m - \tau^r\right)^2} \left(1 + \tau^m - \tau^r\right) \ln \dfrac{\tau^r}{\tau^m} + \dfrac{\tau^b}{\left(\tau^m - \tau^b\right)^2} \left(1 + \tau^m - \tau^b\right) \ln \dfrac{\tau^b}{\tau^m} \right] \end{array} \right\}. \tag{36}$$

In this simulation one uses the fact that the present model reduces to the model of Santos et al. (2003) to allow a comparison of the results.

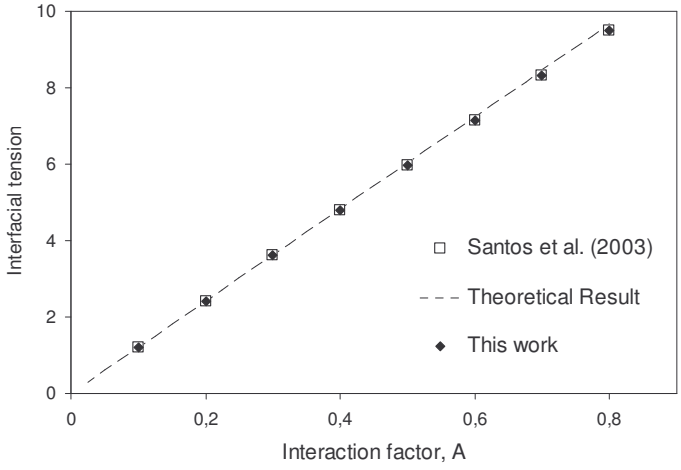

Figure 1 – Interaction factor versus interfacial tension

For this simulation, a unidimensional lattice with 2000 sites was used, where the two phases are initially segregated and periodic boundary conditions were used. The values for the parameters are the following $\tau^r = 1/\lambda_\theta^{rr} = 1.0$, $\tau^b = 1/\lambda_\theta^{bb} = 3.0$, $\theta = 3,\ldots,8$ e $\tau^m = 1/\lambda_\theta^{rb} = 1.0$, $\theta = 1,\ldots,8$. Results are shown in Fig. 1, and are in excellent agreement with theoretical prediction.

4.2 Laplace's Law

Immiscible fluid models must obey Laplace's Law, which predicts a linear dependence between pressure drop and droplet radius, at equilibrium, through interfacial tension σ^{rb}, in such a way that

$$\Delta p = \frac{\sigma^{rb}}{R}. \tag{37}$$

The initial condition for the simulation is a 2D *r*-phase droplet with radius *R*, placed in a 10*R* x 10*R* lattice domain, in order to avoid boundary influence in the simulation results.

Figure 2 shows the pressure difference against $1/R$ in seven runs. Initial density is $\rho_r = \rho_b = 1.0$, interaction factor *A=0.*4 and relaxation times $\lambda_3^{rr} = 0.65$, $\lambda_4^{rr} = 0.75$, $\lambda_6^{rr} = 0.7$, $\lambda_8^{rr} = 0.8$, $\lambda_3^{bb} = 0.75$, $\lambda_4^{bb} = 0.7$, $\lambda_6^{bb} = 0.65$, $\lambda_8^{bb} = 0.8$, $\lambda_1^{rb} = 1.0$, $\lambda_3^{rb} = 0.95$, $\lambda_4^{rb} = 0.9$, $\lambda_6^{rb} = 0.95$ e $\lambda_8^{rb} = 1.1$.

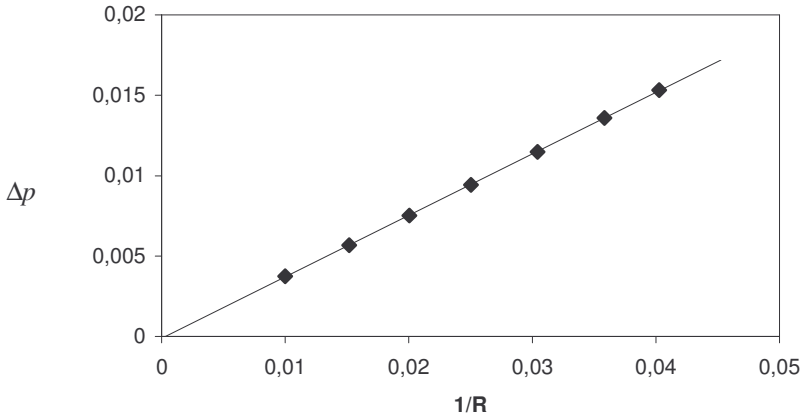

Figure 2 – Laplace's Law

In this way, the interfacial tension, which is precisely the slope of the curve, could be determined by a simple linear curve fitting. By this method, interfacial tension is 0.3827 net units, very near to the value given by the method in the former section, which gives 0.3744 n.u.

4.3 Capillary Waves

The dispersion of capillary waves is a problem commonly used to test LBM for immiscible fluids.The initial condition for this problem can be seen in Fig. 3, where a L×2L (y=2L) domain is filled with *r*-fluid if y<L and filled with *b*-fluid otherwise. A sinusoidal wave is imposed as initial condition to the interface. For this problem, an analytical formulation is described in Landau & Lifschitz (1987) which gives the relation

$$\omega^2 = \frac{\sigma^{rb} k^3}{2\rho}, \tag{38}$$

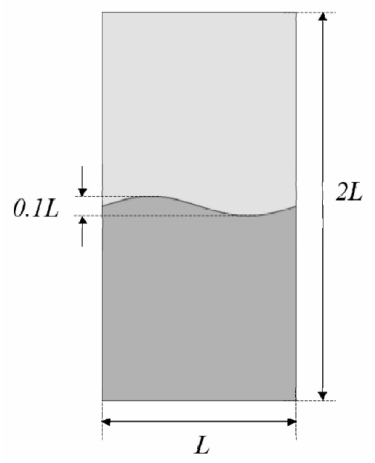

Figure 3 – Initial condition for the capillary waves problem

where k is the wave number and ω is related to the damping. The following parameters were used in the simulation: $\tau^r = \tau^b = 0.52$, $\tau^m = 1.0$, interaction factor $A = 0.4$ and $\rho = 1.0$. The results are shown in Fig. 4, and agree well with the theoretical prediction.

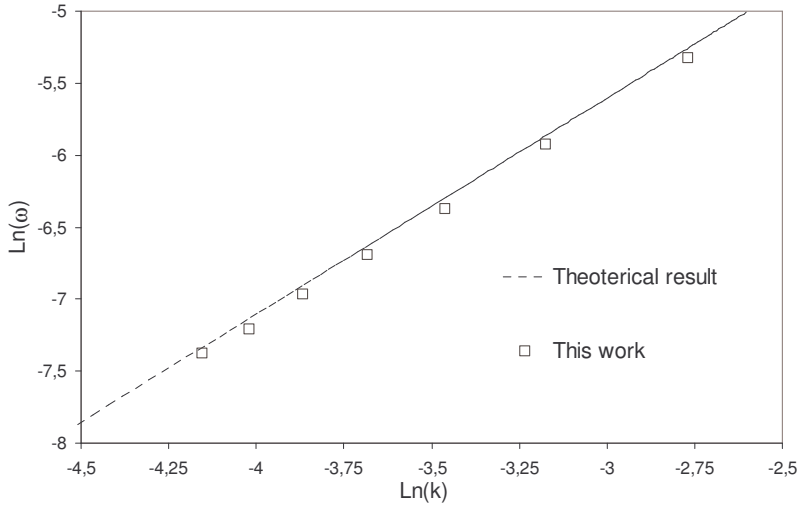

Figure 4 – Comparison between theoretical and simulated results for the cappilary waves problem

5. Conclusions

In the present paper, a model for immiscible fluids with multiple relaxation times based in the lattice Boltzmann equation was proposed. The collision term was splitted, considering cross and mutual collisions between the two species of fluids in moment space. Long range field forces were simulated taken into account long range interaction. Usual simulations for immiscible fluids models were carried out numerical results are in agreement with theoretical ones. For future works, one should perform the Von Neumann stability analysis, and also the Chapman-Enskog expansion for the transition layer. A point that should be emphasized is the easy extensibility of this model to the 3D case, using for that the corresponding lattice and equilibrium distribution function.

6. Acknowledgements

Authors are greatly indebted to ANP (Agência Nacional de Petróleo), CNPq (Conselho Nacional de Desenvolvimento Científico e Tecnológico), FINEP (Financiadora de Estudos e Projetos) and Petrobras S.A. for the financial support.

7. References

Facin, P. C., Philippi, P. C., Santos, L. O. E., 2004, "A non-linear lattice-Boltzmann model for miscible fluids". Future Generation Computer Systems, 20(6), pp. 945-949.

Frisch, U., Hasslacher, B., Pomeau, Y., 1986, "Lattice-Gas Automata for the Navier-Stokes Equation". Physical Review Letters, 56, pp. 1505-1508.

Gustensen, A. K., Rothman, D. H., Zaleski, S., Zanetti, G., 1991, "A lattice-Boltzmann model of immiscible fluids". Physical Review A, 43, pp. 4320-4327.

Gustensen, A. K., Rothman, D. H., 1992, "Microscopic modeling of immiscible fluidsin three dimensions by a lattice-Boltzmann method". Europhysics Letters, 18, pp. 157-161.

d'Humières, D., 1992, "Generalized Lattice-Boltzmann Equation", Prog. Aeronaut. Astronaut., 159, pp. 450-45.

Landau, L. & Lifshitz, E. M., 1987, "Fluid Mechanics", 2ª ed., Butterworth-Heinemann.

Santos, L. O. E., Philippi, P. C., 2002, "Lattice gas model based on field mediators for immiscible fluids". Physical Review E, 65, 46305.

Santos, L. O. E., Facin, P. C., Philippi, P. C., 2003, “Lattice-Boltzmann model based on field mediators for immiscible fluids”. Physical Review E, 68, 56302.

Shan, X., Chen, H., 1993, “Lattice Boltzmann model for simulating flows with multiple phases and components”. Physical Review E, 47, pp. 1815-1819.

Swift, M. R., Osborn, W. R., Yeomans, J.M., 1995, “Lattice Boltzmann Simulation of Nonideal Fluids”. Physical Review Letters, 75, 830.

8. Responsibility notice

The authors are the only responsible for the printed material included in this paper.

APPENDIX C

The following paper was published in *Physical Review E* in 2006.

From the continuous to the lattice Boltzmann equation: The discretization problem and thermal models

Paulo C. Philippi,* Luiz A. Hegele, Jr.,† Luís O. E. dos Santos,‡ and Rodrigo Surmas§
LMPT Mechanical Engineering Department, Federal University of Santa Catarina, 88040-900 Florianópolis, SC, Brazil
(Received 31 August 2005; published 9 May 2006)

The velocity discretization is a critical step in deriving the lattice Boltzmann (LBE) from the continuous Boltzmann equation. This problem is considered in the present paper, following an alternative approach and giving the minimal discrete velocity sets in accordance with the order of approximation that is required for the LBE with respect to the continuous Boltzmann equation and with the lattice structure. Considering N to be the order of the polynomial approximation to the Maxwell-Boltzmann equilibrium distribution, it is shown that solving the discretization problem is equivalent to finding the inner product in the discrete space induced by the inner product in the continuous space that preserves the norm and the orthogonality of the Hermite polynomial tensors in the Hilbert space generated by the functions that map the velocity space onto the real numbers space. As a consequence, it is shown that, for each order N of approximation, the even-parity velocity tensors are isotropic up to rank $2N$ in the discrete space. The norm and the orthogonality restrictions lead to space-filling lattices with increased dimensionality when compared with presently known lattices. This problem is discussed in relation with a discretization approach based on a finite set of orthogonal functions in the discrete space. Two-dimensional square lattices intended to be used in thermal problems and their respective equilibrium distributions are presented and discussed.

DOI: 10.1103/PhysRevE.73.056702 PACS number(s): 47.11.−j, 05.10.−a, 51.10.+y

I. INTRODUCTION

In accordance with Lallemand and Luo [1], the presently known lattice Boltzmann equation (LBE) has not been able to handle realistic thermal (and fully compressible flow) problems with satisfaction. Simulation of the thermal lattice Boltzmann equation is hampered by numerical instabilities when the local velocity increases.

The first thermal lattice Boltzmann models were introduced in about 1990 and there are several reasons that may be conjectured for their failure in handling nonisothermal flows [1].

Considering the kinetic nature of the LBE, establishing a formal link connecting the LBE to the continuous Boltzmann equation, and enabling the conceptual analysis of this discrete numerical scheme could perhaps shed some light on this question.

Indeed, there are several features that cause the lattice Boltzmann regular-lattice based framework to be far removed from the continuous Boltzmann equation, which would be desirable to be its conceptual support. These features include the particles, collision, and long-range interaction models, and the approach used for the time and the velocity space discretization.

Historically, the LBE was introduced by McNamara and Zanetti [2], replacing the Boolean variables in the discrete collision-propagation equations by their *ensemble* averages. Higuera and Jimenez [3] proposed a linearization of the collision term derived from the Boolean models, recognizing that this full form was unnecessarily complex when the main purpose was to retrieve the hydrodynamic equations. Following this line of reasoning, Chen *et al.* [4] suggested replacing the collision term by a single relaxation-time term, followed by Qian *et al.* [5] and Chen *et al.* [6], who introduced a model based on the celebrated kinetic-theory idea of Bhatnagar, Gross, and Krook (BGK) [7], but adding rest particles and retrieving the correct incompressible Navier-Stokes equations, with third-order nonphysical terms in the local speed, u.

The BGK collision term describes the relaxation of the distribution function to an equilibrium distribution. This discrete equilibrium distribution was settled by writing it as a second-order polynomial expansion in the particle velocity $\boldsymbol{c}_i$, with parameters adjusted to retrieve the mass density, the local velocity, and the momentum flux equilibrium moments, which are necessary conditions for satisfying the Navier-Stokes equations.

Thermal lattice BGK schemes included higher-order terms in the equilibrium distribution function [8,9], requiring one to increase the lattice dimensionality [8–10], i.e., the number of vectors in the finite and discrete velocity set $\{\boldsymbol{c}_i, i=0,\ldots,b\}$.

In thermal problems, the BGK single relaxation-time collision term restricts the models to a fixed Prandtl number. The correct description of fluids and fluid flow requires multiple relaxation-time models (MRT). A two-parameter model was introduced by He *et al.* [11] using two sets of distributions for the particle number density and the thermodynamic internal energy, coupled through a viscous dissipation term. Full MRT models were first introduced in the LBE framework by d'Humières [12,13] by modifying the collision step, considering it to be given by the relaxation to the equilibrium of a set of nonpreserved kinetic moments.

*Email address: philippi@lmpt.ufsc.br
†Email address: hegele@lmpt.ufsc.br
‡Email address: emerich@lmpt.ufsc.br
§Email address: surmas@lmpt.ufsc.br

Most lattice Boltzmann simulations are based on an explicit numerical scheme, although some lattice BGK models have been simulated with implicit numerical schemes [14,15] or LBE modified explicit numerical schemes [11], increasing by 1 the order of the time step errors.

With a few exceptions, in all the above works there is no formal link connecting LBE to the continuous Boltzmann equation, although the main ideas were based on the kinetic theory fundamentals.

He and Luo [16] have directly derived the LBE from the continuous Boltzmann equation for some widely known lattices (D2Q9, D2Q6, D2Q7, D3Q27) by the discretization of the velocity space, using the Gauss-Hermite and Gauss-Radau quadrature. Unfortunately, excluding the above-mentioned lattices, the discrete velocity sets obtained by this kind of quadrature do not generate regular, space-filling, lattices.

Succi [17], referring to He and Luo's work, suggests that establishing the exact nature of the link between the LBE and the continuum kinetic theory could be useful for systematic analysis and for the potential derivation of novel LBE numerical schemes.

The present paper deals with the aspects involved in deriving space-filling lattices that should be suitable for thermohydrodynamic problems. We start from the continuous Boltzmann equation, and the derivation of discrete velocity sets is considered as a quadrature problem, i.e., (a) to find a set of discrete velocities, $\boldsymbol{c}_i$, and weights W_i such that all the desired macroscopic moments are *exactly* retrieved as moments of the discrete equilibrium distribution f_i^{eq}, and (b) to ensure isotropy for the even-parity rank velocity tensors and, consequently, for the fluid transfer properties.

In doing that, two questions must be solved.

The first question is how to avoid the temperature dependence of the particles discrete velocities. This is a common drawback when performing Gauss-Hermite and related quadratures, using the dimensionless particle velocity $\boldsymbol{\mathcal{C}} = c/\sqrt{2k/Tm}$ as the integration variable, and leads to temperature-dependent particle velocities [18]. This problem is solved here by letting the particle velocity, c^2, be free from the temperature T in the exponential part $e^{-\mathcal{C}^2}$ of the Maxwell-Boltzmann (MB) distribution, and leads to writing the equilibrium distribution as a Taylor expansion in terms of the temperature deviation Θ. A similar approach is presented in [19].

The second question is how to derive *space-filling* lattices from the quadrature of the continuous Boltzmann equation.

Shan and He [20] showed that by discretizing the Boltzmann-BGK equation at a set of velocity vectors that correspond to the nodes of a Gauss-Hermite quadrature in the velocity space, the Boltzmann equation is effectively projected on a subspace spanned by the leading Hermite polynomials. Nevertheless, the quadrature problem leading to a minimum number of nodes for a given degree of accuracy was considered by these authors as a still unsolved problem. In addition, these authors mention the use of alternative numerical schemes such as the finite differences method, considering that these nodes do not, in general, coincide with the vertices of a regular lattice. More recently, Pavlo *et al.* [18] proposed a temperature-dependent velocity model based on an octagonal lattice, which is not space-filling, but ensures the isotropy of sixth-rank velocity tensors.

Given that the velocity discretization is a critical step in deriving lattice Boltzmann equations, this problem is considered in the present paper, following an alternative approach and giving the minimal discrete velocity sets in accordance with the order of approximation that is required for the LBE with respect to the continuous Boltzmann equation and with the lattice structure.

Considering N to be the order of the polynomial approximation to the MB equilibrium distribution, it is shown that solving the quadrature problem is *equivalent* to finding the inner product $(f^*g)_d$ in the discrete space induced by the inner product $(f^*g)_c$ in the continuous space, which preserves the norm and the orthogonality of the Hermite polynomial tensors $\Psi_{\theta,(r_\theta)}$. As a consequence, it is also shown that for each $\theta=1,\ldots,N$, the 2θ-rank velocity tensors are isotropic in the discrete space.

Two-dimensional square lattices intended to be used in thermal problems and their respective discrete equilibrium distributions are presented and discussed.

Finally, a discretization approach based on a set of orthogonal functions in the discrete space is discussed in detail, in relation with the presently proposed velocity discretization method.

II. THE DISCRETIZATION PROBLEM IN THE LATTICE BOLTZMANN FRAMEWORK

The classical lattice Boltzmann method is based on (i) a regular lattice generated by a space-filling discrete velocity set $\{\boldsymbol{c}_i, i=0\ldots,b\}$ and (ii) a discrete form of the Boltzmann equation, with a single or multiple relaxation time collision model and an equilibrium solution.

A Chapman-Enskog analysis of the lattice BGK equation [10] shows that a set of *necessary* conditions for the correct thermohydrodynamic equations to be retrieved is given by assuring that the discrete distributions f_i^{eq} satisfy

$$\langle\varphi_p\rangle^{\mathrm{eq}} = \frac{1}{n_d}\int f^{\mathrm{eq}}(\boldsymbol{c})\varphi_p(\boldsymbol{c})d\boldsymbol{c} = \frac{1}{n}\sum_i f_i^{\mathrm{eq}}\varphi_p(\boldsymbol{c}_i) \qquad (1)$$

for $\{\varphi_p=1, c_\alpha, c_\alpha c_\beta, c_\alpha c_\beta c_\gamma, c^2 c_\alpha c_\beta\}$, where $f^{\mathrm{eq}}(\boldsymbol{c})$ is the MB distribution written in terms of the particle velocity $\boldsymbol{c}$ in the continuous space, n_d is the number density of particles, n is the number of particles per site, and $\langle\varphi_p\rangle^{\mathrm{eq}}$ denotes a macroscopic equilibrium moment of φ_p.

Frequently, in athermal and thermal lattice Boltzmann models (e.g., [9]), the *unknown* discrete equilibrium distributions $f_{i,N}^{\mathrm{eq}}$ for a given order of approximation, N, are derived as *finite* expansions in the particle velocity $\boldsymbol{c}_i$,

$$\frac{f_{i,N}^{\mathrm{eq}}}{n} = A + B_\alpha c_{i\alpha} + D_{\alpha\beta}c_{i\alpha}c_{i\beta} + \cdots + O(N), \qquad (2)$$

with free parameters that are determined considering the symmetries of a previously chosen lattice

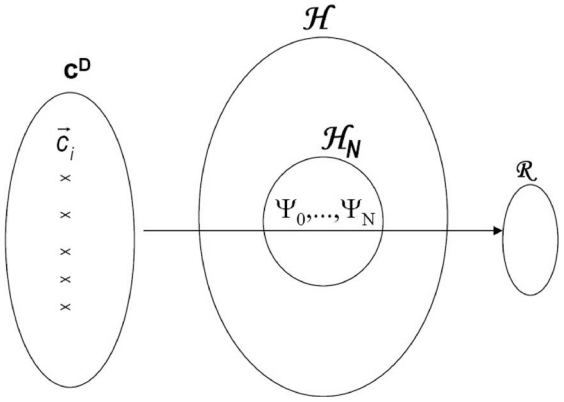

FIG. 1. The Hilbert space and the discretization problem.

$\ell=\{\boldsymbol{c}_i, i=0,\ldots,b\}$ and adjusted to satisfy Eq. (1) for all $\langle\varphi_p\rangle^{\mathrm{eq}}$ of interest.

This approach is equivalent to replacing the full MB distribution on the left-hand side of Eq. (1) by a finite expansion in $\boldsymbol{c}$. In this manner, the moments, $A, B_\alpha, D_{\alpha\beta},\ldots$ in Eq. (2) are calculated to fit the MB distribution at each order of approximation and, as a consequence, are dependent on N.

Since we cannot expect to find any relationship between $f^{\mathrm{eq}}(\boldsymbol{c}_i)$ and $f^{\mathrm{eq}}_{i,N}$, consider now the question of finding the relationship between $f^{\mathrm{eq}}_N(\boldsymbol{c})$ and $f^{\mathrm{eq}}_{i,N}$ when $\boldsymbol{c}\to\boldsymbol{c}_i$. Distribution $f^{\mathrm{eq}}_N(\boldsymbol{c})$ is the projection of the full MB distribution on the function space spanned by functions $\{1, c_\alpha, c_\alpha c_\beta,\ldots\}$. Given that distributions $f^{\mathrm{eq}}_{i,N}$ are only required to retrieve the equilibrium moments, there are no means to assure that $f^{\mathrm{eq}}_N(\boldsymbol{c})$ approaches $f^{\mathrm{eq}}_{i,N}$ (in fact, a weighted $f^{\mathrm{eq}}_{i,N}$) when $\boldsymbol{c}\to\boldsymbol{c}_i$.

The result is that, although the equilibrium moments are preserved with these finite expansions, the equilibrium distribution $f^{\mathrm{eq}}_{i,N}$ has no local identification with the projection $f^{\mathrm{eq}}_N(\boldsymbol{c})$ of the full MB distribution on the function space spanned by $\{1, c_\alpha, c_\alpha c_\beta,\ldots\}$. Section IV gives a more detailed discussion about this problem.

In the present work, discretization is considered as a quadrature problem. In this manner, f^{eq}_i is replaced by a weighted f^{eq}, preventing the above drawback.

Let $\mathcal{H}$ be the Hilbert weighted L_2 space generated by functions $f: c^D\to\mathcal{R}$ that map the D-dimensional continuous velocity space, c^D, onto the real variables space, $\mathcal{R}$ (Fig. 1). Velocity discretization means replacing the entire velocity space c^D by some few velocity vectors. When discretization is considered as a *quadrature* problem, the discrete distributions f^{eq}_i/n on the right-hand side of Eq. (1) must be replaced by $f^{\mathrm{eq}}(\boldsymbol{c}_i)/n_d$, i.e., by the value of the MB distribution evaluated at the pole $\boldsymbol{c}_i$ multiplied by a parameter ω_i, which denotes the weight to be attributed to each velocity vector $\boldsymbol{c}_i$ to satisfy the quadrature condition, considering that, for each coordinate axis α, the lattice speeds $c_{i\alpha}$ form a discrete and finite set and the continuous velocity space is continuous and extends to infinity.

In this manner, the discretization restrictions, Eq. (1), are replaced by the following quadrature equations:

$$\langle\varphi_p\rangle^{\mathrm{eq}} = \int \frac{f^{\mathrm{eq}}(\boldsymbol{c})}{n_d}\varphi_p(\boldsymbol{c})d\boldsymbol{c} = \sum_i \omega_i\left(\frac{2kT}{m}\right)^{D/2}\frac{f^{\mathrm{eq}}(\boldsymbol{c}_i)}{n_d}\varphi_p(\boldsymbol{c}_i), \tag{3}$$

where the factor $(2kT/m)^{D/2}$ was introduced to assure ω_i is a dimensionless, real number, since $f^{\mathrm{eq}}(\boldsymbol{c})/n_d$ is the number of particles per unit volume of the velocity space.

The role of the integration variable

Considering T to be the local temperature, $\boldsymbol{c}$ the particle velocity, $\boldsymbol{u}$ the macroscopic local velocity, m the mass of each particle, and $\boldsymbol{\mathcal{C}}_f=(\boldsymbol{c}-\boldsymbol{u})/\sqrt{2kT/m}$ the dimensionless peculiar velocity, the Maxwell-Boltzmann equilibrium distribution can be written as

$$f^{\mathrm{eq}} = n_d\left(\frac{m}{2\pi kT}\right)^{D/2} e^{-\boldsymbol{\mathcal{C}}_f^2}. \tag{4}$$

Returning to Eq. (3), when performing the quadrature, an integration variable must be chosen. If the dimensionless peculiar velocity, $\boldsymbol{\mathcal{C}}_f$, is chosen as the integration variable,

$$\langle\varphi_p\rangle^{\mathrm{eq}} = \frac{1}{\pi^{D/2}}\int e^{-\boldsymbol{\mathcal{C}}_f^2}\varphi_p(\boldsymbol{\mathcal{C}}_f)d\boldsymbol{\mathcal{C}}_f = \sum_{i=0}^{b} W_i\varphi_p(\boldsymbol{\mathcal{C}}_{fi}), \tag{5}$$

where $\boldsymbol{\mathcal{C}}_{fi}$ is a discrete peculiar velocity (a constant vector) dependent, basically, on b and on the kind of quadrature that was performed and

$$W_i = W_i(|\boldsymbol{\mathcal{C}}_{fi}|) = \frac{\omega_i e^{-\boldsymbol{\mathcal{C}}_{fi}^2}}{\pi^{D/2}} \tag{6}$$

are the dimensionless weights to be attributed to each discrete velocity $\boldsymbol{\mathcal{C}}_{fi}$.

For the first kinetic moment, n,

$$\langle 1\rangle = \frac{1}{\pi^{D/2}}\int e^{-\boldsymbol{\mathcal{C}}_f^2}1\,d\boldsymbol{\mathcal{C}}_f = \sum_{i=0}^{b} W_i 1 = \sum_{i=0}^{b} W_i, \tag{7}$$

resulting in

$$f^{\mathrm{eq}}_i = W_i n. \tag{8}$$

This means that the discrete equilibrium distribution does not depend, *explicitly*, on the macroscopic velocity $\boldsymbol{u}$ and on the temperature T. Nevertheless, the temperature and local velocity dependences are included in the particle velocities through

$$\boldsymbol{c}_i = \boldsymbol{u} + \left(\frac{2kT}{m}\right)^{1/2}\boldsymbol{\mathcal{C}}_{fi} = \boldsymbol{c}_i(T,\boldsymbol{u}). \tag{9}$$

In this manner, the *physical* grid, $(\boldsymbol{x},\boldsymbol{c}_i)$, i.e., the *physical* grid points where the particles will be located after each time step, will be time-dependent. Simulation tends to be very cumbersome and, at first glance, boundary conditions will be difficult to satisfy.

Another choice is the dimensionless particle velocity $\boldsymbol{\mathcal{C}}=\boldsymbol{c}/(2kT/m)^{1/2}$. This is the usual choice in LBM and requires us to rewrite the equilibrium distribution as

$$f^{\mathrm{eq}}=n_d\left(\frac{m}{2\pi kT}\right)^{D/2}e^{-\mathcal{C}^2}e^{2\mathcal{U}\cdot\mathcal{C}-\mathcal{U}^2}, \tag{10}$$

where $\boldsymbol{\mathcal{U}}=\boldsymbol{u}/(2kT/m)^{1/2}$ is a dimensionless local velocity and $\boldsymbol{\mathcal{C}}=\boldsymbol{c}/(2kT/m)^{1/2}$. The use of $\boldsymbol{\mathcal{C}}$ as the integration variable instead of $\boldsymbol{\mathcal{C}}_f$ requires us to develop $e^{2\mathcal{U}\cdot\mathcal{C}-\mathcal{C}^2}$ as an infinite series of Hermite polynomial tensors $\Psi_{\theta,(r_\theta)}$ [21], resulting in

$$f^{\mathrm{eq}}=n_d\frac{e^{-\mathcal{C}^2}}{\pi^{D/2}}\left(\frac{m}{2kT}\right)^{D/2}\sum_{\theta}a^{\mathrm{eq}}_{\theta,(r_\theta)}(\boldsymbol{\mathcal{U}})\Psi_{\theta,(r_\theta)}(\boldsymbol{\mathcal{C}}), \tag{11}$$

where (r_θ) is a sequence of indexes $r_1,r_2,\ldots,r_\theta$ (repeated indexes mean summation),

$$\Psi_0=1, \tag{12}$$

$$\Psi_{1,\alpha}=2C_\alpha, \tag{13}$$

$$\Psi_{2,\alpha\beta}=2\left(C_\alpha C_\beta-\frac{1}{2}\delta_{\alpha\beta}\right), \tag{14}$$

$$\Psi_{3,\alpha\beta\gamma}=\frac{4}{3}\left[C_\alpha C_\beta C_\gamma-\frac{1}{2}(C_\alpha\delta_{\beta\gamma}+C_\beta\delta_{\alpha\gamma}+C_\gamma\delta_{\alpha\beta})\right], \tag{15}$$

$$\Psi_{4,\alpha\beta\gamma\delta}=\frac{2}{3}\left[C_\alpha C_\beta C_\gamma C_\delta-\frac{1}{2}(C_\alpha C_\beta\delta_{\gamma\delta}+C_\alpha C_\gamma\delta_{\beta\delta}+C_\alpha C_\delta\delta_{\beta\gamma}+C_\beta C_\gamma\delta_{\alpha\delta}+C_\beta C_\delta\delta_{\alpha\gamma}+C_\gamma C_\delta\delta_{\alpha\beta})+\frac{1}{4}\Delta_{\alpha\beta\gamma\delta}\right], \tag{16}$$

and so on. Tensor Δ is defined as $\Delta_{\alpha\beta\gamma\delta}=\delta_{\alpha\beta}\delta_{\gamma\delta}+\delta_{\alpha\gamma}\delta_{\beta\delta}+\delta_{\alpha\delta}\delta_{\beta\gamma}$. The above tensors are orthogonal in the Hilbert space $\boldsymbol{\mathcal{H}}$, with respect to the inner product

$$(h*g)_c=\frac{1}{\pi^{D/2}}\int e^{-C^2}hg\,d\boldsymbol{\mathcal{C}}, \tag{17}$$

and symmetric with respect to any index permutation.

The coefficients $a^{\mathrm{eq}}_{\theta,(r_\theta)}$ in Eq. (11) are the macroscopic moments $a^{\mathrm{eq}}_0=1$, $a^{\mathrm{eq}}_{1,\alpha}=U_\alpha$, $a^{\mathrm{eq}}_{2,\alpha\beta}=U_\alpha U_\beta$, $a^{\mathrm{eq}}_{3,\alpha\beta\gamma}=U_\alpha U_\beta U_\gamma$, $a^{\mathrm{eq}}_{4,\alpha\beta\gamma\delta}=U_\alpha U_\beta U_\gamma U_\delta$, and so on.

Second-order approximations to the MB distribution are widely used in LBM athermal simulation, but, as seen in the beginning of the present section, thermohydrodynamics require fourth-order approximations for the equilibrium distribution. Consider a given Nth-order approximation to the MB distribution,

$$f^{\mathrm{eq}}_N=n_d\frac{e^{-C^2}}{\pi^{D/2}}\left(\frac{m}{2kT}\right)^{D/2}\sum_{\theta=0}^{N}a^{\mathrm{eq}}_{\theta,(r_\theta)}(\boldsymbol{\mathcal{U}})\Psi_{\theta,(r_\theta)}(\boldsymbol{\mathcal{C}}), \tag{18}$$

which can be viewed as an Nth-order Taylor expansion of the full MB distribution, in fact $f^{\mathrm{eq}}e^{C^2}$ (up to some local factors), on the local velocity $\vec{U}$, with errors $O(U^{N+1})$.

After quadrature, the equilibrium distribution becomes

$$f^{\mathrm{eq}}_{i,N}=W_i n\sum_{\theta=0}^{N}a^{\mathrm{eq}}_{\theta,(r_\theta)}(\boldsymbol{\mathcal{U}})\Psi_{\theta,(r_\theta)}(\boldsymbol{\mathcal{C}}_i), \tag{19}$$

where, as above, the constant velocity vectors $\boldsymbol{\mathcal{C}}_i$ are dependent on b and on the kind of quadrature that was performed.

The resulting $\boldsymbol{c}_i$ remains temperature-dependent, through

$$\boldsymbol{c}_i=\left(\frac{2kT}{m}\right)^{1/2}\boldsymbol{\mathcal{C}}_i=\boldsymbol{c}_i(T), \tag{20}$$

which means that after each time step, particles will be propagated to intermediate positions between next-neighboring sites, requiring us to write allocation rules that preserve, locally, the mass, momentum, and energy of the particles packet [18].

III. QUADRATURE BASED ON PRESCRIBED ABSCISSAS

Avoiding the $\boldsymbol{c}_i$ temperature dependence requires us to consider the particle velocity $\boldsymbol{c}$ as the integrating variable when performing the quadrature, i.e., to let c^2 be free from T in the exponential part e^{-C^2} of the equilibrium distribution. This can be accomplished by writing

$$e^{-(c-u)^2/(2kT/m)}=(e^{-C^2_{fo}})^{T_0/T}, \tag{21}$$

where T_0 is a reference (and constant) temperature and $\boldsymbol{\mathcal{C}}_{fo}=(\boldsymbol{c}-\boldsymbol{u})/(2kT_0/m)^{1/2}$ is a new dimensionless peculiar velocity referred to the temperature T_o.

When T is near T_0, i.e., when the departures from thermal equilibrium are small, the above expression may be developed in a Taylor series around $T/T_o=1$. Considering $\Theta=T/T_o-1$ to be the temperature deviation, this development gives

$$(e^{-C^2_{fo}})^{T_0/T}=e^{-C^2_{fo}}\left[1+C^2_{fo}\Theta+\frac{1}{2}C^2_{fo}(C^2_{fo}-2)\Theta^2+\cdots\right], \tag{22}$$

which terms are increasing powers of C^2_{fo}.

In this way,

$$f^{\mathrm{eq}}=n_d\left(\frac{T_0}{T}\right)^{D/2}\left[1+C^2_{fo}\Theta+\frac{1}{2}C^2_{fo}(C^2_{fo}-2)\Theta^2+\cdots\right]\times\frac{1}{\pi^{D/2}}\left(\frac{m}{2kT_0}\right)^{D/2}\times e^{-C^2_o}\sum_{\theta}a^{\mathrm{eq}}_{\theta,(r_\theta)}(\boldsymbol{\mathcal{U}}_0)\Psi_{\theta,(r_\theta)}(\boldsymbol{\mathcal{C}}_{0,i}), \tag{23}$$

where $\boldsymbol{\mathcal{U}}_0=\boldsymbol{u}/(2kT_0/m)^{1/2}$.

When the term $(T_0/T)^{D/2}$ is also developed in a Taylor series in terms of the temperature deviation Θ, replacing $\boldsymbol{\mathcal{C}}_{fo}=\boldsymbol{\mathcal{C}}_o-\boldsymbol{\mathcal{U}}_0$, Eq. (23) can be written, after mutiplying the several terms and reorganizing the resulting expression in terms of increasing order of the Hermite polynomials $\Psi_{\theta,(r_\theta)}$, as

$$f^{\mathrm{eq}} = \frac{1}{\pi^{D/2}}\left(\frac{m}{2kT_0}\right)^{D/2} e^{-C_0^2} \sum_{\theta} a^{\mathrm{eq}}_{\theta,(r_\theta)}(n_d, \mathcal{U}_0, \Theta)\Psi_{\theta,(r_\theta)}(\mathcal{C}_o), \tag{24}$$

where

$$a^{\mathrm{eq}}_0 = n_d, \tag{25}$$

$$a^{\mathrm{eq}}_{1,\alpha} = n_d \mathcal{U}_{0,\alpha}, \tag{26}$$

$$a^{\mathrm{eq}}_{2,\alpha\beta} = n_d \mathcal{U}_{0,\alpha}\mathcal{U}_{0,\beta} + \frac{1}{2} n_d \Theta \delta_{\alpha\beta}, \tag{27}$$

$$a^{\mathrm{eq}}_{3,\alpha\beta\gamma} = n_d \mathcal{U}_{0,\alpha}\mathcal{U}_{0,\beta}\mathcal{U}_{0,\gamma} + \frac{3}{2} n_d \Theta \mathcal{U}_{0,\gamma}\delta_{\alpha\beta}, \tag{28}$$

$$a^{\mathrm{eq}}_{4,\alpha\beta\gamma\delta} = n_d \mathcal{U}_{0,\alpha}\mathcal{U}_{0,\beta}\mathcal{U}_{0,\gamma}\mathcal{U}_{0,\delta} + 3 n_d \Theta \mathcal{U}_{0,\alpha}\mathcal{U}_{0,\beta}\delta_{\gamma\delta} + \frac{3}{4} n_d \Theta^2 \delta_{\alpha\beta}\delta_{\gamma\delta}, \tag{29}$$

related, respectively, to following macroscopic properties at equilibrium: the number density of particles n_d, the local momentum $n_d U_{0,\alpha}$, the momentum flux $\Pi^{\mathrm{eq}}_{\alpha\beta}$, the energy flux $e^{\mathrm{eq}}_{\alpha\beta\gamma}$, and a hyperflux of momentum, $\Xi^{\mathrm{eq}}_{\alpha\beta\gamma\delta}$.

Since each $\varphi_p(\boldsymbol{c})$ is a p-order monomial tensor in $\boldsymbol{c}$, functions $\Psi_{\theta,(r_\theta)}$ can be written as

$$\Psi_{\theta,(r_\theta)} = \sum_{\eta=0}^{\theta} a^{\theta}_{\eta,(s_\eta)} \varphi_\eta. \tag{30}$$

In this manner, for a given order θ, after multiplying Eq. (3) by the constants $a^{\theta}_{\eta,(s_\eta)}$, $\eta = 0, \ldots, \theta$ and adding the resulting equations, the quadrature equation, Eq. (3), can be rewritten in terms of quadrature equations for each $\Psi_{\theta,(r_\theta)}$ in the orthogonal basis of $\mathcal{H}$,

$$\int \frac{f^{\mathrm{eq}}(\boldsymbol{c})}{n_d}\Psi_{\theta,(r_\theta)} d\boldsymbol{c} = \sum_i \omega_i \left(\frac{2kT_0}{m}\right)^{D/2} \frac{f^{\mathrm{eq}}(\boldsymbol{c}_i)}{n_d}\Psi_{\theta,(r_\theta)}(\boldsymbol{c}_i). \tag{31}$$

Using the development, Eq. (24),

$$\sum_{\eta} a^{\mathrm{eq}}_{\eta,(s_\eta)} \frac{1}{\pi^{D/2}} \int e^{-C_0^2}\Psi_{\eta,(s_\eta)}(\mathcal{C}_o)\Psi_{\theta,(r_\theta)}(\mathcal{C}_o) d\mathcal{C}_o = \sum_{\eta} a^{\mathrm{eq}}_{\eta,(s_\eta)} \sum_i W_i \Psi_{\theta,(r_\theta)}(\mathcal{C}_{o,i})\Psi_{\eta,(s_\eta)}(\mathcal{C}_{o,i}), \tag{32}$$

where

$$W_i = W_i(|\mathcal{C}_{0i}|) = \frac{1}{\pi^{D/2}} \omega_i e^{-\mathcal{C}_{0i}^2}. \tag{33}$$

Since each $a^{\mathrm{eq}}_{\eta,(s_\eta)}$ is an independent equilibrium moment, Eq. (32) gives

$$\sum_i W_i \Psi_{\theta,(r_\theta)}(\mathcal{C}_{o,i})\Psi_{\eta,(s_\eta)}(\mathcal{C}_{o,i}) = \frac{1}{\pi^{D/2}} \int e^{-C_0^2}\Psi_{\eta,(s_\eta)}(\mathcal{C}_o)\Psi_{\theta,(r_\theta)}(\mathcal{C}_o) d\mathcal{C}_o. \tag{34}$$

Consider the inner products in the continuous and discrete space, respectively;

$$(f * g)_c \equiv \frac{1}{\pi^{D/2}} \int e^{-C_0^2} f g d\mathcal{C}_0, \tag{35}$$

$$(f * g)_d \equiv \sum_i W_i f(\mathcal{C}_{o,i}) g(\mathcal{C}_{o,i}), \tag{36}$$

and their induced norms

$$\|f\|_c^2 \equiv \frac{1}{\pi^{D/2}} \int e^{-C_0^2} f^2 d\mathcal{C}_0, \tag{37}$$

$$\|f\|_d^2 \equiv \sum_i W_i f^2(\mathcal{C}_{o,i}). \tag{38}$$

Since functions $\Psi_{\theta,(r_\theta)}(\mathcal{C}_o)$ are orthogonal in the continuous space with respect to the inner product Eq. (35), Eq. (34) requires the orthogonality of $\Psi_{\theta,(r_\theta)}(\mathcal{C}_{o,i})$ in the discrete space, with respect to the inner product Eq. (36). In addition, Eq. (34) requires the norm preservation of $\Psi_{\theta,(r_\theta)}$,

$$\sum_i W_i \Psi^2_{\theta,(r_\theta)}(\mathcal{C}_{o,i}) = \frac{1}{\pi^{D/2}} \int e^{-C_0^2}\Psi^2_{\theta,(r_\theta)}(\mathcal{C}_o) d\mathcal{C}_o. \tag{39}$$

In this manner, the still unknown weights W_i and the discrete velocities $\mathcal{C}_{o,i}$ must be chosen in such a manner that the orthogonality of the Hermite polynomial tensors $\Psi_{\theta,(r_\theta)}$ is assured in the discrete space and satisfying the norm preservation equation, Eq. (39).

In Appendix A, it is shown that the norm-preservation equation warrants the orthogonality of $\Psi_{\theta,(r_\theta)}(\mathcal{C}_{o,i})$ with respect to the inner product, Eq. (36), when the discrete velocity space is a Bravais lattice.

The above conclusion is very important because it shows that the norm-preservation equation warrants the orthogonality of $\Psi_{\theta,(r_\theta)}(\mathcal{C}_{o,i})$ in the discrete space, with respect to the inner product, Eq. (36). This reduces our discretization problem to find the weights W_i and the poles $\mathcal{C}_{oi}$ satisfying, solely, the norm restrictions, Eq. (39).

Let $\mathcal{H}_N$ be the subspace of $\mathcal{H}$ generated by the first Hermite polynomials with order $s \leqslant N$ and $f^{\mathrm{eq}}_N(c)$ be the projection of the MB distribution, $f^{\mathrm{eq}}(c)$, on this subspace. Function $f^{\mathrm{eq}}_N e^{\mathcal{C}_0^2}$ is an Nth -order $\boldsymbol{c}$-polynomial tensor and f^{eq}_N can be written as

$$f^{\mathrm{eq}}_N = \frac{e^{-C_0^2}}{\pi^{D/2}} \sum_{\theta=0}^{N} a^{\mathrm{eq},N}_{\theta,(r_\theta)}(n_d, \mathcal{U}_0, \Theta)\Psi_{\theta,(r_\theta)}. \tag{40}$$

Due to the orthogonality and completeness of $\Psi_{\theta,(r_\theta)}$,

$$a^{\mathrm{eq},N}_{\theta,(r_\theta)}(n_d, \mathcal{U}_0, \Theta) = a^{\mathrm{eq}}_{\theta,(r_\theta)}(n_d, \mathcal{U}_0, \Theta) \tag{41}$$

for $\theta \leqslant N$, meaning that the moments $a^{\mathrm{eq}}_{\theta,(r_\theta)}$ of the *full* MB

distribution are *preserved* when calculated in $\mathcal{H}_N$ with the approximation f_N^{eq}. Although this is a trivial consequence of the functional structure of the Hilbert space $\mathcal{H}$, the above equation is of great importance in lattice Boltzmann theory and means that an Nth-order approximation to the equilibrium distribution is required when Nth-order macroscopic equilibrium moments are to be correctly described in LBM. In addition, since LBM is a kinetic method based on a special discrete form of the Boltzmann equation, the degree of accuracy of the solution will be limited by N.

The above considerations also mean that if real positive weights W_i and velocities $\boldsymbol{\mathcal{C}}_{oi}$ can be found satisfying the norm-preservation conditions, the 2θ-rank velocity tensors

$$\Lambda_{(r_\theta),(s_\theta)} = \sum_i W_i C_{0,i,r_0} \cdots C_{0,i,r_\theta} C_{0,i,s_0} \cdots C_{0,i,s_\theta} \qquad (42)$$

are isotropic for all $\theta=1,\ldots,N$. This property follows directly from the isotropy of these velocity tensors in the continuous space. Indeed, each function $C_{0,i,r_0}\cdots C_{0,i,r_\theta}$ can be written in terms of a linear combination of the orthogonal functions $\Psi_{\eta,(t_\eta)}$ and the individual products $\Psi_{\eta,(t_\eta)}\Psi_{\eta,(v_\eta)}$ give nonzero values only when $t=v$, when the above equation gives $\|\Psi_{\eta,(t_\eta)}\|_d^2$, which is the same as the one calculated in continuous space.

With the exception of a very few lattices, Gaussian-like quadratures do not give a Bravais discrete set $\boldsymbol{\mathcal{C}}_{oi}$. Nevertheless, if any regular set $\{\boldsymbol{e}_i\}$, giving a Bravais lattice, is chosen, the quadrature problem can be considered as to find the weights W_i and a scaling factor a such that $\boldsymbol{\mathcal{C}}_{o,i}=a\boldsymbol{e}_i$, satisfying Eq. (39). Considering that the poles $\boldsymbol{e}_i$ are previously known, this quadrature method was denoted as *quadrature with prescribed abcissas*.

In this manner, when the order of approximation N of the Hermite polynomial expansion to the MB equilibrium distribution is chosen, a set $\Psi_{\theta,(r_\theta)}$, $\theta=0,\ldots,N$, is established, and the infinite and enumerable basis of the Hilbert space $\mathcal{H}:c^D\rightarrow R$, which generates the solutions of the continuous Boltzmann equation, is replaced by a *finite* set of Hermite polynomial tensors, restricting the solutions to Nth-degree polynomials in the velocity $\boldsymbol{c}$. The quadrature problem is now to select a regular lattice $\{\boldsymbol{e}_i\}$ in such a manner that functions $\Psi_{\theta,(r_\theta)}$ preserve the orthogonality with respect to the inner product in the discrete space, and this can be accomplished by assuring that the norm of *each one* of these functions $\Psi_{\theta,(r_\theta)}$ is retrieved, *exactly*, in the discrete space. The number b of the required lattice vectors is dependent on the order N of the polynomial approximation, $b=b(N)$. In addition, we have shown that when the quadrature problem is solved, the 2θ-rank tensors given by Eq. (42) are isotropic in the discrete space for $\theta=1,\ldots,N$.

IV. TWO-DIMENSIONAL SQUARE LATTICES

We restrict our attention to two-dimensional square lattices, although the above presented quadrature procedure is general and may be used for deriving other two- or three-dimensional lattices.

When the equilibrium distribution is an Nth-order polynomial approximation to the MB distribution, quadrature will be exact for all moments of order $p\leqslant N$, if the weights W_iW are chosen so as to satisfy Eq. (39) for all the functions,

$$\Psi = \left\{1, 2C_{ox}, 2C_{oy}, 2\left(C_{ox}^2 - \frac{1}{2}\right), 2\left(C_{oy}^2 - \frac{1}{2}\right), 2C_{ox}C_{oy}, \ldots\right\}. \qquad (43)$$

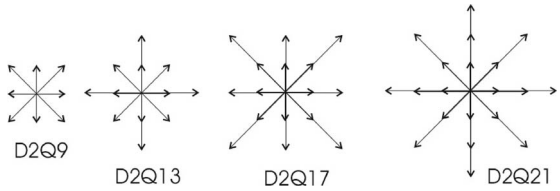

FIG. 2. Two-dimensional square lattices.

Each one of these functions gives a quadrature equation. Some equations will be linearly dependent in accordance with the lattice symmetry.

In two dimensions, square lattices such as the D2Q9, D2Q13, and other DQ-like lattices have four discrete velocities at each energy level C_o. Figure 2 summarizes some square lattices that are being used in lattice Boltzmann simulation: each set of four discrete velocities is superposed to the previous lattice vectors set when adding a single energy level, following the sequence $(0,1,\sqrt{2},2,2\sqrt{2},3,3\sqrt{2},\ldots)$.

When $N=2$, there will be four linearly independent equations for four unknowns related to the scaling factor a, and the D2Q9 weights W_0, W_1, W_2. This set has a unique solution leading to the widely known values $W_0=16/36$, $W_1=4/36$, $W_2=1/36$, and $a=\sqrt{3/2}$. This is shown in Appendix B.

In this manner, a *second-order approximation* to the full MB distribution is the equilibrium distribution in the D2Q9 lattice, and this distribution may be written as a linear combination of the first *six* Hermite orthogonal polynomials Ψ_0, $\Psi_{1,x}$, $\Psi_{1,y}$, $\Psi_{2,xx}$, $\Psi_{2,yy}$, and $\Psi_{2,xy}$. The addition of further restrictions, related to the norm preservation of the third-order Hermite polynomials $\Psi_{3,xxy}$, $\Psi_{3,yyx}$, gives a system of equations with the same solution, but additional restrictions related to $\Psi_{3,xxx}$ or $\Psi_{3,yyy}$ gives a system *without solution*. Further, a ninth polynomial tensor that fits to the D2Q9 lattice can be found by considering a Gram-Schmidt orthogonalization of the function C_o^4, using the previous Hermite polynomials and the inner product Eq. (35). Nevertheless, the addition of these third- and fourth-order functions to the second-order polynomial expansion of the discrete equilibrium distribution f_i^{eq} does not appear to be helpful, since it does not change the order of approximation of f_i^{eq} and will not be considered in this paper.

The dimensionless local velocity $\boldsymbol{\mathcal{U}}_0=\boldsymbol{u}/(2kT_0/m)^{1/2}$ can be scaled to enable us to work with unitary lattice units. In this manner, the spatial and the time scales, h and δ, respectively, can be chosen so as to satisfy

$$\frac{h}{\delta} = \left(\frac{2kT_0}{m}\right)^{1/2}, \qquad (44)$$

and, since

$$\boldsymbol{\mathcal{U}}_0 = \sum_i f_i \boldsymbol{\mathcal{C}}_{oi} = a \sum_i f_i \boldsymbol{e}_i, \tag{45}$$

where $\boldsymbol{e}_i$ are the usual lattice vectors in 2D lattices, a new local velocity can be defined as

$$\boldsymbol{u}^* = \frac{\boldsymbol{\mathcal{U}}_0}{a} = \sum_i f_i \boldsymbol{e}_i. \tag{46}$$

The equilibrium distribution for the D2Q9 lattice is then

$$f_{i,2}^{\mathrm{eq}} = W_i n \left(1 + 2a^2 u_\alpha^* e_{i,\alpha} + 2a^2 u_\alpha^* u_\beta^* \left(a^2 e_{i,\alpha} e_{i,\beta} - \frac{1}{2}\delta_{\alpha\beta} \right) + \Theta(a^2 e_i^2 - 1) \right), \tag{47}$$

with third-order errors $O(\Theta u^*, u^{*3})$.

The effect of temperature on the equilibrium distribution can be clearly seen from Eq. (47). In higher temperature sites, the amount of rest particles is reduced and redistributed to higher energy levels, trying to mimic the temperature dependence of the continuous MB distribution. This effect is highly desirable in thermal LBE simulation. An equilibrium distribution similar to Eq. (47) is given as Eq. (18) of Shan and He [20].

When the macroscopic velocity $\boldsymbol{\mathcal{U}}_0$ is replaced by $\boldsymbol{u}^*$, the moments $a_{\theta,(r_\theta)}^{\mathrm{eq}}$ in Eqs. (25)–(29) are then

$$a_0^{\mathrm{eq}} = n, \tag{48}$$

$$a_{1,\alpha}^{\mathrm{eq}} = n a u_\alpha^*, \tag{49}$$

$$a_{2,\alpha\beta}^{\mathrm{eq}} = n a^2 u_\alpha^* u_\beta^* + \frac{1}{2} n \Theta \delta_{\alpha\beta}, \tag{50}$$

$$a_{3,\alpha\beta\gamma}^{\mathrm{eq}} = n a^3 u_\alpha^* u_\beta^* u_\gamma^* + \frac{3}{2} n \Theta a u_\gamma^* \delta_{\alpha\beta}, \tag{51}$$

$$a_{4,\alpha\beta\gamma\delta}^{\mathrm{eq}} = n a^4 u_\alpha^* u_\beta^* u_\gamma^* u_\delta^* + 3 n \Theta a^2 u_\alpha^* u_\beta^* \delta_{\gamma\delta} + \frac{3}{4} n \Theta^2 \delta_{\alpha\beta}\delta_{\gamma\delta}. \tag{52}$$

In the same manner, the velocity functions $\Psi_{\theta,(r_\theta)}$ $(\boldsymbol{\mathcal{C}}_{o,i})$, Eqs. (12)–(16), can be rewritten in terms of the lattice vectors $\boldsymbol{e}_i$,

$$\Psi_0 = 1, \tag{53}$$

$$\Psi_{1,\alpha} = 2a e_{i\alpha}, \tag{54}$$

$$\Psi_{2,\alpha\beta} = 2\left(a^2 e_{i\alpha} e_{i\beta} - \frac{1}{2}\delta_{\alpha\beta} \right), \tag{55}$$

$$\Psi_{3,\alpha\beta\gamma} = \frac{4}{3}\left[a^3 e_{i\alpha} e_{i\beta} e_{i\gamma} - \frac{a}{2}(e_{i\alpha}\delta_{\beta\gamma} + e_{i\beta}\delta_{\alpha\gamma} + e_{i\gamma}\delta_{\alpha\beta}) \right], \tag{56}$$

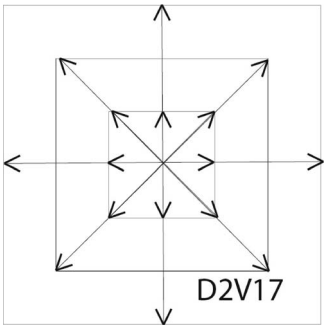

FIG. 3. The D2V17 lattice.

$$\Psi_{4,\alpha\beta\gamma\delta} = \frac{2}{3}\left[a^4 e_{i\alpha} e_{i\beta} e_{i\gamma} e_{i\delta} - \frac{a^2}{2}(e_{i\alpha}e_{i\beta}\delta_{\gamma\delta} + e_{i\alpha}e_{i\gamma}\delta_{\beta\delta} + e_{i\alpha}e_{i\delta}\delta_{\beta\gamma} + e_{i\beta}e_{i\gamma}\delta_{\alpha\delta} + e_{i\beta}e_{i\delta}\delta_{\alpha\gamma} + e_{i\gamma}e_{i\delta}\delta_{\alpha\beta}) + \frac{1}{4}\Delta_{\alpha\beta\gamma\delta} \right]. \tag{57}$$

The D2Q13 and the next lattices are also able to run second-order models. In these cases, the number of unknowns is greater than the number of disposable equations, and several solutions will be available, satisfying the quadrature problem.

Nevertheless, contrary to the results of McNamara and Alder [10] and to the results that would be expected with fitting methods (see Sec. IV), this lattice is *not able* to run *full* third-order models. Indeed, when $N=3$, it is impossible to find real positive values for a, W_0, W_1, W_2, W_3 satisfying all the norm restrictions, Eq. (39), related to $\Psi_{3,\alpha\beta\gamma}$. This result is the same for the D2Q17 lattice.

Considering the D2Q21 lattice as a next candidate for third-order models, there will be, in this case, seven unknowns a, W_0, W_1, W_2, W_3, W_4, W_5 for six norm restrictions, after eliminating identical equations. Letting a be a free variable, the system gives a solution with real positive roots when a is inside the interval $0.659836 \leqslant a \leqslant 1.16208$.

The values $a=0.659836$ and $a=1.16208$ (in fact, $a=1/12\sqrt{5}\sqrt{\sqrt{193}+25}$) are roots of the polynomials $W_0(a)$ and $W_3(a)$, respectively. In this manner, when the value $a=1.16208$ is chosen, $W_3=0$ and the lattice loses an energy level, giving a modification of the D2Q17 lattice, which has been named D2V17, shown in Fig. 3. The weights, with six significant digits, are $W_0=0.402005$, $W_1=0.116155$, $W_2=0.0330064$, $W_3=0$, $W_4=0.0000790786$, and $W_5=0.000258415$.

This modified square lattice is less expensive considering computer requirements and has the same properties when compared with the D2Q21 lattice, i.e., it retrieves, exactly, all the equilibrium moments up to the third order and gives isotropic tensors up to the sixth rank. Therefore, the present method can also be considered as a tool for investigating the structure of minimal velocity sets giving regular lattices. The D2V17 equilibrium distribution can be written as

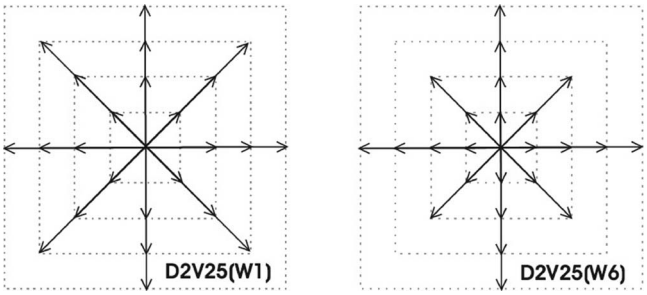

FIG. 4. The D2V25 lattices.

$$f_{i,3}^{\mathrm{eq}} = f_{i,2}^{\mathrm{eq}} + W_i a_{3,\alpha\beta\gamma}^{\mathrm{eq}} \Psi_{3,\alpha\beta\gamma}(i)$$
$$= W_i n \Bigg[1 + 2a^2 u_\alpha^* e_{i,\alpha} + 2(a^2 u_\alpha^* u_\beta^*) \left(a^2 e_{i,\alpha} e_{i,\beta} - \frac{1}{2}\delta_{\alpha\beta} \right) + \Theta(a^2 e_i^2 - 1) + \frac{4}{3} a^3 u_\alpha^* u_\beta^* u_\gamma^* \Bigg[a^3 e_{i,\alpha} e_{i,\beta} e_{i,\gamma} - \frac{a}{2}(e_{i,\alpha}\delta_{\beta\gamma} + e_{i,\beta}\delta_{\alpha\gamma} + e_{i,\gamma}\delta_{\alpha\beta}) \Bigg] + 2\Theta a^2 (a^2 e_i^2 - 2) u_\gamma^* e_{i,\gamma} \Bigg] \tag{58}$$

with fourth-order errors $O(\Theta u^{*2}, u^{*4})$.

In addition to the equilibrium moments up to third order, thermohydrodynamics requires the fourth-order equilibrium moments $\langle C_0^2 C_{0,x}^2 \rangle^{\mathrm{eq}}$, $\langle C_0^2 C_{0,y}^2 \rangle^{\mathrm{eq}}$, and $\langle C_0^2 C_{0,x} C_{0,y} \rangle^{\mathrm{eq}}$ to be retrieved [10]. Since these functions are not orthogonal in the continuous velocity space, a Gram-Schmidt orthogonalization procedure was used to find orthogonal polynomials from this set by using the previous Hermite polynomials and the inner product Eq. (35).

The result was

$$\Psi_{4,1} = C_o^2 C_{o,x}^2 - \frac{7}{2} C_{o,x}^2 - \frac{1}{2} C_{o,y}^2 + 1, \tag{59}$$

$$\Psi_{4,2} = \frac{1}{7}[C_o^2 (7C_{o,y}^2 - C_{o,x}^2) - 24 C_{o,y}^2 + 6], \tag{60}$$

$$\Psi_{4,3} = C_{o,x} C_{o,y} (C_o^2 - 3). \tag{61}$$

When we require the norm preservation of the functions $\Psi_{4,1}$, $\Psi_{4,2}$, and $\Psi_{4,3}$, this gives a system of eight independent equations for nine unknowns. In this case, a is again a free parameter and the solution gave real positive weights for $0.590193 \leqslant a \leqslant 0.760569$.

Further, when a is, respectively, taken as 0.590193 or 0.760569, the weights W_1 or W_6 are null, giving two D2V25 lattices that retrieve the correct thermohydrodynamics equations. These lattices are shown in Fig. 4. For the first lattice, called D2V25(W1), $a=0.590193$ and the calculated weights are $W_0=0.235184$, $W_1=0$, $W=0.101817$, $W_3=5.92134\times10^{-2}$, $W_4=2.00409\times10^{-2}$, $W_5=6.79523\times10^{-3}$, $W_6=1.14376\times10^{-3}$, and $W_7=2.19788\times10^{-3}$. Lattice D2V25(W6) has $a=0.760569$ and $W_0=0.239059$, $W_1=0.063158$, $W_2=8.75957\times10^{-2}$, $W_3=3.11800\times10^{-2}$, $W_4=6.19896\times10^{-3}$, $W_5=2.02013\times10^{-3}$, $W_6=0$, and $W_7=8.38224\times10^{-5}$.

Therefore, thermohydrodynamic equations are correctly retrieved with the LBE based on these lattices, but isotropy of eighth-rank tensors cannot be assured. The equilibrium distribution for this lattice can be written as

$$f_{i,\mathrm{th}}^{\mathrm{eq}} = f_{i,3}^{\mathrm{eq}} + W_i [a_{4,1}^{\mathrm{eq}} \Psi_{4,1}(i) + a_{4,2}^{\mathrm{eq}} \Psi_{4,2}(i) + a_{4,3}^{\mathrm{eq}} \Psi_{4,3}(i)], \tag{62}$$

with, nevertheless, fourth-order errors $O(\Theta u^{*2}, u^{*4}, \Theta^2)$ with respect to the full MB distribution. Parameters $a_{4,\theta}^{\mathrm{eq}}$ can be found by using the orthogonality properties of $\Psi_{4,\theta}$ $(\boldsymbol{\mathcal{C}}_0)$ in the continuous space, giving,

$$a_{4,1}^{\mathrm{eq}} = \frac{2}{7}[2a^4 u_x^{*2} u^{*2} + \Theta a^2 (6u_x^{*2} + u^{*2}) + 2\Theta^2], \tag{63}$$

$$a_{4,2}^{\mathrm{eq}} = \frac{1}{12}(7a^4 u_y^{*4} - a^4 u_x^{*4} + 6a^4 u_x^{*2} u_y^{*2} + 24a^2 u_y^{*2}\Theta + 6\Theta^2), \tag{64}$$

$$a_{4,3}^{\mathrm{eq}} = \frac{4}{3} a^2 u_x^* u_y^* (3\Theta + a^2 u^{*2}). \tag{65}$$

For the full fourth-order model, the norm preservation of a full set of Hermite orthogonal polynomials until the fourth order is required, giving a set of nine norm restrictions. This system will only be closed for a lattice with eight energy levels. The D2Q29 lattice, with eight weights $W_0,\ldots, W_7$, is a natural candidate to be the *minimal* square lattice to run fourth-order models in the square lattice hierarchy. For this lattice, there are nine linearly independent equations. This closed set of nine independent equations has, nevertheless, no solution.

This result was the same for the next D2Q33 lattice, when a is allowed to be a free parameter.

Since each function $\Psi_{\theta,(r_\theta)}$ is a linear combination of the monomials $\varphi=\{1, C_{ox}, C_{oy}, C_{ox}^2, C_{oy}^2, C_{ox}C_{oy}, \ldots\}$, the norm restrictions, Eq. (39), can be indifferently used on the set Ψ of orthogonal functions or on set φ of monomials. The last choice is, in the present case, preferable for identifying a symmetry deficiency in the DQ-series hierarchy of square lattices (Fig. 2). Indeed, consider the fourth-order functions $\varphi_{4,1}=C_{oy}^2 C_{ox}^2$ and $\varphi_{4,2}=C_{ox}^3 C_{oy}$. These functions have different norms in the continuous space, respectively, $3/4$ and $\sqrt{15/16}$. Nevertheless, since $\varphi_{4,1}=(C_{oy}C_{ox})^2$ and $\varphi_{4,2}=(C_{ox}C_{oy})C_{ox}^2$, the only contributions for their norms in the discrete space came from the diagonal vectors and are the same because along these directions $|C_{o,iy}|=|C_{o,ix}|$.

This is an important result, since it means that the Q-series of square lattices are unable to run full fourth-order LBE models.

In this way, we have tried another building structure for the lattices, filling completely the available Cartesian space around each site following the sequence $|e_i|=0, 1, \sqrt{2}, 2, \sqrt{5}, 2\sqrt{2}, 3, \sqrt{10}$ with sequentially increasing values for $|e_i|$.

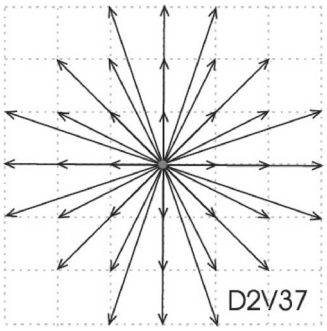

FIG. 5. The D2V37 lattice.

Figure 5 shows a D2V37 lattice, constructed in such a manner, with 37 velocity vectors but eight weights W_i. Solution of the nine norm equations is unique and gives, when six significant digits are considered, $a=0.846393$, $W_0=0.233151$, $W_1=0.107306$, $W_2=0.0576679$, $W_3=0.0142082$, $W_4=0.00535305$, $W_5=0.00101194$, $W_6=0.000245301$, and $W_7=0.000283414$. This lattice came from the solution of a closed system with nine linearly independent norm restriction for nine unknowns.

Since, in the D2V37 lattice, all the fourth-order Hermite polynomial tensors belong to the orthogonal basis of this lattice, the equilibrium distribution can be written as

$$
\begin{aligned}
f_{i,4}^{\mathrm{eq}} &= f_{i,3}^{\mathrm{eq}} + W_i a_{4,\alpha\beta\gamma\delta}^{\mathrm{eq}} \Psi_{4,\alpha\beta\gamma\delta}(i) \\
&= W_i n \Bigg\{ 1 + 2a^2 u_\alpha^* e_{i,\alpha} + 2(a^2 u_\alpha^* u_\beta^*) \left(a^2 e_{i,\alpha} e_{i,\beta} - \frac{1}{2}\delta_{\alpha\beta} \right) \\
&\quad + \Theta(a^2 e_i^2 - 1) + \frac{4}{3} a^3 u_\alpha^* u_\beta^* u_\gamma^* \Bigg[a^3 e_{i,\alpha} e_{i,\beta} e_{i,\gamma} \\
&\quad - \frac{a}{2}(e_{i,\alpha}\delta_{\beta\gamma} + e_{i,\beta}\delta_{\alpha\gamma} + e_{i,\gamma}\delta_{\alpha\beta}) \Bigg] + 2\Theta a^2 (a^2 e_i^2 - 2) u_\gamma^* e_{i,\gamma} \\
&\quad + \frac{2}{3} \Bigg[\Bigg[a^8 (u_\alpha^* e_{i\alpha})^4 - 3a^6 u^{*2} (u_\alpha^* e_{i\alpha})^2 + \frac{3}{4} a^4 u^{*4} \Bigg] \\
&\quad + \Theta \Bigg[3a^6 (u_\alpha^* e_{i\alpha})^2 e_i^2 - \frac{3}{2} a^4 [D(u_\alpha^* e_{i\alpha})^2 + 4(u_\alpha^* e_{i\alpha})^2 \\
&\quad + u^{*2} e_i^2] + \frac{3}{4} a^2 u^{*2} (D+2) \Bigg] \\
&\quad + \frac{3}{4}\Theta^2 \Bigg[a^4 e_i^4 - \frac{1}{2} a^2 (D+2) e_i^2 + \frac{1}{4} D(D+2) \Bigg] \Bigg] \Bigg\}. \qquad (66)
\end{aligned}
$$

The D2V37 lattice, with the above equilibrium distribution, can be considered as the *minimal* square lattice giving a fourth-order approximation to the continuous Boltzmann equation, wih errors $O(\Theta^2 u^*, u^{*5})$.

The weights W_i, in general, decrease with i and attain very small values when i is large. The smallness of W_i for large i is expected and is a consequence of (a) the restriction that was imposed on the lattice to be space filling, requiring the norm of each added lattice vector, $\boldsymbol{e}_i$ to be, frequently, an integer multiple of the norm of the lattice vectors forming the D2Q9 lattice unitary cell in square lattices, and (b) the required degree of approximation leading to polynomials with terms of $O(e_b^N)$.

V. DISCUSSION: A DISCRETIZATION APPROACH BASED ON A FINITE SET OF ORTHOGONAL FUNCTIONS IN THE DISCRETE SPACE

Consider a previously assigned velocity set $\ell=\{\boldsymbol{c}_0,\ldots,\boldsymbol{c}_b\}$ giving a regular lattice. Returning to Eq. (1),

$$
\langle \varphi_\eta \rangle^{\mathrm{eq}} = \int \frac{f^{\mathrm{eq}}(\boldsymbol{c})}{n_d} \varphi_\eta(\boldsymbol{c}) d\boldsymbol{c} = \sum_i \frac{f_i^{\mathrm{eq}}}{n} \varphi_\eta(\boldsymbol{c}_i) \qquad (67)
$$

for $\eta=0,1,2,\ldots,b$, but now φ_η forms a set of $b+1$ linearly independent velocity monomials in a given lattice with $b+1$ degrees of freedom. Considering, e.g., the D2Q9 lattice, this set can be chosen as

$$
\varphi = \{1, c_{ix}, c_{iy}, c_{ix}^2, c_{iy}^2, c_{ix}c_{iy}, c_{ix}^2 c_{iy}, c_{iy}^2 c_{ix}, c_i^4\}, \qquad (68)
$$

since, in this lattice, there are only two third-degree linearly independent monomials and a fourth-degree additional monomial is required.

The orthogonal functions $\Psi_{\theta,(r_\theta)}(\boldsymbol{c}_i)$ are now considered to be derived from the set φ_η. This can be accomplished by using an orthogonalization procedure, such as the Gram-Schmidt process, and is the basis of the LB moments method [13]. Since the particular forms of $\Psi_{\theta,(r_\theta)}(\boldsymbol{c}_i)$ are dependent on the lattice, on functions φ_η, and on the manner in which the Gram-Schmidt method is used, these functions will be noted as $\Psi_{\theta,(r_\theta)}^{\ell}(\boldsymbol{c}_i)$ to distinguish them from the above Hermite polynomial tensors.

In this case, an inner product must be defined in the discrete space generated by the functions $f:\{\boldsymbol{c}_0,\ldots,\boldsymbol{c}_b\}\rightarrow R$. Considering

$$
(a * b)_d = \sum_i a_i b_i \qquad (69)
$$

to be such a product each element of the orthogonal basis can be written in terms of the monomials φ_η as

$$
\Psi_{\theta,(r_\theta)}^{\ell} = \sum_{\eta=0}^{\theta} a_{\eta,(s_\eta)}^{\theta,\ell} \varphi_\eta, \qquad (70)
$$

where $a_{\eta,(s_\eta)}^{\theta,\ell}$ are real numbers, dependent on the assigned lattice. After multiplying Eq. (67) by $a_{\eta,(s_\eta)}^{\theta,\ell}$ for each η and adding the resulting equations, we obtain

$$
\int \frac{f^{\mathrm{eq}}(\boldsymbol{c})}{n_d} \Psi_{\theta,(r_\theta)}^{\ell}(\boldsymbol{c}) d\boldsymbol{c} = \sum_i \frac{f_i^{\mathrm{eq}}}{n} \Psi_{\theta,(r_\theta)}^{\ell}(\boldsymbol{c}_i). \qquad (71)
$$

Expanding f_i^{eq}/n in terms of functions $\Psi_{\theta,(r_\theta)}^{\ell}(\boldsymbol{c}_i)$,

$$
\frac{f_i^{\mathrm{eq}}}{n} = \sum_{\theta=0}^{b} a_{\theta,(r_\theta)}^{\mathrm{eq},\ell} \Psi_{\theta,(r_\theta)}^{\ell}(\boldsymbol{c}_i). \qquad (72)
$$

Since $\Psi_{\theta,(r_\theta)}^{\ell}(\boldsymbol{c}_i)$ are orthogonal (in the discrete space), the following relationship follows directly from Eq. (71):

$$\int \frac{f^{\mathrm{eq}}(\boldsymbol{c})}{n_d}\Psi^{\ell}_{\theta,(r_\theta)}(\boldsymbol{c})d\boldsymbol{c} = a^{\mathrm{eq},\ell}_{\theta,(r_\theta)}\lambda_\theta, \tag{73}$$

where

$$\lambda_\theta = \sum_i (\Psi^{\ell}_{\theta,(r_\theta)})^2, \tag{74}$$

resulting in

$$a^{\mathrm{eq},\ell}_{\theta,(r_\theta)} = \frac{\int \frac{f^{\mathrm{eq}}(\boldsymbol{c})}{n_d}\Psi^{\ell}_{\theta,(r_\theta)}(\boldsymbol{c})d\boldsymbol{c}}{\sum_i (\Psi^{\ell}_{\theta,(r_\theta)})^2}. \tag{75}$$

The above equation gives the equilibrium moment $a^{\mathrm{eq},\ell}_{\theta,(r_\theta)}$ in terms of the MB distribution function for a given order θ of the function $\Psi^{\ell}_{\theta,(r_\theta)}$.

In this manner, Eq. (71) can be regarded as a *discretization equation* giving the unknowns f_i^{eq} in terms of the MB distribution function, requiring the moments $a^{\mathrm{eq},\ell}_{\theta,(r_\theta)}$ to be the projections of the full MB distribution, $f^{\mathrm{eq}}(\boldsymbol{c})$, on a (not orthogonal) basis $\Psi^{\ell}_{\theta,(r_\theta)}(\boldsymbol{c})$ of $\mathcal{H}_N$, Eq. (75).

The discrete velocities $\boldsymbol{c}_i$ can be related to the dimensionless lattice vectors $\mathbf{e}_i$ through

$$\boldsymbol{c}_i = \frac{h}{\delta}\boldsymbol{e}_i, \tag{76}$$

where h and δ are, respectively, the space and time scales.

The next step is now to find the polynomial approximation, $f_N^{\mathrm{eq}}(\boldsymbol{c})$, to the full MB equilibrium distribution that is generated by functions $\Psi^{\ell}_{\theta,(r_\theta)}(\boldsymbol{c})$ of $\mathcal{H}_N$ and see what is the relationship between $f_N^{\mathrm{eq}}(\boldsymbol{c}_i)$ and the above derived f_i^{eq}.

It is important to emphasize that although functions $\Psi^{\ell}_{\theta,(r_\theta)}$ are orthogonal in the subspace $\mathcal{H}_N$ of $\mathcal{H}$, generated by $\Psi^{\ell}_{\theta,(r_\theta)}$ with respect to the inner product, Eq. (69), these functions are, in general, *not orthogonal* in this subspace, with respect to the inner product of $\mathcal{H}$, Eq. (17). Thus, consider replacing $f^{\mathrm{eq}}(\boldsymbol{c})$ on the left-hand side of Eq. (73) by the projection $f_N^{\mathrm{eq}}(\boldsymbol{c})$ of the MB distribution on the subspace spanned by functions $\Psi^{\ell}_{\theta,(r_\theta)}(\boldsymbol{c})$.

Written in terms of $\Psi^{\ell}_{\eta,(s_\eta)}$, this projection will have a form analogous to Eq. (18),

$$f_N^{\mathrm{eq}} = n_d \frac{e^{-C^2}}{\pi^{D/2}}\left(\frac{m}{2kT}\right)^{D/2}\sum_{\theta=0}^{N} a^{\mathrm{eq},\ell}_{\eta,(s_\eta)}\Psi^{\ell}_{\eta,(s_\eta)}(\boldsymbol{\mathcal{C}}). \tag{77}$$

Since functions $\Psi^{\ell}_{\eta,(s_\eta)}$ are not orthogonal with respect to Eq. (17), Eq. (73) gives

$$\sum_\eta a^{\mathrm{eq},\ell}_{\eta,(s_\eta)}\frac{1}{\pi^{D/2}}\int e^{-C^2}\Psi^{\ell}_{\eta,(s_\eta)}\Psi^{\ell}_{\theta,(r_\theta)}d\boldsymbol{\mathcal{C}} = a^{\mathrm{eq},\ell}_{\theta,(r_\theta)}\lambda_\theta, \tag{78}$$

which is a closed system of equations for the unknows $a^{\mathrm{eq},\ell}_{\eta,(s_\eta)}$. When $a^{\mathrm{eq},\ell}_{\theta,(r_\theta)}$ on the right-hand side of the above equation is considered to be either given by Eq. (75) or to be unknown, this system can only be expected to have the same solution, Eq. (75), when functions $\Psi^{\ell}_{\eta,(s_\eta)}$ are orthogonal with respect to the inner product Eq. (17) and

$$\frac{1}{\pi^{D/2}}\int e^{-\mathcal{C}^2}\Psi^{\ell}_{\eta,(s_\eta)}\Psi^{\ell}_{\theta,(r_\theta)}d\boldsymbol{\mathcal{C}} = \sum_i \Psi^{\ell}_{\eta,(s_\eta)}(\boldsymbol{\mathcal{C}}_i)\Psi^{\ell}_{\theta,(r_\theta)}(\boldsymbol{\mathcal{C}}_i), \tag{79}$$

which is not generally true.

This means that, analogous to the previous approach discussed in the beginning of Sec. I, $f_N^{\mathrm{eq}}(\boldsymbol{c})$ has no identification with f_i^{eq} and does not converge to f_i^{eq} (or to a weighted f_i^{eq}) when $\boldsymbol{c}$ approaches the poles $\boldsymbol{c}_i$.

In this manner, although the above exposed discretization procedure leads to the correct macroscopic equilibrium moments and, as a consequence, to the correct hydrodynamic equations, the generated discrete equilibrium distribution loses any local identification with its continuous counterpart.

LBM is a kinetic method based on the solution of a discrete kinetic equation (and not on the solution of the hydrodynamic equations themselves), and the next question to be answered is, to what extent does this lack of identification affect the solution of a given hydrodynamic problem?

VI. CONCLUSION

The present paper deals with the discretization problem in generating the lattice Boltzmann equation from the continuous Boltzmann equation.

In the quadrature problem, lattices with temperature-dependent particle velocities were avoided by letting the particle velocity, c^2, be free from the temperature T in the exponential part e^{-C^2} of the MB distribution and writing the equilibrium distribution as a Taylor expansion in terms of the temperature deviation Θ.

It was shown that the LBE can be derived from the continuous Boltzmann equation when the orthogonality of the Hermite polynomial tensors in the continuous space is maintained. It was also shown that this can be assured when the norms of these tensors are preserved in discrete space, leading to increasingly accurate lattice Boltzmann models.

In this manner, the preservation of the functional structure of the Hilbert space, $\mathcal{H}_N$, when its inner product and induced norm are replaced by discrete sums, appears to be a fundamental rule for the velocity discretization problem when the discrete equilibrium distribution is required to give increasingly accurate approximations with respect to the continuous MB distribution. Although equilibrium moments are preserved, this rule is not, in general, satisfied by the lattices, which structure is derived from a finite polynomial expansion in the discrete space.

These restrictions lead to space-filling lattices with increased dimensionality when compared with presently known square lattices. In this manner, it was concluded that a 17-velocities lattice is required for third order and a 25-velocities lattice is needed for thermal model approximations, compared with, respectively, the D2Q13 and D2Q17 lattices, which are shown to retrieve the correct macroscopic equations related to these moments. In particular, considering thermal problems, the D2Q17 lattice, which equilibrium distributions f_i^{eq} are obtained with the method exposed in Sec.

TABLE I. Parity indexes of some leading Hermite polynomial tensors.

$\Psi_{\theta,(r_\theta)}$	m_x	m_y
Ψ_0	0	0
$\Psi_{1,x}$	1	0
$\Psi_{1,y}$	0	1
$\Psi_{2,xx}$	2	0
$\Psi_{2,yy}$	0	2
$\Psi_{2,xy}$	1	1
$\Psi_{3,xxx}$	3	0
$\Psi_{3,xyy}$	1	2
$\Psi_{3,yyy}$	0	3

IV, retrieves the thermohydrodynamic equations, but its equilibrium distribution and the derived lattice Boltzmann equation cannot be considered as reliable approximations to the MB distribution and the Boltzmann equation, respectively.

ACKNOWLEDGMENTS

The authors are greatly indebted to ANP (Brazilian Petroleum Agency), CNPq (Brazilian Research Council), Finep (Brazilian Agency for Research and Projects), and Petrobras (Brazilian Petroleum Company) for the financial support. The authors thank Diogo Nardelli Siebert for very helpful discussions.

APPENDIX A: ORTHOGONALITY OF THE HERMITE POLYNOMIAL TENSORS IN THE DISCRETE SPACE

Let $\Psi_{\theta,(r_\theta)}$ be a set of Hermite polynomial tensors, orthogonal with respect to the inner product Eq. (35). Consider a Bravais lattice, where to each velocity vector $\boldsymbol{\mathcal{C}}_{0,i}$, $\boldsymbol{\mathcal{C}}_{0,i} \neq 0$, corresponds a discrete velocity $\boldsymbol{\mathcal{C}}_{0,-i}=-\boldsymbol{\mathcal{C}}_{0,i}$.

Let $m_\alpha(\Psi_{\theta,(r_\theta)})$ be a parity index giving the number of times the index α appears in $\Psi_{\theta,(r_\theta)}$. Table I gives the parity indexes of some leading Hermite polynomial tensors in two dimensions.

Index $m_\alpha(\Psi_{\theta,(r_\theta)})$ gives the parity of $\Psi_{\theta,(r_\theta)}$ with respect to the α component of the particle velocity $\boldsymbol{\mathcal{C}}_0$. In this manner, the Hermite polynomials $\Psi_{\theta,(r_\theta)}$ can be also written as a three-index function $\Psi_{\theta,m_{x\theta},m_{y\theta}}$. This last notation is more convenient for the present purpose.

When making the inner product in either its continuous, Eq. (35), and discrete, Eq. (36), forms,

$$(\Psi_{\theta,m_{x\theta},m_{y\theta}} * \Psi_{\eta,m_{x\eta},m_{y\eta}})_{c \text{ or } d'},$$

this product is trivially null whenever

$$m_x(\Psi_{\theta,m_{x\theta},m_{y\theta}}\Psi_{\eta,m_{x\eta},m_{y\eta}}) = m_{x\theta} + m_{x\eta}$$

or

$$m_y(\Psi_{\theta,m_{x\theta},m_{y\theta}}\Psi_{\eta,m_{x\eta},m_{y\eta}}) = m_{y\theta} + m_{y\eta}$$

are odd.

When both parity indexes $m_x(\Psi_{\theta,m_{x\theta},m_{y\theta}}\Psi_{\eta,m_{x\eta},m_{y\eta}})$ and $m_y(\Psi_{\theta,m_{x\theta},m_{y\theta}}\Psi_{\eta,m_{x\eta},m_{y\eta}})$ are even, the resulting polynomial is invariant under changes $C_{0x}\rightarrow -C_{0x}$ and $C_{0y}\rightarrow -C_{0y}$, therefore it has only quadratic forms in the monomials 1, C_{0x}, C_{0y}, C_{0x}^2, C_{0y}^2, $\boldsymbol{\mathcal{C}}_{0x}\boldsymbol{\mathcal{C}}_{0y}$,…. When both parity indexes $m_x(\Psi_{\theta,m_{x\theta},m_{y\theta}}\Psi_{\eta,m_{x\eta},m_{y\eta}})$ and $m_y(\Psi_{\theta,m_{x\theta},m_{y\theta}}\Psi_{\eta,m_{x\eta},m_{y\eta}})$ are even, the resulting polynomial is invariant under changes $C_{0x}\rightarrow -C_{0x}$ and $C_{0y}\rightarrow -C_{0y}$, therefore it has only quadratic forms in the monomials

$$C = \{C_{\theta,m_{x\theta},m_{y\theta}} = 1, C_{0x}, C_{0y}, C_{0x}^2, C_{0y}^2, C_{0x}C_{0y}, \dots\}$$

. The squared monomials can be written as linear combinations of $\Psi_{i,j,k}^2$. This comes from the consideration that each square $\Psi_{\theta,m_{x\theta},m_{y\theta}}^2$ depends on a leading term related to $C_{\theta,m_{x\theta},m_{y\theta}}^2$ and on lower-order degree monomials. In this manner, letting Ψ^2 and C^2 be vectors,

$$\Psi^2 = [\Psi_0^2, \Psi_{1,1,0}^2, \dots, \Psi_{\theta,m_{x\theta},m_{y\theta}}^2]$$

and

$$C^2 = [C_0^2, C_{1,1,0}^2, \dots, C_{\theta,m_{x\theta},m_{y\theta}}^2],$$

respectively, the linear system of equations

$$\Psi^2 = AC^2 \tag{A1}$$

can be easily inverted since A is a triangular matrix, with non-null terms in the diagonal. Consequently, the products will be

$$\Psi_{\theta,m_{x\theta},m_{y\theta}}\Psi_{\eta,m_{x\eta},m_{y\eta}} = \sum_{i=0}^{(\theta+\eta)/2}\sum_{j=0}^{i} a_{i,j,i-j}\Psi_{i,j,i-j}^2, \tag{A2}$$

where the parameters $a_{i,j,i-j}$ are constants.

As a consequence, when $(\Psi_{\theta,m_{x\theta},m_{y\theta}}{}^*\Psi_{\eta,m_{x\eta},m_{y\eta}})_d$ is not trivially null, i.e., when $m_x(\Psi_{\theta,m_{x\theta},m_{y\theta}}\Psi_{\eta,m_{x\eta},m_{y\eta}})$ and $m_y(\Psi_{\theta,m_{x\theta},m_{y\theta}}\Psi_{\eta,m_{x\eta},m_{y\eta}})$ are even, this inner product will be given by

$$\begin{aligned}(\Psi_{\theta,m_{x\theta},m_{y\theta}} * \Psi_{\eta,m_{x\eta},m_{y\eta}})_d &= \sum_{i=0}^{(\theta+\eta)/2}\sum_{j=0}^{i} a_{i,j,i-j}\|\Psi_{i,j,i-j}\|_d^2 = \sum_{i=0}^{(\theta+\eta)/2}\sum_{j=0}^{i} a_{i,j,i-j}\|\Psi_{i,j,i-j}\|_c^2 \\ &= (\Psi_{\theta,m_{x\theta},m_{y\theta}} * \Psi_{\eta,m_{x\eta},m_{y\eta}})_c\end{aligned} \tag{A3}$$

because (i) the norms of functions Ψ_θ are preserved and (ii) Eq. (A2) is true in both continuous and discrete space.

In this manner, since functions Ψ_θ are orthogonal in continuous space, they will also be orthogonal in discrete space with respect to the inner product, Eq. (36).

This result can be easily generalized for three-dimensional lattices.

APPENDIX B

Considering the D2Q9 lattice, the norm and orthogonality restrictions give for the functions

$$\{\Psi_0, \Psi_{1,x}, \Psi_{1,y}, \Psi_{2,xx}, \Psi_{2,yy}, \Psi_{2,xy}\} \tag{B1}$$

the following system of equations:

$$\frac{1}{\pi}\left[\int_{-\infty}^{\infty} e^{-C_{0y}^2}\left(\int_{-\infty}^{\infty} e^{-C_{0x}^2} 1 dC_{0x}\right) dC_{0y}\right] = 1 = W_0 + 4W_1 + 4W_2,$$

$$\frac{1}{\pi}\left[\int_{-\infty}^{\infty} e^{-C_{0y}^2}\left(\int_{-\infty}^{\infty} e^{-C_{0x}^2}(2C_{0x})^2 dC_{0x}\right) dC_{0y}\right] = 2 = 8a^2 W_1 + 16a^2 W_2,$$

$$\frac{1}{\pi}\left(\int_{-\infty}^{\infty} e^{-C_{0y}^2}\left\{\int_{-\infty}^{\infty} e^{-C_{0x}^2}\left[2\left(C_{0x}^2 - \frac{1}{2}\right)\right]^2 dC_{0x}\right\} dC_{0y}\right) = 2 = W_0 + 4W_2(2a^2-1)^2 + W_1[2(2a^2-1)^2 + 2],$$

$$\frac{1}{\pi}\left[\int_{-\infty}^{\infty} e^{-C_{0y}^2}\left(\int_{-\infty}^{\infty} e^{-C_{0x}^2}(2C_{0x}C_{0y})^2 dC_{0x}\right) dC_{0y}\right] = 1 = 16a^4 W_2,$$

$$\frac{1}{\pi}\left\{\int_{-\infty}^{\infty} e^{-C_{0y}^2}\left[\int_{-\infty}^{\infty} e^{-C_{0x}^2} 1 \times 2\left(C_{0x}^2 - \frac{1}{2}\right) dC_{0x}\right] dC_{0y}\right\} = 0 = W_1(4a^2-4) - W_0 + W_2(8a^2-4),$$

$$\frac{1}{\pi}\left\{\int_{-\infty}^{\infty} e^{-C_{0y}^2}\left[\int_{-\infty}^{\infty} e^{-C_{0x}^2} 2\left(C_{0x}^2 - \frac{1}{2}\right) \times 2\left(C_{0y}^2 - \frac{1}{2}\right) dC_{0x}\right] dC_{0y}\right\} = 0 = W_0 + W_1(4-8a^2) + 4W_2(2a^2-1)^2,$$

where identical equations and the inner products giving odd velocity functions were previously excluded.

There are only four independent equations. The solution of the above system gives the classically known values $a = \sqrt{3/2}$, $W_0 = 16/36$, $W_1 = 4/36$, and $W_2 = 1/36$, which are also the solutions when only the first four equations, related to the norm restrictions, are considered. In this manner, the two linearly independent orthogonality conditions are satisfied by the solution of the norm equations. This outcome was the same for all the lattice that have been analyzed in this work, and Appendix A shows that this result is, in fact, a consequence of general properties of Hermite polynomials and of the Bravais lattices structure.

[1] P. Lallemand and L. S. Luo, Phys. Rev. E **68**, 036706 (2003).
[2] G. R. McNamara and G. Zanetti, Phys. Rev. Lett. **61**, 2332 (1988).
[3] F. J. Higuera and J. Jimenez, Europhys. Lett. **9**, 663 (1989).
[4] S. Chen, H. Chen, D. Martinez, and W. H. Matthaeus, Phys. Rev. Lett. **67**, 3776 (1991).
[5] Y. H. Qian, D. d'Humières, and P. Lallemand, Europhys. Lett. **17**, 479 (1992).
[6] H. Chen, S. Chen, and W. H. Matthaeus, Phys. Rev. A **45**, R5339 (1992).
[7] P. Bhatnagar, E. Gross, and M. Krook, Phys. Rev. **94**, 511 (1954).
[8] F. J. Alexander, S. Chen, and J. D. Sterling, Phys. Rev. E **47**, R2249 (1993).
[9] Y. Chen, H. Ohashi, and M. Akiyama, Phys. Rev. E **50**, 2776 (1994).
[10] G. McNamara and B. J. Alder, Physica A **194**, 218 (1993).
[11] X. He, S. Chen, and G. D. Doolen, J. Comput. Phys. **146**, 282 (1998).
[12] D. d'Humières, in *Progress in Astronautics and Aeronautics*, edited by B. D. Shizgal and D. P. Weaver (AIAA, Washington, D.C., 1992), Vol. 159, pp. 450–458.
[13] D. d'Humières, M. Bouzidi, and P. Lallemand, Phys. Rev. E **63**, 066702 (2001).
[14] J. Tolke, M. Krafczyk, M. Schulz, E. Rank, and R. Berrios, Int. J. Mod. Phys. C **9**, 1143 (1998).
[15] K. Sankaranarayanan, X. Shan, I. G. Kevrekidis, and S. Sundaresan, J. Fluid Mech. **452**, 61 (2002).
[16] X. He and L. S. Luo, Phys. Rev. E **56**, 6811 (1997).
[17] S. Succi, *The Lattice Boltzmann Equation* (Clarendon Press, Oxford, 2001).
[18] P. Pavlo, G. Vahala, and L. Vahala, J. Stat. Phys. **107**, 499 (2002).
[19] X. He and G. D. Doolen, J. Stat. Phys. **107**, 309 (2002).
[20] X. Shan and X. He, Phys. Rev. Lett. **80**, 65 (1998).
[21] H. Grad, in *Handbuch der Physik* (Springer, New York, 1958), Vol. 12.

APPENDIX D

The following paper was published in the *International Journal of Modern Physics C*, in 2007.

International Journal of Modern Physics C
Vol. 18, No. 4 (2007) 546–555

World Scientific
www.worldscientific.com

THERMAL LATTICE BOLTZMANN IN TWO DIMENSIONS

DIOGO NARDELLI SIEBERT*, LUIZ ADOLFO HEGELE, Jr.†, RODRIGO SURMAS‡, LUÍS ORLANDO EMERICH DOS SANTOS§ and PAULO CESAR PHILIPPI¶

Mechanical Engineering Department, Federal University of Santa Catarina
88040-900 Florianópolis, SC, Brazil
**diogo@lmpt.ufsc.br*
†*hegele@lmpt.ufsc.br*
‡*surmas@lmpt.ufsc.br*
§*emerich@lmpt.ufsc.br*
¶*philippi@lmpt.ufsc.br*

The velocity discretization is a critical step in deriving the lattice Boltzmann (LBE) from the Boltzmann equation. The velocity discretization problem was considered in a recent paper (Philippi et al., *From the continuous to the lattice Boltzmann equation: the discretization problem and thermal models*, *Physical Review E* 73: 56702, 2006) following a new approach and giving the minimal discrete velocity sets in accordance with the order of approximation that is required for the LBE with respect to the Boltzmann equation. As a consequence, two-dimensional lattices and their respective equilibrium distributions were derived and discussed, considering the order of approximation that was required for the LBE. In the present work, a Chapman-Enskog (CE) analysis is performed for deriving the macroscopic transport equations for the mass, momentum and energy for these lattices. The problem of describing the transfer of energy in fluids is discussed in relation with the order of approximation of the LBE model. Simulation of temperature, pressure and velocity steps are also presented to validate the CE analysis.

Keywords: LBE; thermal models; BGK; quadrature.

PACS Nos.: 47.11.-j, 05.10.-a, 51.10.+y.

1. Introduction

A Lattice-Boltzmann model that can handle thermal problems in a satisfactory manner have been the subject of several works.[1,2,3] Unfortunately these models present difficulties, most of them due to deviations in the hydrodynamic equations and numerical instability.

Recently, an alternative procedure to discretize the Maxwell-Boltzmann (MB) distribution was proposed.[4,5] Based on the quadrature of a Hermite polynomial expansion of this distribution, the procedure allows to obtain a lattice Boltzmann equation (LBE) that can recover the moments of the MB distribution up to a desired order.

The objective of this work is to study in more detail the lattices and the equilibrium distributions obtained using the procedure proposed in Ref. 4. We begin with a brief review of the velocity discretization in Section 2. In Section 3 we present

a Chapman-Enskog (CE) analysis for the obtained LBE. Simulation results confronting the transport coefficients obtained in the CE analysis are presented and discussed in Section 4.

2. Velocity discretization in two dimensional problems

The velocity discretization step intends to replace the entire continuous velocity space $\Re^2$ by a finite set of discrete velocities $\boldsymbol{\xi}_i$. A set of *necessary* conditions for the correct hydrodynamic equations to be retrieved is given by assuring that the discrete distributions f_i^{eq} used in the LBE equation satisfy:

$$\langle\varphi\rangle_p^{eq} = \int f^{eq}(\boldsymbol{\xi})\varphi_p(\boldsymbol{\xi})d\boldsymbol{\xi} = \sum_i f_i^{eq}\varphi_p(\boldsymbol{\xi}_i) \tag{1}$$

for all the equilibrium moments, $\langle\varphi_p\rangle^{eq}$, of interest.

Considering discretization as a quadrature problem, the discrete distributions f_i^{eq} in the right-hand side of Eq. (1) are replaced by $f^{eq}(\boldsymbol{\xi}_i)$, i.e., by the value of the MB distribution evaluated at the pole $\boldsymbol{\xi}_i$, multiplied by the weight to be attributed to each velocity vector $\boldsymbol{\xi}_i$ in order to satisfy the quadrature condition.

In this manner, the discretization restrictions, Eq. (1), are replaced by the following quadrature,

$$\langle\varphi_p\rangle^{eq} = \int f^{eq}(\boldsymbol{\xi})\varphi_p(\boldsymbol{\xi})d\boldsymbol{\xi} = \sum_i W_i e^{\frac{m\xi_i^2}{2k_BT_o}}\left(\frac{2\pi k_BT_o}{m}\right) f^{eq}(\boldsymbol{\xi}_i)\varphi_p(\boldsymbol{\xi}_i), \tag{2}$$

where the factor (k_BT_o/m) was introduced to assure W_i to be a dimensionless real number, since $f^{eq}(\boldsymbol{\xi})$ is the number of particles per unit area of the velocity space.

Given a reference temperature T_0, dimensionless velocities can be introduced, defining $\boldsymbol{\xi}_o = (k_BT_o/m)^{-1/2}\boldsymbol{\xi}$ and $\boldsymbol{u}_o = (k_BT_o/m)^{-1/2}\boldsymbol{u}$. Using the dimensionless velocities and a temperature deviation Θ, defined by $\Theta \equiv (T/T_o - 1)$, the MB distribution can be written

$$f^{eq}(\boldsymbol{\xi}_o) = \frac{m}{2\pi k_BT_o}e^{-\xi_o^2/2}\sum_{n=0}^{\infty}\frac{1}{n!}a_{r_n}^{(n)}\mathscr{H}_{r_n}^{(n)}(\boldsymbol{\xi}_o), \tag{3}$$

where $\mathscr{H}_{r_n}^{(n)}(\boldsymbol{\xi}_o)$ are the Hermite polynomial tensors[a] and $r_n = \{\alpha_1, \alpha_2, \ldots, \alpha_n\}$ is a sequence of indexes that characterize a particular element of the n order tensor. The Einstein's summing convention is also used.

The coefficients $a_{r_n}^{(n)}$, can be obtained considering the orthogonality of the Hermite polynomial tensors:

$$a_{r_n}^{(n)} = \left(\frac{k_BT_o}{m}\right)\int f^{eq}(\boldsymbol{\xi}_o)\mathscr{H}_{r_n}^{(n)}(\boldsymbol{\xi}_o)d\boldsymbol{\xi}_o. \tag{5}$$

[a]The Hermite polynomial tensors are defined by the Rodrigues formula

$$\mathscr{H}^{(n)}(\boldsymbol{\xi}_o) = \frac{(-1)^n}{e^{-\xi_o^2/2}}\boldsymbol{\nabla}^n[e^{-\xi_o^2/2}]$$

Now we simplify our description of the equilibrium distribution by cutting off terms of order higher then N, denoting this approximated function by $f^{eq,N}(\boldsymbol{\xi})$. One of the features of the expansion in Eq.(3) is that if a moment of φ_p have an order lower or equal than N:

$$\langle\varphi_p\rangle = \int f^{eq}(\boldsymbol{\xi})\varphi_p(\boldsymbol{\xi})d\boldsymbol{\xi} = \int f^{eq,N}(\boldsymbol{\xi})\varphi_p(\boldsymbol{\xi})d\boldsymbol{\xi}. \tag{6}$$

If we use this property, replacing $f^{eq}(\boldsymbol{\xi})$ by $f^{eq,N}(\boldsymbol{\xi})$ in Eq. (2) and using the expanded form of this function, we retrieve the following relation;

$$\frac{1}{2\pi}\int e^{-\boldsymbol{\xi}_o^2/2}\mathscr{H}^{(j)}_{r_j}(\xi_o)\mathscr{H}^{(n)}_{r_n}(\xi_o)d\boldsymbol{\xi}_o = \sum_i W_i\mathscr{H}^{(j)}_{r_j}(\xi_{o,i})\mathscr{H}^{(n)}_{r_n}(\xi_{o,i}) \tag{7}$$

for all n and $m \leq N$, where $\boldsymbol{\xi}_{o,i}$ is the dimensionless form of the discrete velocities $\boldsymbol{\xi}_i$.

In this manner, the still unknown weights W_i and the discrete velocities $\boldsymbol{\xi}_{o,i}$ must be chosen in such a manner that the orthogonality and norm of the Hermite polynomial tensors $\mathscr{H}^{(n)}_{r_n}$ are assured in the discrete space. In Ref. 4, it was shown that when the discrete velocity space is invariant under $\pi/2$ rotations and reflections about the x and y axes, the norm preservation for all Hermite polynomials of order lower than N in the discrete velocity space results on the orthogonality between these functions.

The former conclusion is very important because it reduces our discretization problem to find the weights W_i and the poles $\boldsymbol{\xi}_{o,i}$ satisfying, solely, the norm restrictions, i.e , Eq. (7) when $n = j$ and $r_n = r_j$. With the exception of a very few lattices, Gaussian-like quadratures does not give a regular discrete set $\boldsymbol{\xi}_{o,i}$. Nevertheless, if a dimensionless velocity set $\{\boldsymbol{c}_i\}$, giving a space-filling lattice, is chosen, the quadrature problem can be considered as the problem of finding the weights W_i and a scaling factor a such that $\boldsymbol{\xi}_{o,i} = a\boldsymbol{c}_i$, satisfying the norm preservation. Considering that the poles $\boldsymbol{c}_i$ are previously known, this quadrature method was named as *quadrature with prescribed abscissae.*

Finally, if we compare the Eq. (1) and Eq.(2) using the expansion in Eq. (3) cutting off terms of order higher then N, we obtain:

$$f_i^{eq} = W_i\sum_{n=0}^{N}\frac{1}{n!}a^{(n)}_{r_n}\mathscr{H}^{(n)}_{r_n}(a\boldsymbol{c}_i) \tag{8}$$

The set of velocity vectors $\boldsymbol{c}_i$ of these models for third (D2V17) and fourth (D2V37) are shown in Fig. (1) and Fig. (2). For the scale factor a and the weights W_i see the Tables 1 and 2. Another lattice that is suitable for thermal problems is the D2V25, because it can recover the moments $\langle\xi^2\xi_\alpha\xi_\beta\rangle$ (for more details see Ref. 4).

3. Chapman-Enskog Analysis

As usual in the Lattice Boltzmann context[2], we begin the CE analysis by a Taylor series expansion of $f(\boldsymbol{x}+\boldsymbol{\xi}_i, t+\delta)$ around the position $\boldsymbol{x}$ and time t and replacing

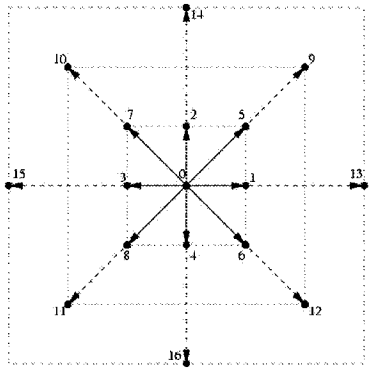

Fig. 1. D2V17 lattice

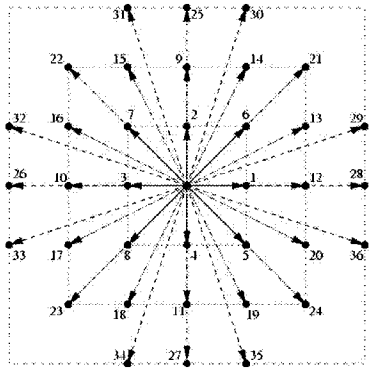

Fig. 2. D2V37 lattice

Table 1. D2V17 weights

i	W_i
0	$\frac{575+193\sqrt{193}}{8100}$
1-4	$\frac{3355-91\sqrt{193}}{18000}$
5-8	$\frac{655+17\sqrt{193}}{27000}$
9-12	$\frac{685-49\sqrt{193}}{54000}$
13-16	$\frac{1445-101\sqrt{193}}{162000}$
a	$\sqrt{\frac{5(25+\sqrt{193})}{72}}$

the resulting expression in the collision/propagation equation with a BGK operator.

Expanding the distribution function and the time derivative in power series of the Knudsen's number (the ratio between the microscopic and the macroscopic length scales) and equating the terms of the same order, we obtain the following equations for the first and second orders:

$$\partial_0 f_i^{(0)} + \xi_{i,\alpha}\partial_\alpha f_i^{(0)} = -\epsilon\frac{f_i^{(1)}}{\tau}, \tag{9}$$

$$\partial_1 f_i^{(0)} + \left(1 - \frac{\delta}{2\tau}\right)\left(\partial_0 f_i^{(1)} + \xi_{i,\alpha}\partial_\alpha f_i^{(1)}\right) = -\epsilon\frac{f_i^{(2)}}{\tau}. \tag{10}$$

The analysis is performed without writing an explicit expression for the equilibrium distribution $f_i^{(0)}$, restricting the attention to the properties this distribution is required to satisfy. These restrictions will be checked latter considering each lattice and respective equilibrium distribution function.

Table 2. D2V37 weights, where $R = (67 + 36\sqrt{30})^{1/3}$

i	W_i
0	$\frac{56266R^2 - 7^{2/3}(19991 - 338\sqrt{30})R + 7^{4/3}(14323 + 6238\sqrt{30})}{264600R^2}$
1-4	$\frac{31206R^2 - 7^{2/3}(3201 + 466\sqrt{30})R - 7^{4/3}(2427 - 706\sqrt{30})}{264600R^2}$
5-8	$\frac{29232R^2 + 7^{2/3}(3888 + 265\sqrt{30})R + 7^{4/3}(216 - 1027\sqrt{30})}{529200R^2}$
9-12	$\frac{42R^2 + 7^{2/3}(33 + 2\sqrt{30})R - \sqrt[3]{7}(3 + 62\sqrt{30})}{3600R^2}$
13-20	$\frac{1638R^2 + 7^{2/3}(1647 + 4\sqrt{30})R - 7^{4/3}(891 + 496\sqrt{30})}{264600R^2}$
21-24	$\frac{-126R^2 + 7^{2/3}(1161 + 194\sqrt{30})R + 7^{4/3}(1107 - 242\sqrt{30})}{1058400R^2}$
25-28	$\frac{14R^2 + 7^{2/3}(131 + 10\sqrt{30})R + 7^{4/3}(17 - 34\sqrt{30})}{264600R^2}$
29-36	$\frac{-168R^2 + 7^{2/3}(228 + 71\sqrt{30})R + 7^{4/3}(516 - 29\sqrt{30})}{1058400R^2}$
a	$\frac{1}{6}\sqrt{49 - \frac{17(7)^{2/3}}{R} + 7^{1/3}R}$

Using the relations:

$$\rho = m \sum_i f_i^{(0)}, \tag{11}$$

$$\rho u_\alpha = m \sum_i f_i^{(0)} \xi_{i,\alpha}, \tag{12}$$

and adding over all velocities in Eq. (9) and Eq. (10) the mass conservation equation is obtained:

$$\partial_t \rho + \partial_\alpha (\rho u_\alpha) = 0. \tag{13}$$

It can be shown that the relations given by Eq. (11) and Eq. (12) together with

$$\rho u_\alpha u_\beta + \rho e \delta_{\alpha\beta} = m \sum_i f_i^{(0)} \xi_{i,\alpha} \xi_{i,\beta}, \tag{14}$$

where $e = \frac{k_B T}{m} = \frac{(k_B T_o)}{m}(\Theta + 1)$ is the internal energy. The former equations leads to the following expression for the macroscopic momentum conservation:

$$\partial_t (\rho u_\alpha) + \partial_\beta (\rho u_\alpha u_\beta) + \partial_\alpha (\rho e) + \left(1 - \frac{\delta}{2\tau}\right) \partial_\beta \Pi_{\alpha\beta}^{(1)} = 0. \tag{15}$$

The tensor $\Pi_{\alpha\beta}^{(1)} \equiv \sum_i f_i^{(1)} \xi_{i,\alpha} \xi_{i,\beta}$ can be obtained by using Eq. (9). If we want the viscous stress tensor to assume the usual form it is necessary that the third order equilibrium moments obey the expression:

$$\rho u_\alpha u_\beta u_\gamma + \rho e (u_\gamma \delta_{\alpha\beta} + u_\alpha \delta_{\gamma\beta} + u_\beta \delta_{\gamma\alpha}) = m \sum_i f_i^{(0)} \xi_{i,\alpha} \xi_{i,\beta} \xi_{i,\gamma}. \tag{16}$$

With this assumption, the momentum conservation equation takes the final form

$$\partial_t(\rho u_\alpha) + \partial_\beta(\rho u_\alpha u_\beta) + \partial_\alpha(\rho e) + \partial_\beta\left[\mu(\partial_\alpha u_\beta + \partial_\beta u_\alpha)\right] - \partial_\beta\left[\lambda(\partial_\gamma u_\gamma)\right] = 0, \quad (17)$$

where the transport coefficients are given by $\mu = \lambda = \rho e\left(\tau - \frac{\delta}{2}\right)$.

The energy equation was obtained using a similar approach. We first multiply the Eq. (9) and Eq. (10) by ξ_i^2 than we sum over all directions. Subtracting from the resulting equation the part relative to the mechanical energy a equation for the evolution of the internal energy is found:

$$\partial_t(\rho e) + \partial_\alpha(\rho e u_\alpha) + \rho e(\partial_\alpha u_\alpha) + \left(1 - \frac{\delta}{2\tau}\right)\left(\partial_\alpha q_\alpha^{(1)} + \Pi_{\alpha\beta}^{(1)}\partial_\alpha u_\beta\right) = 0, \quad (18)$$

where, as in the case of the momentum equation, $q_\alpha^{(1)} \equiv \sum_i \xi_i^2 \xi_{i,\alpha} f_i^{(1)} - u_\beta \Pi_{\alpha\beta}^{(1)}$.

Eq. (9) can be used to calculate $q_\alpha^{(1)}$. Using the Eq. (11), Eq. (12), Eq. (14) and Eq. (16) together with

$$(4\rho e^2 + \rho u^2 e)\delta_{\alpha\beta} + (6\rho e + \rho u^2)u_\alpha u_\beta = m\sum_i f_i^{(0)} \xi_i^2 \xi_{i,\alpha}\xi_{i,\beta} \quad (19)$$

the desired form for the energy equation is recovered,

$$\partial_t(\rho e) + \partial_\alpha(\rho e u_\alpha) + \partial_\alpha[k(\partial_\alpha e)] + [\rho e\delta_{\alpha\beta} + \mu(\partial_\alpha u_\beta + \partial_\beta u_\alpha) + \lambda(\partial_\gamma u_\gamma)\delta_{\alpha\beta}]\partial_\alpha u_\beta = 0, \quad (20)$$

with the thermal diffusivity $k = 2\rho e\left(\tau - \frac{\delta}{2}\right)$.

All the models discussed in the previous section recover the moments up to the third order, consequently these models obey the mass conservation in Eq. (13) and the momentum equation described in Eq. (17). The equilibrium distribution function for the lattice D2V17 cannot recover the moments of fourth order, therefore the internal energy calculated with this lattice does not follow Eq. (20). On the other hand, the distributions for the lattices D2V25 and D2V37 satisfy Eq. (19), thus satisfying the macroscopic energy conservation.

4. Results

In this section, the results obtained in the CE analysis are validated by the measurement of the kinematic viscosity and thermal diffusivity. This is done by comparing the analytical solution of the diffusive problem with simulations. The shock tube problem is also analyzed. The main objective of this analysis is to compare the different lattices. This problem was chosen because predicted analytical solutions are available, boundary conditions are not necessary (the boundary conditions can be very difficult to set in multispeeds schemes) and the computational cost is low (only 1D problems are considered).

4.1. *Diffusive problem*

The diffusive problem can be described as follow:

$$\frac{\partial g(x,t)}{\partial t} = D\frac{\partial^2 g(x,t)}{\partial x^2}, \quad g(0,t) = g_o, \quad g(\infty,t) = 0, \quad g(x,0) = 0 \quad (21)$$

where $x \geq 0$ and $t \geq 0$. The analytical solution of this problem is:

$$D = \frac{1}{t}\left[\frac{x}{2\ \mathrm{invErfc}\left(g(x)/g_o\right)}\right]^2, \tag{22}$$

where x and t are the position and time at the measurement point. This expression can be usefull to calculate the kinematic viscosity (D) if the function $g(x,t)$ is replaced by $u_y(x,t)$ and g_o by a prescribed velocity. If $g(x,t)$ is replaced by $(T(x,t) - T_\infty)/(T_o - T_\infty)$, D will mean the thermal diffusivity.

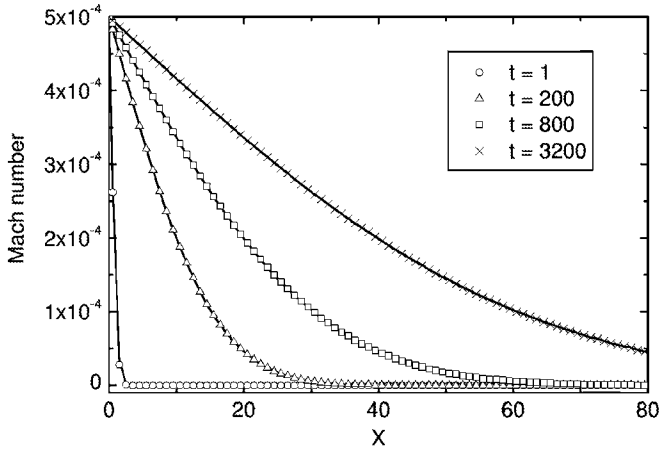

Fig. 3. Momentum diffusion in a D2V37 lattice. The dots are the simulated results and lines are the analytical solutions.

4.2. *Kinematic Viscosity Measurement*

We use a 20000×1 domain with periodic boundary conditions. Considering $x = 0$ in the middle of the simulation domain, we set $u_y = 0.001$ for $x < 0$ and $u_y = 0$ for $x > 0$. Initially the temperature and density are constants in all the domain.

The evolution of this problem is shown in Fig. 3. The simulation results agree with the results of the Chapman-Enskog analysis, with relative errors around 0.01% (see Fig. 4.2 and Fig. 4.2). If the velocity difference is increased, the viscous dissipation can affect the results, but this was not observed until a Mach number difference equal to 0.6. The D2V17 lattice became unstable to Θ less than -0.1 (the same behavior occurred in the temperature and pressure step problems).

4.3. *Thermal Diffusivity Measurement*

For this measurement the same domain of the former simulation was used. The initial condition was a temperature step ($\Theta = 0.001 + \Theta_o$ for $x < 0$ and $\Theta = \Theta_o$ for

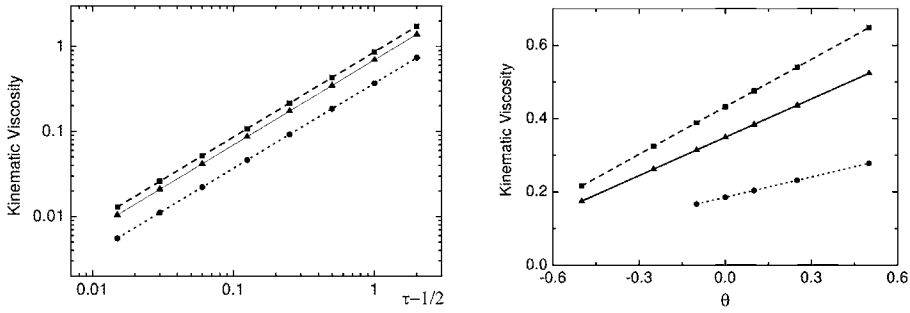

Fig. 4. The variation of the kinematic viscosity (a) with Θ for $\tau = 1$ and (b) with τ for $\Theta = 0$. Simulation results for (●) D2V17, (■) D2V25(W6) and (▲) D2V37 are compared with analytical predictions.

$x > 0$) and the density was set in order to obtain a constant pressure throughout the whole simulation domain.

If Θ_o is zero, as in Fig. 4.3, the thermal diffusivity is correctly recovered in all the lattices with error of the order of 0.01%. If Θ_o deviates even a little from 0 the D2V17 starts to present errors that can be related to the lack of conservation of the fourth order moments. The D2V25(w6) lattice and the D2V37 lattice presented very good agreement with the Chapman-Enskog results in the range $-0.5 < \Theta_o < 0.5$.

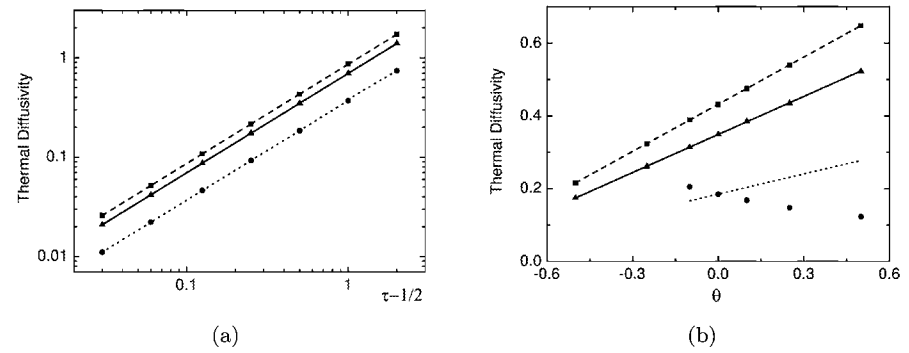

Fig. 5. Thermal diffusivity variation (a) with τ for $\Theta_o = 0$ and (b) with Θ_o for $\tau = 1$. Simulation results for (●) D2V17, (■) D2V25(W6) and (▲) D2V37 are compared with analytical predictions.

4.4. *Shock Tube*

The shock tube problem was also simulated in a 20000×1 domain with periodic boundary conditions. The initial condition used was a density step ($\rho = 1.001$ for

$x < 0$ and $\rho = 1.000$ for $x > 0$) and a constant temperature. The spatial and temporal evolutions are shown in Fig. 4.4 and Fig. 4.4.

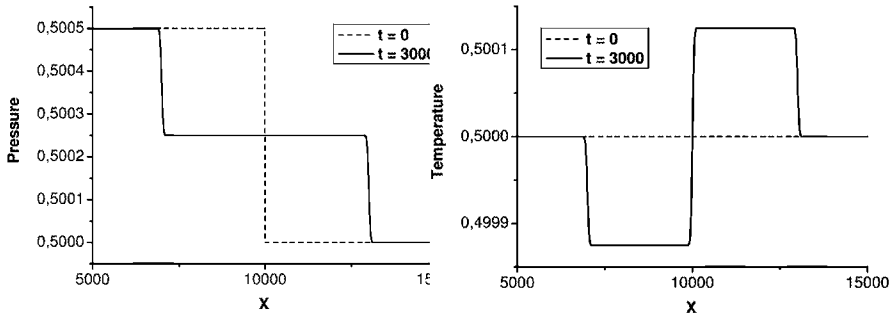

(a) (b)

Fig. 6. Shocktube profile in lattice units for the (a) pressure and (b) temperature.

The sound speed was measured to study its dependence with the temperature. This is shown in Fig. 7. All the lattices presented excelent results (even the D2V17 lattice), with relative errors smaller than 0.01%.

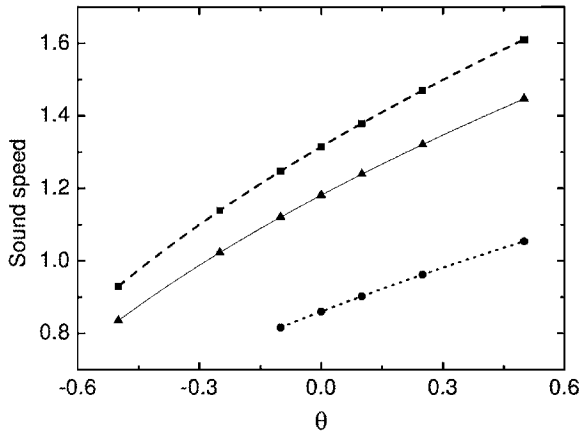

Fig. 7. Sound speed dependence with Θ for the (●) D2V17, (■) D2V25(W6) and (▲) D2V37 lattices. The lines are given by the analyticial expression $c_s = \sqrt{2(\theta + 1)}/a$.

5. Conclusions

In this work, a Chapman-Enskog analysis was performed for deriving the macroscopic transport equations for the mass, momentum and energy for some two-

dimensional multi-speed LBE that were derived using a quadrature with prescribed abscissas method. The problem of describing the transfer of energy in fluids was discussed in relation with the order of approximation of the LBE. Simulation of the temperature, pressure and velocity steps were also presented and used to validate the Chapman-Enskog analysis

Present results did not show any meaningful difference between the D2V25 constructed to recover the $\langle \xi^2 \xi_\alpha \xi_\beta \rangle$ moments and the full fourth order D2V37, when the transport coefficients and sound speed were measured from LB simulations and compared with the Chapman-Enskog theoretical predictions. Both models presented an excellent agreement and showed a comparable stability range, $-0.5 < \Theta < 0.5$, when the relaxation time τ is around 1 or greater.

A von-Neumann stability analysis is, presently, being performed to estimate the Θ stability limits when the relaxation time τ approaches its lower limit $1/2$.

Acknowledgments

Authors are greatly indebted with Capes (Coordenation Foundation of Improvement of Superior Level Personal), CNPq (Brazilian Research Council) and Finep (Brazilian Agency for Research and Projects) for the financial support.

References

1. G. McNamara and B. Alder, *Physica A* **194**, 218 (1993).
2. F. J. Alexander, S. Chen and J. D. Sterling, *Phys. Rev. E* **47**, R2249 (1993).
3. Y. Chen, H. Ohashi and M. Akiyama *Phys. Rev. E* **50**, 2776 (1994).
4. P. C. Philippi, L. A. Hegele Jr., L. O. E. dos Santos and R. Surmas, *Phys. Rev. E* **73**, 056702 (2006).
5. X. Shan, X. Yuan and H. Chen, *J. Fluid Mech.* **550**, 413 (2006).
6. P. L. Bhatnagar, E. P. Gross and M. Krook, *Phys. Rev.* **94**, 511 (1954).

APPENDIX E

The following paper was published in the *International Journal of Modern Physics C*, in 2007.

International Journal of Modern Physics C
Vol. 18, No. 4 (2007) 556–565

World Scientific
www.worldscientific.com

FROM THE BOLTZMANN TO THE LATTICE-BOLTZMANN EQUATION: BEYOND BGK COLLISION MODELS

PAULO CESAR PHILIPPI*, LUIZ ADOLFO HEGELE, Jr.†, RODRIGO SURMAS‡, DIOGO NARDELLI SIEBERT§ and LUÍS ORLANDO EMERICH DOS SANTOS¶

Mechanical Engineering Department, Federal University of Santa Catarina
88040-900 Florianópolis, SC, Brazil
**philippi@lmpt.ufsc.br*
†*hegele@lmpt.ufsc.br*
‡*surmas@lmpt.ufsc.br*
§*diogo@lmpt.ufsc.br*
¶*emerich@lmpt.ufsc.br*

In this work, we present a derivation for the lattice-Boltzmann equation directly from the linearized Boltzmann equation, combining the following main features: multiple relaxation times and thermodynamic consistency in the description of non isothermal compressible flows. The method presented here is based on the discretization of increasingly order kinetic models of the Boltzmann equation. Following a Gross-Jackson procedure, the linearized collision term is developed in Hermite polynomial tensors and the resulting infinite series is diagonalized after a chosen integer N, establishing the order of approximation of the collision term. The velocity space is discretized, in accordance with a quadrature method based on prescribed abscissas (Philippi *et al.*, *Phys. Rev E* 73, 056702, 2006). The problem of describing the energy transfer is discussed, in relation with the order of approximation of a two relaxation-times lattice Boltzmann model. The velocity-step, temperature-step and the shock tube problems are investigated, adopting lattices with 37, 53 and 81 velocities.

Keywords: Lattice Boltzmann equation; thermal models; multiple relaxation times.

PACS Nos.: 47.11.-j, 05.10.-a, 51.10.+y.

1. Introduction

The lattice-Boltzmann equation (LBE) was introduced by McNamara & Zanetti [1], replacing the Boolean variables in the discrete collision-propagation equations of the lattice gas model by their *ensemble* averages. Higuera & Jimenez [2] proposed a linearization of the collision operator derived from the Boolean models, recognizing that this full form was unnecessarily complex when the main purpose was to retrieve the hydrodynamic equations. Following this line of reasoning, Chen *et al.* [3] suggested replacing the collision term by a single relaxation-time term, followed by Qian *et al.* [4], who introduced a model based on the Bhatnagar, Gross and Krook (BGK) collision term [5], retrieving the incompressible Navier-Stokes equations with third-order non-physical terms in the local speed, u. The BGK collision term describes the relaxation of the distribution function to a prescribed equilibrium. This discrete

equilibrium distribution was settled by writing it as a second-order polynomial expansion in the particle-velocity $\boldsymbol{c}_i$, with coefficients adjusted to retrieve the mass density, the local velocity and the momentum flux, which are necessary conditions for satisfying the Navier-Stokes equations.

Thermal lattice-BGK schemes included higher order terms in the equilibrium distribution function [6,7], requiring to increase the number of vectors in the velocity set $\{\boldsymbol{c}_i, i = 0, ..., b\}$. Nevertheless, the polynomial expansion form in the particle-velocity $\boldsymbol{c}_i$, with adjustable parameters, was retained, and the numerical simulations were performed on arbitrary lattices.

In thermal problems, the BGK collision term restricts the models to a fixed Prandtl number. To allow a variable Prandtl number, at least two relaxation times are needed. In this way, a two-parameters model was introduced by He *et al.* [8] using two sets of distributions for the particles number density and the thermodynamic internal energy, coupled through a viscous dissipation term and proposed to be run in a two-dimensional nine-velocities lattice. Full multiple relaxation time (MRT) models were firstly introduced in the LBE framework by d'Humières [9]. In that model, dispersion relations are used as constraints for the adjustable parameters related to the short wave-length non-hydrodynamic moments, and numerical stability is assured by damping these higher frequency moments [10].

The presently known lattice-Boltzmann equations have not been able to handle realistic thermal and fully compressible flow problems with satisfaction, since the simulation of the LBE is, frequently, followed by numerical instabilities when the local velocity increases [11,12]. In fact, in previous works dealing with MRT models, the main concern is the *numerical stability* and *not* the description of non-isothermal or multi-component fluid flows, which, effectively, require additional relaxation parameters.

In a previous paper [13], a construction principle for the LBE was derived considering the velocity discretization problem as a quadrature problem with prescribed abscissas. When the N_f^{th} order of approximation of a Hermite polynomial expansion to the Maxwell-Boltzmann (MB) equilibrium distribution is chosen, the infinite and enumerable basis of the Hilbert space is replaced by a *finite* set of Hermite polynomial tensors, restricting the solutions to N_f^{th}-degree polynomials in the velocity $\boldsymbol{c}$. The quadrature problem was, then, considered as to select a regular lattice $\{\boldsymbol{c}_i\}$, in such a manner that the Hermite polynomials preserve the orthogonality. This was shown to be possible by assuring that the norm of *each one* of these functions is retrieved, *exactly*, by the quadrature. It was,also, shown that when the quadrature problem is solved, the 2θ-rank velocity tensors are isotropic, for $\theta = 1, ...N_f$. Similar results were, almost simultaneously, obtained by Shan *et al.* [14], although using a different formulation.

In this paper, the collision model is obtained in accordance with a Gross-Jackson procedure [15], using its development in Hermite polynomial tensors. The resulting infinite series is diagonalized after a chosen order N, establishing the order of approximation to the linearized Boltzmann equation.

For validating the model, the velocity-step, temperature-step, and shock tube problems are investigated, using the 37, 53 and 81 velocities lattices for several different combinations of parameters.

2. Kinetic models for the Boltzmann equation

The Boltzmann equation [16,17], without external forces, reads

$$\partial_t f + \boldsymbol{c}.\nabla f = \Omega, \tag{1}$$

where $\boldsymbol{c}$ is the particles velocity and Ω the collision integral.

The equilibrium solution of the Boltzmann equation is the Maxwell-Boltzmann distribution,

$$f^{eq} = n_d \left(\frac{m}{2\pi kT}\right)^{D/2} e^{-\frac{(\boldsymbol{c}-\boldsymbol{u})^2}{\frac{2kT}{m}}}, \tag{2}$$

satisfying

$$\int f^{eq} d\boldsymbol{c} = n_d, \tag{3}$$

$$\int f^{eq} \boldsymbol{c} d\boldsymbol{c} = n_d \boldsymbol{u}, \tag{4}$$

$$\int \frac{1}{2} m f^{eq} \left(\boldsymbol{c} - u\right)^2 d\boldsymbol{c} = \frac{D}{2} n_d kT, \tag{5}$$

where n_d is the number density of the particles with mass m, $\boldsymbol{u}$ is the local velocity, T is the thermodynamic temperature, and D the dimension of the physical space.

Writing the distribution $f = f^{eq} + f^{neq}$, with $f^{neq} = f^{eq}\phi$, when f is near f^{eq}, the collision term can be written as

$$\Omega = f^{eq}\mathcal{L}\{\phi\}, \tag{6}$$

where $\mathcal{L}$ is a linear operator.

Considering the dimensionless peculiar velocity $\boldsymbol{\mathcal{C}}_f = \left(\frac{m}{2kT}\right)^{1/2} (\boldsymbol{c} - \boldsymbol{u})$, $\mathscr{H}_{\theta,(r_\theta)}$ to be an Hermite polynomial tensor [13], where (r_θ) is a sequence of indexes $r_1, r_2, ...r_\theta$, the perturbation ϕ can be developed as [17,18,19],

$$\phi = \sum_\theta a_{\theta,(r_\theta)}(\boldsymbol{x}, t)\, \mathscr{H}_{\theta,(r_\theta)}(\boldsymbol{\mathcal{C}}_f), \tag{7}$$

where repeated indexes means summation. The coefficients a_θ can be related to the macroscopic moments of f. Clearly, $a_0 = 0$, $a_{1,\alpha} = 0$.

The viscous stress tensor,

$$P_{\alpha\beta} = \int m f \left(c_\alpha - u_\alpha\right)\left(c_\beta - u_\beta\right) d\boldsymbol{c}, \tag{8}$$

is related to the second order perturbation coefficient as

$$a_{2,\alpha\beta} = \frac{P_{\alpha\beta}}{2p}, \tag{9}$$

where $p = n_d kT$ is the thermodynamic pressure. Due to the energy conservation, the trace of P is null. Similarly, the net heat flux, q_α, can be related to the contracted third order perturbation coefficient $a_{3,\alpha\gamma\gamma}$, and so forth with the higher order moments.

Using the development of perturbation ϕ, Eq. (7),

$$\mathcal{L}\{\phi\} = \sum_\theta a_{\theta,(r_\theta)} \mathcal{L}\{\mathscr{H}_{\theta,(r_\theta)}\}. \tag{10}$$

The resulting function from $\mathcal{L}\left(\mathscr{H}_{\theta,(r_\theta)}\right)$ can be developed in terms of the θ-order Hermite tensors that belong to the orthogonal basis of this space,

$$\mathcal{L}\{\mathscr{H}_{\theta,(r_\theta)}\} = \sum_{(s_\theta)} \gamma_{(r_\theta),(s_\theta)} \mathscr{H}_{\theta,(s_\theta)}, \tag{11}$$

where $\gamma_{(r_\theta),(s_\theta)}$ designate the $(r_\theta),(s_\theta)$ components of 2θ-order *relaxation tensors*. As $\mathcal{L}$ is a self-adjoint operator, its eigenvalues are non-positive. When the terms above a chosen order N are diagonalized, following a Gross-Jackson procedure [15,16], Eq. (10) reads

$$\mathcal{L}\{\phi\} = -\sum_{\theta=0}^{N} \lambda_{(r_\theta),(s_\theta)} a_{\theta,(r_\theta)} \mathscr{H}_{\theta,(s_\theta)} - \gamma_{N+1}\phi, \tag{12}$$

where $\lambda_{(r_\theta),(s_\theta)} = -\gamma_{(r_\theta),(s_\theta)} - \gamma_{N+1}\delta_{(r_\theta),(s_\theta)}$ is positive for all r_θ, s_θ, since $\lambda_{(r_\theta),(s_\theta)} = -\gamma_{(r_\theta),(s_\theta)}$ for all off-diagonal components, and the diagonal components $\gamma_{(r_\theta),(r_\theta)}$ are negative with an absolute value that is greater than γ_{N+1} for all θ smaller or equal to N. Eq. (12) can be considered as an N^{th}-order kinetic model to the collision term, with an absorption term $\gamma_{N+1}\phi$ resulting from the diagonalization of the relaxation tensors after a given N. Therefore, all the moments of order higher than N are collapsed into a single non-equilibrium term. When $N = 0$ or $N = 1$, Eq. (12) gives the well known BGK model, when all the collision operator spectra is replaced by a single relaxation term. Each term in the sum, Eq. (12), gives the relaxation to the equilibrium of second or higher order kinetic moments that are not preserved in collisions.

2.1. *Second Order Collision Model*

We focus our analysis to the two dimensional space and second order models ($N = 2$). From Eq. (12)

$$\lambda_{(r_2),(s_2)} a_{2,(r_2)} \mathscr{H}_{2,(s_2)} = \lambda_{\alpha\beta\gamma\delta} a_{2,\alpha\beta} \mathscr{H}_{2,\gamma\delta}. \tag{13}$$

Requiring isotropy of the 4^{th} rank relaxation tensor, it reads

$$\lambda_{\alpha\beta\gamma\delta} = \lambda_1 \delta_{\alpha\beta}\delta_{\gamma\delta} + \lambda_2 \delta_{\alpha\gamma}\delta_{\beta\delta} + \lambda_3 \delta_{\alpha\delta}\delta_{\beta\gamma}. \tag{14}$$

After some straightforward algebra, Eq. (13) reads

$$\lambda_{\alpha\beta\gamma\delta} a_{2,\alpha\beta} \mathscr{H}_{2,\gamma\delta} = \frac{\lambda_\mu}{p}\left[\tau_{xx}\mathcal{C}_{fx}^2 + \tau_{yy}\mathcal{C}_{fy}^2 + 2\tau_{xy}\mathcal{C}_{fx}\mathcal{C}_{fy}\right], \tag{15}$$

since $a_{2,\alpha\alpha} = 0$, and $\lambda_\mu = \lambda_1 + \lambda_2$. Finally, from Eq. (12), the second order collision term model in two dimensions, together with the advection term of the Boltzmann equation, can be written as

$$\partial_t f + \boldsymbol{c}.\nabla_r f = -f^{eq}\left(\frac{2\lambda_\mu}{p}\left[\tau_{xx}\mathcal{C}_{fx}^2 + \tau_{yy}\mathcal{C}_{fy}^2 + 2\tau_{xy}\mathcal{C}_{fx}\mathcal{C}_{fy}\right] + \gamma_3\phi\right). \tag{16}$$

2.2. *Chapman-Enskog analysis for the second order model in two dimensions*

Considering $f^{(0)}$ in the asymptotic expansion

$$f = f^{(0)} + K_n f^{(1)} + ..., \tag{17}$$

to be the Maxwell-Boltzmann equilibrium distribution $f^{eq}(n, \boldsymbol{u}, T)$, where K_n is the Knudsen number, the zeroth order time derivative, resulting from the Chapman-Enskog induced decomposition of the time derivative ($\partial_t = \partial_0 + K_n\partial_1 + ...$), reads,

$$\begin{aligned}\frac{\partial_0 f^{(0)}}{f^{(0)}} &= 2\left(\mathcal{C}_{f\alpha}\mathcal{C}_{f\beta} - \frac{1}{2}\delta_{\alpha\beta}\right)\partial_\beta u_\alpha - \left(\mathcal{C}_f^2 - 1\right)\nabla.\boldsymbol{u} \\ &\quad + \left(\frac{2kT}{m}\right)^{1/2}\left(\mathcal{C}_f^2 - 2\right)\boldsymbol{\mathcal{C}}_f.\nabla \ln T.\end{aligned} \tag{18}$$

Using Eqs. (18) and (16),

$$\begin{aligned}&2\left(\mathcal{C}_{fx}^2 - \frac{1}{2}\right)\partial_x u_x + 2\left(\mathcal{C}_{fy}^2 - \frac{1}{2}\right)\partial_y u_y + 2\mathcal{C}_{fx}\mathcal{C}_{fy}\left(\partial_x u_y + \partial_y u_x\right) \\ &- \left[\left(\mathcal{C}_{fx}^2 - \frac{1}{2}\right) + \left(\mathcal{C}_{fy}^2 - \frac{1}{2}\right)\right]\nabla.\boldsymbol{u} + \left(\frac{2kT}{m}\right)^{1/2}\left(\mathcal{C}_f^2 - 2\right)\boldsymbol{\mathcal{C}}_f.\nabla \ln T \\ &= -\frac{2\lambda_\mu}{p}\left[\tau_{xx}\mathcal{C}_{fx}^2 + \tau_{yy}\mathcal{C}_{fy}^2 + 2\tau_{xy}\mathcal{C}_{fx}\mathcal{C}_{fy}\right] - \gamma_3\phi.\end{aligned} \tag{19}$$

Eqs. (18) and (19) are used to derive, in a formal way, constitutive equations for the viscous stress tensor, $\tau_{\alpha\beta}$, and the net heat flux, q_α. The transport coefficients found by this procedure are the first and the second viscosity coefficients, namely

$$\mu = \eta = \frac{nkT}{2\lambda_\mu + \gamma_3}, \tag{20}$$

and the thermal conductivity, according to the Fourier's Law $q_\alpha = -\kappa\partial_\alpha T$,

$$\kappa = \frac{2nk^2T}{m}\frac{1}{\gamma_3}. \tag{21}$$

In this manner, the present second-order continuous kinetic model is thermodynamically consistent and able for analyzing non-isothermal and fully compressible flows, which are described by independently tunable Reynolds and Prandtl numbers. Consideration of third-order collision models will be, only, necessary, in multicomponent systems, for correctly describing third-order coupling, for instance, the Soret and Dufour effects [19].

3. Two-dimensional lattices for thermal problems

The discretized advection term of the Boltzmann equation, adopted here, is the usual *propagation* term of the Lattice Boltzmann Equation or, formally, an explicit first order upwind finite-difference scheme. Hence, with the discretized collision term, for two dimensions, the particle evolution equation reads as

$$f_i(\boldsymbol{x}^* + \boldsymbol{e_i}, t^* + 1) - f_i(\boldsymbol{x}^*, t^*) = \frac{1}{\tau}\left(f_i^{eq}(\boldsymbol{x}^*, t^*) - f_i(\boldsymbol{x}^*, t^*)\right) - \frac{1}{\tau_\mu} f_i^{eq}(\boldsymbol{x}^*, t^*) \frac{P^*_{\alpha\beta}}{p^* e^*}(e_{i\alpha} - u^*_\alpha)(e_{i\beta} - u^*_\beta) \tag{22}$$

where, $\frac{1}{\tau} = \gamma_3 \delta$, $\frac{1}{\tau_\mu} = \lambda_\mu \delta$, δ is the physical time increment, and the star tagged variables are dimensionless variables.

The N_f^{th}- order approximation for the equilibrium distribution, in the discrete space, can be written as [13]

$$f^{eq}_{i,N_f} = w_i \sum_{\theta=0}^{N_f} a^{eq}_{\theta,(r_\theta)}\left(n, \boldsymbol{u}^*, \Theta\right) \mathscr{H}_{\theta,(r_\theta)}\left(\boldsymbol{e}_i\right), \tag{23}$$

where w_i is the discrete weight associated with the speed of the i-direction, and Θ is the temperature deviation, defined as $\Theta = \frac{T}{T_0} - 1$ (where T_0 is a reference temperature) and related to the lattice internal energy e^* through

$$e^* = \frac{\Theta + 1}{2a^2}, \tag{24}$$

where a is a scaling factor, depending on a chosen lattice. The sound speed is related to the scaling factor through

$$c_s = \frac{\sqrt{\Theta + 1}}{a}. \tag{25}$$

For this evolution equation, when performing the Chapman-Enskog analysis, the calculation of the momentum flux requires the 4^{th}-order moments to be correctly retrieved. The kinematic viscosity is given by

$$\nu = \frac{\Theta + 1}{2a^2}\left(\frac{1}{\frac{2}{\tau_\mu} + \frac{1}{\tau}} - \frac{1}{2}\right), \tag{26}$$

which is closely related to Eq. (20). The parameter $-1/2$ is due to the spatial discretization. A lattice with 37 velocities (D2V37) [13] was found to be the *minimal* space filling lattice correctly retrieving the momentum flux, for this two collision-parameters model. The set of velocity vectors composing this lattice is the following one, $|e_i| = \left\{0, 1, \sqrt{2}, 2, \sqrt{5}, 2\sqrt{2}, 3, \sqrt{10}\right\}$.

The thermal diffusivity coefficient has the following form,

$$\alpha = \frac{\Theta + 1}{2a^2}\left(\tau - \frac{1}{2}\right). \tag{27}$$

although the heat flux vector contains errors $\mathcal{O}(u^{*6}, \Theta u^{*4}, \Theta^2 u^{*2})$. The D2V37 lattice is able to retrieve only 4^{th}-order moments, and a 5^{th}-order approximation to the equilibrium distribution lattice proved to be necessary. A lattice with 53 velocities (D2V53) fulfilling these constraints was, then, obtained, according to the method exposed in Ref. 13. The velocity vectors follow the sequence $|e_i| = \left\{0, 1, \sqrt{2}, 2, \sqrt{5}, 2\sqrt{2}, 3, \sqrt{10}, \sqrt{13}, 4, \sqrt{17}\right\}$. The D2V53 lattice was found to be the minimal two-dimensional space-filling lattice for the *correct* description of the flow of energy with this two relaxation time collision model, without any Knudsen first order errors.

4. Numerical Simulations

In the simulations, the D2V37 and D2V53 lattices and also a 81 velocity lattice (D2V81), with a 6^{th} order approximation to the maxwellian equilibrium distribution, were used. We numerically measured the sound speed, kinematic viscosity and thermal diffusivity. We also present results for the shock tube problem.

4.1. *Transport coefficients*

Several numerical simulations for the transport coefficients were carried out. The measured results are compared with the analytical results. Fig. 1.a shows the results for the sound speed versus the temperature deviation Θ. The sound speed increases with the number of lattice discrete velocities. Excellent agreement has been found between the numerical experiments and the analytical results. The measurement of the kinematic viscosity was done using a velocity-step. The results for the kinematic viscosity was plotted versus the Prandtl number (Pr) for the different lattices. The temperature deviation Θ was set to 0, and the Prandtl number varies from 0.01 to 100. The results are presented in Fig. 1.b and show excellent agreement between the theory and simulation. For the measurement of the thermal diffusivity, a temperature-step was used. The thermal diffusivity was plotted against the temperature deviation and the results are shown in Fig. 2. All the results show excellent agreement between numerical experiments and theoretical predictions.

4.2. *Shock tube*

For the shock tube problem, a D2V81 lattice and a domain with 10^5 sites was used. The temperature deviation was set to 0 at $t^* = 0$, and $Pr = 1$. The ratio between the densities is 4. Fig. 3 shows the numerical results for density, temperature, pressure and velocity after 2,000 time steps. The pressure level is correctly predicted when compared with analytical results.

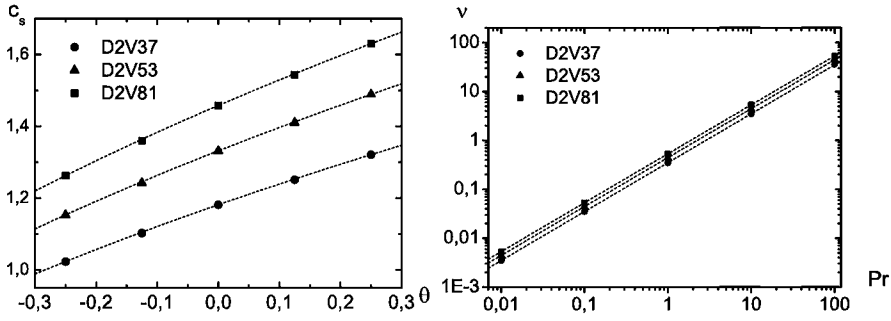

(a) (b)

Fig. 1. Results of the numerical mesurements for the D2V37, D2V53 and D2V81 lattices for: (a) speed of sound versus temperature, and (b) kinematic viscosity versus Prandtl number. In both graphics, the dotted lines are the analytical results.

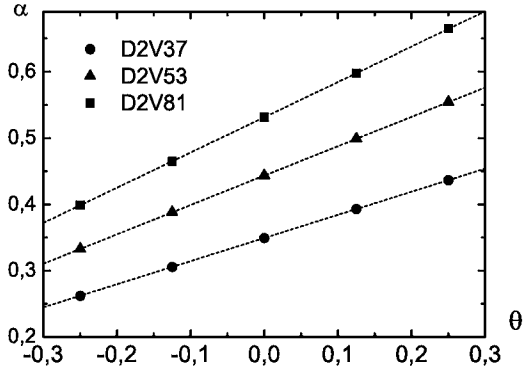

Fig. 2. Results of the numerical measurements of thermal diffusivity versus the temperature deviation Θ for the D2V37, D2V53 and D2V81 lattices. Dotted lines are analytical results.

5. Conclusions

In this work, a method for simulating non-isothermal compressible flows within the lattice Boltzmann framework was presented. The linearized collision term of the Boltzmann equation was expanded in terms of non-equilibrium moments and discretized. Analytical results for the transport coefficients were reported and agree very well with the numerical experiments. The collision model can also be used for

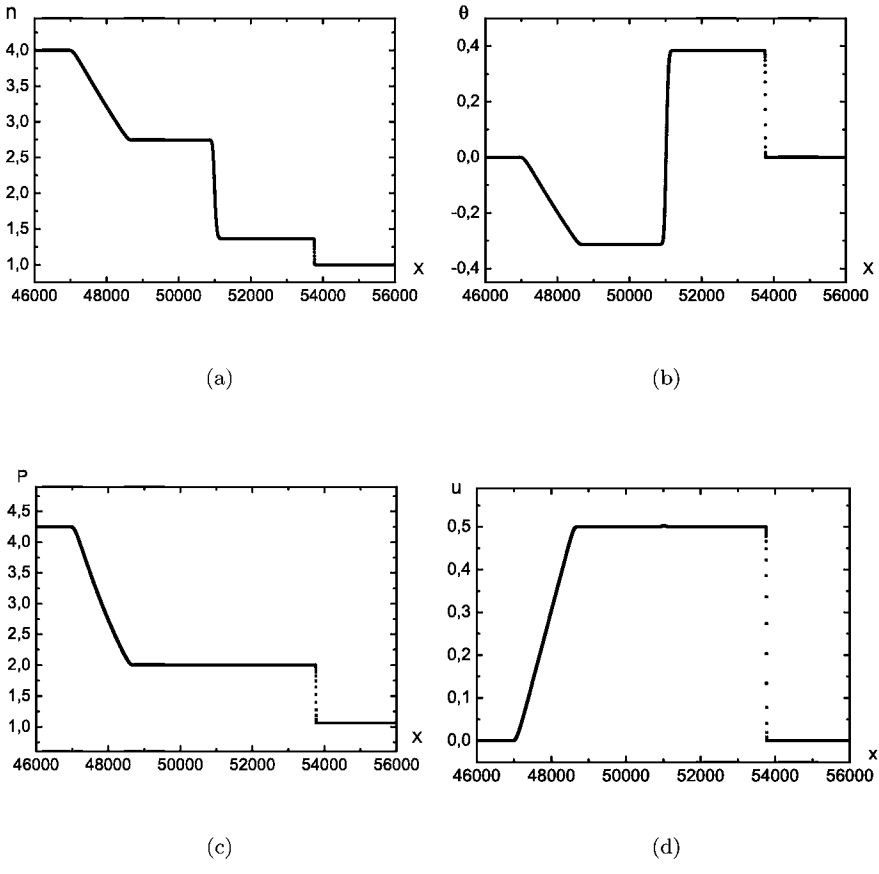

Fig. 3. Results for the (a) density, (b) temperature deviation, (c) pressure and (d) velocity profiles in the shock tube problem ($t^* = 2,000$).

multi-component modeling, if one want to obtain tunable independent parameters for the transport coefficients in the macroscopic equations.

Acknowledgements

The authors would like to acknowledge the financial support of CNPq (Conselho Nacional de Desenvolvimento Científico e Tecnológico), ANP (Agência Nacional do Petróleo) and FINEP (Financiadora de Estudos e Projetos).

References

1. G. R. McNamara and G. Zanetti, *Phys. Rev. Lett.* **61**, 2332 (1988).
2. F. J. Higuera and J. Jimenez, *Europhys. Lett. E* **9**, 663 (1989).
3. H. Chen, S. Chen and W. Mathaeus, *Phys. Rev. A* **45**, R5339 (1992).
4. Y. H. Qian, D. d'Humières and P. Lallemand, *Europhys. Lett.* **17**, 479 (1992).

5. P. L. Bhatnagar, E. P. Gross and M. Krook, *Phys. Rev.* **94**, 511 (1954).
6. F. J. Alexander, S. Chen and J. D. Sterling, *Phys. Rev. E* **47**, R2249 (1993).
7. Y. Chen, H. Ohashi and M. Akyama, *Phys. Rev. E* **50**, 2776 (1994).
8. X. He, S. Chen and G. D. Doolen, *J. Comp. Phys.* **146**, 282 (1998).
9. D. d'Humières, in *Rarefied Gas Dynamics: Theory and Simulations* (ed. B. D. Shizgal & D. P. Weaver). *Prog. Astronaut. Aeronaut.* **159**, 450 (1992).
10. P. Lallemand and L. S. Luo, *Phys. Rev. E* **61**, 6546 (2000).
11. P. Lallemand and L. S. Luo, *Phys. Rev. E* **68**, 036706 (2003).
12. S. Succi, *The Lattice Boltzmann Equation for Fluid Dynamics and Beyond* (Clarendon Press, Oxford, 1998).
13. P. C. Philippi, L. A. Hegele Jr., L. O. E. dos Santos and R. Surmas, *Phys. Rev. E* **73**, 056702 (2006).
14. X. Shan, X. Yuan and H. Chen, *J. Fluid Mech.* **550**, 413 (2006).
15. E. P. Gross and E. A. Jackson, *Phys. Fluids* **2**, 432 (1959).
16. C. Cercignani, *Mathematical Methods in Kinetic Theory* (Macmillan, London, 1969).
17. H. Grad, *Principles of the Kinetic Theory of Gases* in *Handbuch der Physik*, vol. 12, pp. 205-294, (Springer, New York, 1958).
18. X. Shan and X. He, *Phys. Rev. Lett.* **80**, 65 (1998).
19. P. C. Philippi and R. Brun, *Physica A* **105**, 147 (1981).

APPENDIX F

The following paper was published in *Physical Review E* in 2008.

Lattice Boltzmann equation linear stability analysis: Thermal and athermal models

D. N. Siebert,* L. A. Hegele, Jr.,† and P. C. Philippi‡
LMPT Mechanical Engineering Department, Federal University of Santa Catarina, 88040-900 Florianopolis, SC, Brazil
(Received 1 October 2007; published 26 February 2008)

Although several thermal lattice Boltzmann models have been proposed, this method has not yet been shown to be able to describe nonisothermal fully compressible flows in a satisfactory manner, mostly due to the presence of important deviations from the advection-diffusion macroscopic equations and also due to numerical instabilities. In this context, this paper presents a linear stability analysis for some lattice Boltzmann models that were recently derived as discrete forms of the continuous Boltzmann equation [P. C. Philippi, L. A. Hegele, Jr., L. O. E. dos Santos, and R. Surmas, Phys. Rev. E **63**, 056702 (2006)], in order to investigate the sources of instability and to find, for each model, the upper and lower limits for the macroscopic variables, between which it is possible to ensure a stable behavior. The results for two-dimensional (2D) lattices with 9, 17, 25, and 37 velocities indicate that increasing the order of approximation of the lattice Boltzmann equation enhances stability. Results are also presented for an athermal 2D nine-velocity model, the accuracy of which has been improved with respect to the standard D2Q9 model, by adding third-order terms in the lattice Boltzmann equation.

DOI: 10.1103/PhysRevE.77.026707 PACS number(s): 47.11.−j, 05.10.−a, 51.10.+y

I. INTRODUCTION

The main goal of the lattice Boltzmann method is to model the dynamical behavior of a fluid on the kinetic level. This purpose is accomplished by calculating the evolution of the distribution function in space and time, given a discrete set of velocities.

The lattice-Boltzmann equation (LBE) was first introduced by McNamara and Zanetti [1], replacing the lattice gas automata Boolean variables, [2], in the discrete collision-propagation equations, with their ensemble averages.

Higuera and Jiménez [3] proposed a linearization of the collision term derived from the Boolean models, recognizing that this full form was unnecessarily complex when the main purpose was to retrieve the hydrodynamic equations.

Following this line of reasoning, Chen *et al.* [4] suggested replacing the collision term with a single relaxation time term, followed by Qian *et al.* [5], who introduced a model based on the Bhatnagar-Gross-Krook (BGK) model [6], retrieving the incompressible Navier-Stokes equations with third-order errors in the local speed.

The BGK collision term describes the relaxation of the distribution function toward an equilibrium distribution. This discrete equilibrium distribution was settled in lattice Boltzmann models by writing it as a second-order polynomial expansion in the local fluid velocity, with adjustable parameters in order to retrieve the mass density, the local velocity and the momentum flux equilibrium moments, which are necessary conditions for satisfying the Navier-Stokes equations.

Thermal lattice Boltzmann models were firstly treated by Alexander *et al.* [7], who extended the Qian *et al.* second-order equilibrium distribution to a third-order model for solving some thermohydrodynamic problems, resulting in a good agreement when compared with analytical solutions.

McNamara and Alder [8], found a set of 13 and 26 restrictions that this expansion must satisfy to retrieve the correct advection-diffusion macroscopic equations, respectively, in two and three dimensions.

Nonlinear deviations in the momentum and energy equations, in the model of Alexander and co-workers, were found by Chen *et al.* [9], who introduced a fourth order polynomial expansion into the equilibrium distribution, fitting adjustable parameters. These authors used combinations of square lattices for satisfying the restrictions imposed by the Chapman-Enskog analysis and found a 16-velocity lattice in two dimensions and a lattice with 41 velocities in three dimensions.

With the exception of McNamara and Zanetti's unconditionally stable LBE, [1], all the above models have stability issues [8,9].

In these studies the equilibrium distribution was written as finite expansions in the local velocity with free parameters that were adjusted to satisfy some main restrictions to retrieve the full advection-diffusion equations. Consequently, there is no formal link connecting the LBE to the Boltzmann equation.

This connection has been first established by He and Luo [10] who directly derived the LBE from the Boltzmann equation for some widely known lattices (D2Q9, D2Q6, D2Q7, D3Q27) by the discretization of the velocity space, using the Gauss-Hermite and Gauss-Radau quadrature. Excluding the above mentioned lattices, the discrete velocity sets obtained by this kind of quadrature do not generate regular space-filling lattices.

Philippi *et al.* [11] derived a construction principle for the LBE considering the velocity discretization problem as a quadrature problem with prescribed abscissas, starting from the Boltzmann equation. It was formally shown that the number of discrete velocities is directly related to the order of approximation of the discrete equilibrium distribution, with respect to the full Maxwell-Boltzmann (MB) distribution and, consequently, to the highest order of the kinetic

*diogo@lmpt.ufsc.br
†hegele@lmpt.ufsc.br
‡philippi@lmpt.ufsc.br

moments that are to be correctly retrieved. Similar results were, almost simultaneously, obtained by Shan *et al.* [12], although using a different procedure.

In this manner, lattices that are able to retrieve second-, third-, and fourth-order terms in the Maxwellian distribution were derived.

The results of Philippi *et al.* were followed by a rigorous Chapman-Enskog analysis of the derived LBE, [13]. It was shown that, when the collision term is written as a BGK single relaxation-time term, the first-order Knudsen internal energy balance equations are only retrieved without errors with the fourth-order LBE.

Three fourth-order two-dimensional models were derived by Philippi *et al.*: The first two based on a set of 25 discrete velocities and the third on a set of 37 velocities. The 37-velocity model was the only one that was written with a complete set of fourth-order Hermite polynomials and since all these three lattice BGK (LBGK) models give the correct thermohydrodynamics, it appeared to be important to determine in which manner the addition of these high-order Hermite polynomials affects the LBE stability in nonisothermal problems.

The stability limits were also obtained in athermal problems, when the temperature deviations are kept null and the sole source of instability is the local speed.

In both the athermal and thermal models it was found that the main reason for instability is the lack of accuracy of the LBE representation with respect to the full continuous Boltzmann equation and that the attainment of larger stability ranges requires an increase in the order of approximation of the LBE.

This is an important result, since this also requires an increase in the number of velocities and is somewhat in contradiction with past studies dealing with simulations using multispeed models where the addition of speeds being led to an increase in instability [14]. In fact, in past studies, the *a posteriore* nature of these methods provided no means to avoid the stability issues in a satisfactory manner.

In this study, it is shown that the construction principle derived by Philippi *et al.* [11], leads to LB models, in which stability can be enhanced by increasing the number of discrete velocities in a systematic way.

It is also shown that stability can be improved by adding higher order Hermite polynomials in the MB polynomial expansion, when the norm of such polynomials is preserved in the discrete space, although this addition has no effect on its first-order Knudsen number behavior. In this paper, this is shown to be true for the D2Q9 athermal LBE.

This paper is organized as follows. In Sec. II the velocity discretization procedure is briefly presented. In Sec. III, some highlights of linear stability analysis are provided. The stability maps obtained for the various models are also presented. Section IV concludes the paper.

II. DISCRETE VELOCITY MODELS FOR THERMAL PROBLEMS

The LBE for collision-propagation schemes can be formally considered as a particular case of an explicit first-order upwind finite-difference numerical approximation of the continuous Boltzmann equation and can be written, for a given point $\boldsymbol{x}$ at a time t, as

$$f_i(\boldsymbol{x}^* + \boldsymbol{c}_i, t^* + 1) - f_i(\boldsymbol{x}^*, t^*) = \Omega_i, \tag{1}$$

where $\boldsymbol{x}^* = \boldsymbol{x}/h$ and $t^* = t/\delta$ are given in dimensionless lattice units, $\boldsymbol{c}_i$ are the usual dimensionless lattice vectors, h and δ are the spatial and time steps and Ω_i is the discretized collision term, usually a collision model such as the BGK single relaxation time model [6] or a multiple relaxation time model [15,16]. In most cases the collision operator Ω_i depends on the explicit form of the local equilibrium distribution function, so when the velocity discretization is performed it is necessary to choose a suitable form for this distribution.

For the BGK collision operator, a Chapman-Enskog analysis shows that the correct hydrodynamic equations are retrieved when the discrete distributions f_i^{eq} have the same moments as the MB distribution up to a third-order term for isothermal problems and some additional fourth-order terms for thermal problems. In many models this function is obtained by a power series of the local velocity $\boldsymbol{u}$, where the coefficients of this expansion are chosen so that f_i^{eq} follows the relation

$$\langle \varphi_p \rangle^{\mathrm{eq}} = \int f^{\mathrm{eq}}(\boldsymbol{\xi}) \varphi_p(\boldsymbol{\xi}) d\boldsymbol{\xi} = \sum_i f_i^{\mathrm{eq}} \varphi_p(\boldsymbol{\xi}_i), \tag{2}$$

where $f^{\mathrm{eq}}(\boldsymbol{\xi})$ is the MB distribution function.

In Philippi *et al.* [11], the discretization of the velocity space is considered as a quadrature problem, i.e., the discrete distributions f_i^{eq} in the right-hand side of Eq. (2) are replaced by the value of a polynomial approximation of the MB distribution evaluated at the pole $\boldsymbol{\xi}_i$, multiplied by a parameter $\mathcal{W}_i$, which represents the weight to be attributed to each velocity vector $\boldsymbol{\xi}_i$ required by the quadrature condition.

Defining a dimensionless velocity $\boldsymbol{\xi}_o = (kT_0/m)^{-1/2}\boldsymbol{\xi}$, the MB distribution can be written as an infinite series of Hermite polynomial tensors $\mathcal{H}^{(n)}_{r_n}(\boldsymbol{\xi}_o)$ [16,17],

$$f^{\mathrm{eq}}(\boldsymbol{\xi}_o) = \left(\frac{m}{kT_0}\right)^{D/2} \frac{e^{-\xi_0^2/2}}{(2\pi)^{D/2}} \sum_n \frac{1}{n!} a^{(n)}_{r_n} \mathcal{H}^{(n)}_{r_n}(\boldsymbol{\xi}_o), \tag{3}$$

where T_0 is a reference and constant temperature, D is the space dimension, and the coefficients $a^{(n)}_{r_n}$ are related to the macroscopic properties at equilibrium and can be found using the orthogonality properties of the Hermite polynomials [13]. An approximated form of the MB distribution $f_i^{\mathrm{eq},N}$ is obtained when the polynomial expansion in Eq. (3) is truncated in the Nth order. It is, nevertheless, important to note that any moment of a velocity polynomial φ_p whose order is equal to or lower than N will be the same as when it is calculated with the full MB distribution:

$$\int f^{\mathrm{eq}} \varphi_p(\boldsymbol{\xi}) d\boldsymbol{\xi} = \int f^{\mathrm{eq},N} \varphi_p(\boldsymbol{\xi}) d\boldsymbol{\xi}. \tag{4}$$

In this manner, to retrieve the correct moments of the MB equilibrium distribution in a discrete velocity space, based on a few velocity vectors, a quadrature is performed, enabling

the integration of the polynomial velocity functions up to a chosen order, without errors. This allows us to write

$$\int f^{\mathrm{eq}}(\boldsymbol{\xi})\varphi_p(\boldsymbol{\xi})d\boldsymbol{\xi} = \sum_i \mathcal{W}_i f^{\mathrm{eq},N}(\boldsymbol{\xi}_i)\varphi_p(\boldsymbol{\xi}_i). \tag{5}$$

The weights $\mathcal{W}_i$ can be written in terms of the conventional dimensionless weights w_i by using

$$\mathcal{W}_i = w_i e^{\xi_o^2/2}\left(\frac{2\pi k T_0}{m}\right)^{D/2}. \tag{6}$$

In Ref. [11], the use of prescribed abcissas was proposed to perform the quadrature, i.e., the velocity vectors $\boldsymbol{\xi}_{o,i}$ are chosen and weights w_i and a scale factor are determined from the quadrature restrictions. This scale factor relates the dimensionless velocity vectors to the usual lattice vectors through $\boldsymbol{\xi}_{o,i}=a\boldsymbol{c}_i$. The authors also showed that when a lattice that is invariant by coordinate permutation and reflection is chosen, the following norm preservation equations assure the orthogonality of the Hermite polynomials in the discrete space:

$$\sum_{i=0}^{b} \omega_i[\mathcal{H}_{r_n}^{(n)}(\boldsymbol{\xi}_{o,i})]^2 = \frac{1}{(2\pi)^{D/2}}\int e^{-\xi_o^2/2}[\mathcal{H}_{r_n}^{(n)}(\boldsymbol{\xi}_o)]^2 d\boldsymbol{\xi}_o \tag{7}$$

for all Hermite polynomial tensors $\mathcal{H}_{r_n}^{(n)}$ with an order lower than or equal to N. In this manner, the discrete velocities are chosen in such a manner as to make the number of variables—the weights and the scale factor—equal to the number of linearly independent equations given by Eq. (7). When this set of equations has a solution, this condition assures that the norm of the Hermite polynomial tensors in discrete space is the same as in continuous space.

By defining $f_i \equiv \mathcal{W}_i f(\boldsymbol{\xi}_i)$, it is possible to obtain the usual form of the discrete equilibrium distribution used in the lattice LBM,

$$f_i^{\mathrm{eq}} = w_i \sum_{n=0}^{N} \frac{1}{n!} a_{r_n}^{(n)} \mathcal{H}_{r_n}^{(n)}(a\boldsymbol{c}_i). \tag{8}$$

Some sets of velocities and the equilibrium distributions for the third- and fourth-order models, which are used in this study, can be found in the Appendix.

III. LINEAR STABILITY ANALYSIS

Instability is a common feature of numeric discrete methods. Since LBM (i) is based on polynomial approximations of the full continuous Boltzmann equation and (ii) discretization is always performed with errors that are proportional to some power of the spatial scale, h, and time step, δ, (iii) and the method is explicit in time, so the LBE is also subject to numerical instabilities.

As discussed in Sec. II, the LBM can be considered as an explicit first-order finite-difference method, so von Neumann linear stability analysis can be applied to the LBE. In the present von Neumann analysis, the aim is to obtain the response of a system, described by a set of equations, which is slightly removed from a given equilibrium state by a small perturbation. When this perturbation is not absorbed by the system itself, such an equilibrium state is considered to be unstable and the mathematical description for this system is unable to describe the system in this state. This is performed using spatial wave perturbations, the effects of which can be superposed, when this physical system is described by linear equations.

Most LBE are nonlinear because they are based on collision operators that are quadratic in f_i. This requires the linearization of the LBE and, although this simplification limits the analysis to small perturbations, it can provide valuable information about the stability behavior of the LBE models. The LBE linearization is performed by developing the collision term in a Taylor series around a global equilibrium distribution $\bar{f}_i$:

$$\bar{f}_i = f_i^{\mathrm{eq}}|_{\bar{\rho},\bar{\boldsymbol{u}},\bar{e}} \tag{9}$$

related to an equilibrium state given by the set of variables $\bar{\rho}$, $\bar{\boldsymbol{u}}$, and $\bar{e}$, where stability is analyzed.

Noting that the collision operator is a function of f_i, i.e., $\Omega_i \equiv \Omega_i(f_0, f_1, \ldots, f_b)$ this Taylor expansion can be written in the form

$$\Omega_i(f) = \Omega_i|_{\bar{f}} + \sum_j \left.\frac{\partial \Omega_i}{\partial \bar{f}_j}\right|_{\bar{f}} \delta f_j + \mathcal{O}(\delta f_j^2), \tag{10}$$

where $\delta f_i \equiv f_i - \bar{f}_i$. The zeroth-order term in Eq. (10) vanishes because $\bar{f}$ is an equilibrium distribution. Replacing this expansion in Eq. (1) and neglecting the second-order terms in δf_i,

$$\delta f_i(\boldsymbol{x}+\boldsymbol{c}_i, t+1) - \delta f_i(\boldsymbol{x}, t) = \sum_{j=0}^{b} \left.\frac{\partial \Omega_i}{\partial \bar{f}_j}\right|_{\bar{f}} (\delta f_j). \tag{11}$$

Performing a discrete Fourier transform in Eq. (11) the following equation for the $\boldsymbol{k}$ wave number component of δf_i is then obtained:

$$\delta f_i(\boldsymbol{k}, t+1) = e^{-i\boldsymbol{c}_i\cdot\boldsymbol{k}} \sum_{j=0}^{b} \left[\delta_{ij} + \left.\frac{\partial \Omega_i}{\partial \bar{f}_j}\right|_{\bar{f}}\right] \delta f_j(\boldsymbol{k}, t). \tag{12}$$

The above equation gives the time evolution of the fluctuation $\delta f_i(\boldsymbol{k}, t)$ from its initial value $\delta f_i(\boldsymbol{k}, 0)$. For convenience this equation will be rewritten using

$$|\delta f_i(\boldsymbol{k}, t+1)\rangle = \hat{L}|\delta f_i(\boldsymbol{k}, t)\rangle, \tag{13}$$

where the Dirac notation for vectors was used and the operator $\hat{L}$ is related to the matrix,

$$L_{ij} = e^{-i\boldsymbol{c}_i\cdot\boldsymbol{k}}\left[\delta_{ij} + \left.\frac{\partial \Omega_i}{\partial \bar{f}_j}\right|_{\bar{f}}\right]. \tag{14}$$

Let the eigenvectors of L_{ij} be denoted by $|z_l\rangle$ and their respective eigenvalues by z_l. In the present case it is suitable to choose these eigenvectors as a basis for representing the perturbed state at $t=0$, $|\delta f(\boldsymbol{k}, 0)\rangle$, because when the $\hat{L}$ operator is applied on these vectors it results in $\hat{L}|z_l\rangle = z_l|z_l\rangle$. In

this manner, after t repeated applications of $\hat{L}$,

$$|\delta f(\boldsymbol{k},t)\rangle = \hat{L}^t|\delta f(\boldsymbol{k},0)\rangle = \sum_{l=0}^{b} b_l(z_l)^t|z_l\rangle, \tag{15}$$

where $b_l=\langle z_l|\,\delta f(\boldsymbol{k},0)\rangle$. Equation (15) shows that the behavior of $|\delta f(\boldsymbol{k},t)\rangle$ can be determined by its eigenvalues z_l and, consequently, that the solution will not diverge for $t\to\infty$ if the complex modulus of the eigenvalues z_l are less than 1 for all values of l.

In conclusion, the investigation of the stability of a physical state given by $\bar{\rho}$, $\bar{u}$ and $\bar{e}$, requires, in von Neumann stability theory, the calculation of the eigenvalues z_l of the L_{ij} matrix. This state is considered to be stable when $|z_l|$ is smaller than 1 for all values of $\boldsymbol{k}$, whose moduli can assume values from 0 to 2π since the L_{ij} matrix elements depend on the wavenumber through the periodic function $e^{-i\boldsymbol{k}\cdot\boldsymbol{c}_i}$.

A. Stability maps of some two-dimensional LBE

In this section the procedure described in the previous section is used to find the stability maps of some two-dimensional LBE proposed by Philippi *et al.*, [11]. We restrict our attention to the BGK, single relaxation time, collision model [6],

$$\Omega_i = \frac{f_i^{\mathrm{eq}} - f_i}{\tau^*}, \tag{16}$$

where $\tau^*=\tau/\delta$ is the dimensionless form of the relaxation time.

The LAPACK++ (Linear Algebra Package for the C++ language) was used to numerically solve the eigenvalue problem, since analytical solutions are only possible for a few particular cases.

The use of numerical methods for obtaining the stability maps is hindered by the large number of diagonalizations required since the matrix must be evaluated for several values of the wave number $\boldsymbol{k}$. In this manner, the dependence of the L_{ij} eigenvalues on the orientation of $\boldsymbol{k}$ was investigated. The results showed that the most unstable case occurs when vectors $\boldsymbol{k}$ and $\boldsymbol{u}$ are parallel, so in the analysis, the orientation of $\boldsymbol{k}$ is restricted to this case. Previous studies on stability have also considered this restriction [18,19].

In particular, Sterling and Chen, [15] have also considered vectors $\boldsymbol{k}$ and $\boldsymbol{u}$ to be parallel to the x axis. Nevertheless, it is shown in Fig. 1 that this assumption can lead to erroneous conclusions. In this figure, the stability limits of the local speed speed $\boldsymbol{u}$ are shown for three different orientations of $\boldsymbol{k}$, for the D2Q9 athermal LBE. The symbol θ gives the angular orientation of vector $\boldsymbol{k}$ with respect to the x axis. In this case, it can be seen that the most critical orientation corresponds to $\theta=\pi/4$ and not to $\theta=0$ as in Sterling and Chen [15]. Thus it can be concluded that the effect of this orientation on the stability limits must be taken into account for each LBE.

For these reasons, for each LBE the stability is investigated considering several values of the wave number k from zero to π distributed in accordance with a fixed interval $\Delta k=0.005$ and several values of the angle θ in the range of 0 to $\pi/4$ spaced by an interval of $\Delta\theta=\pi/100$.

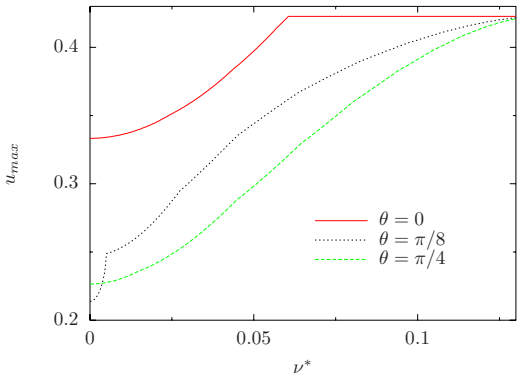

FIG. 1. (Color online) Dependence of the stability limits on the orientation of the wave vector $\boldsymbol{k}$ with respect to the x axis for the D2Q9 LBGK model, where $\nu^*=(\tau^*-1/2)/3$.

1. Athermal models

Our analysis begins with a study of models that use the D2Q9 lattice. The usual D2Q9, first suggested by Qian *et al.* [5], has a second-order equilibrium distribution and can be obtained from the MB distribution by the method described in Sec. II when the order of approximation is set to $N=2$ and the temperature is kept constant and equal to T_o. This lattice was chosen because some third-order moments can be incorporated into this second-order equilibrium distribution using the quadrature procedure described in Sec. II.

In fact, for this LBE, when the weights obtained for the second-order model are used, the norm of the third-order Hermite polynomials $\mathcal{H}^{(3)}_{xxy}$ and $\mathcal{H}^{(3)}_{xyy}$ are also preserved. This allows the inclusion of the related third-order moments in the equilibrium distribution, which takes on the following form:

$$f_i^{\mathrm{eq}} = \rho w_i\left\{1 + 3(\boldsymbol{u}\cdot\boldsymbol{c}_i) + \frac{9}{2}(\boldsymbol{u}\cdot\boldsymbol{c}_i)^2 - \frac{3}{2}u^2 + \frac{27}{2}\left[u_x^2(c_{y,i}u_y)\left(c_{x,i}^2 - \frac{1}{3}\right) + u_y^2(c_{x,i}u_x)\left(c_{y,i}^2 - \frac{1}{3}\right)\right]\right\}. \tag{17}$$

Since this inclusion does not have any effect on the second-order and lower equilibrium moments, the momentum balance macroscopic equations continue to be affected by third-order $\mathcal{O}(u^3)$ errors and the question that remains to be answered is whether the inclusion of these third-order Hermite polynomials has any effect on the LBE stability.

In this manner the D2Q9 stability was analyzed by comparing the D2Q9 LBGK with a second- and a third-order equilibrium distribution. These models were also compared with the Lallemand and Luo, [18], multiple relaxation time (MRT) model, since this model was also built with the aim of improving the LBE stability.

The present analysis can be found in Fig. 2 and is focused on values of the relaxation time very close to its singular limit 1/2. The abscissa was chosen as $1/\tau^*$ in order to compare with previous results from Ref. [18]. It can be observed that both the second- and the third-order LBGK models present a homogeneous decrease in the local speed stability

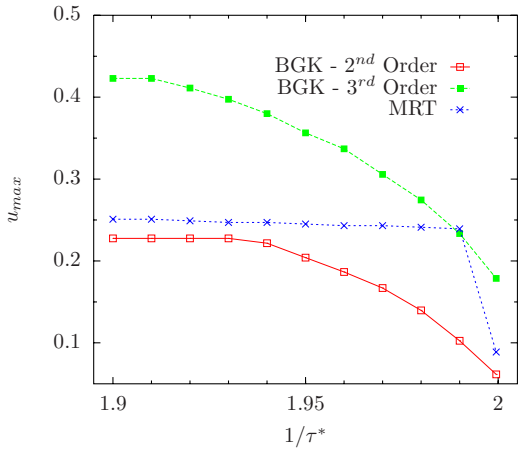

FIG. 2. (Color online) Maximum speed assuring linear stability for models using the D2Q9 lattice.

limit when the relaxation time approaches 1/2, whereas this limit remains insensitive to the τ^* variation in the MRT model, up to $\tau^*=0.50251$. Although the results presented by Lallemand and Luo are not related to quasi-incompressible models, as the present LBGK ones are, they attributed the better performance of the MRT model with respect to the second-order LBGK to the use of high frequency relaxation terms in modeling the collision term.

Figure 2 shows, nevertheless, that the third-order LBGK model has a considerably better performance when compared with the second-order one and with the MRT model in what concerns its stability limits. In this manner, the addition of third-order velocity polynomials largely improve the stability range and this improvement is due to the equilibrium distribution representation itself and not to the use of extra relaxation terms in the collision model. This is an important conclusion, since it avoids the use of MRT dispersion relations for the adjustable parameters—related to the short wavelength nonhydrodynamic moments—to increase numerical stability.

In fact, the improvement of the stability limits by increasing the order of the polynomial approximation to the full MB equilibrium distribution in LBGK models has shown to be a general result. This can be seen in Fig. 3, where the second order LBGK D2Q9 model is compared with the full third-order D2V17 and with the full fourth-order D2V37 models, derived by Philippi *et al.* [11]. These LBE are shown in the Appendix of the present paper. For the athermal results shown in Fig. 3 the temperature T was kept constant, $T=T_0$.

In the use of LBM it is of great interest to solve high Reynolds number flow problems and this usually requires dealing with low values of the kinematic viscosity and, consequently, with relaxation times very close to their lower limits. A Chanpman-Enskog analysis, [13], shows that for these three models the dimensionless kinematic viscosity is given by

$$\nu^* = \frac{1}{a^2}\left(\tau^* - \frac{1}{2}\right). \tag{18}$$

Since the scale factor a is dependent on the lattice, it is better to draw the lattice maps in terms of the dimensionless kine-

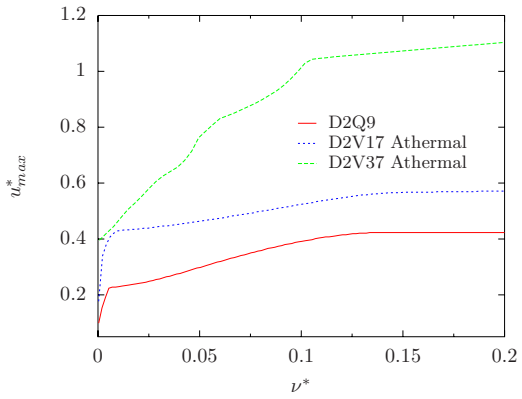

FIG. 3. (Color online) Stability map for the second-, third-, and fourth-order athermal models.

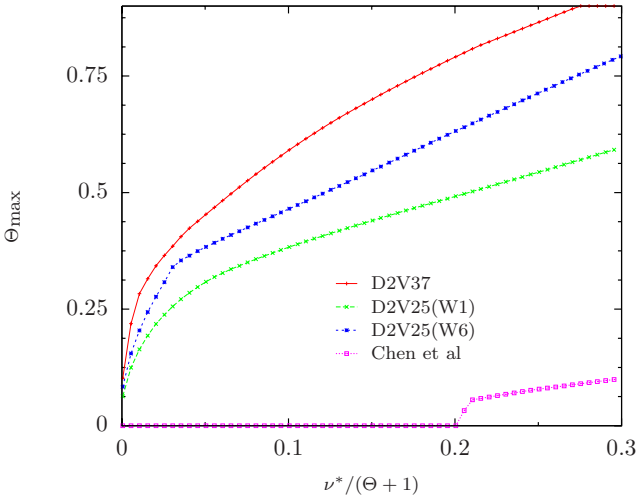

(a) $\Theta > 0$

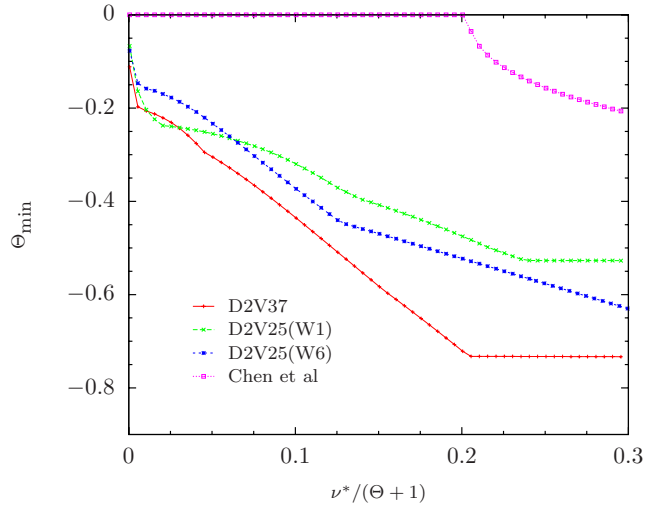

(b) $\Theta < 0$

FIG. 4. (Color online) Positive and negative maximum stable values for deviation of the temperature from T_o for $u^*=0$.

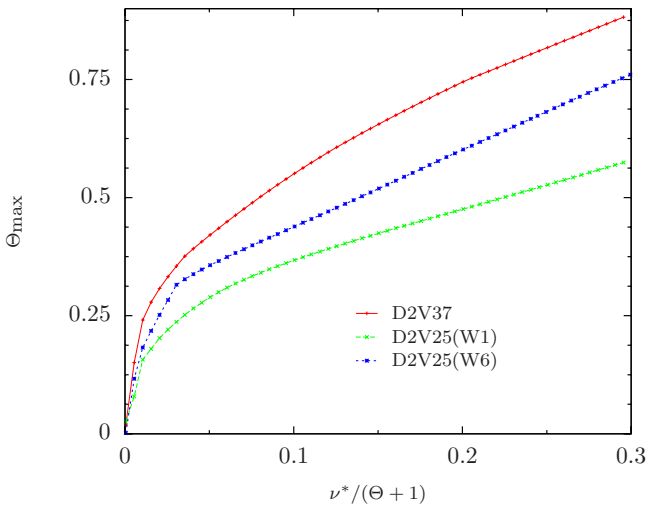

(a) $\Theta > 0$

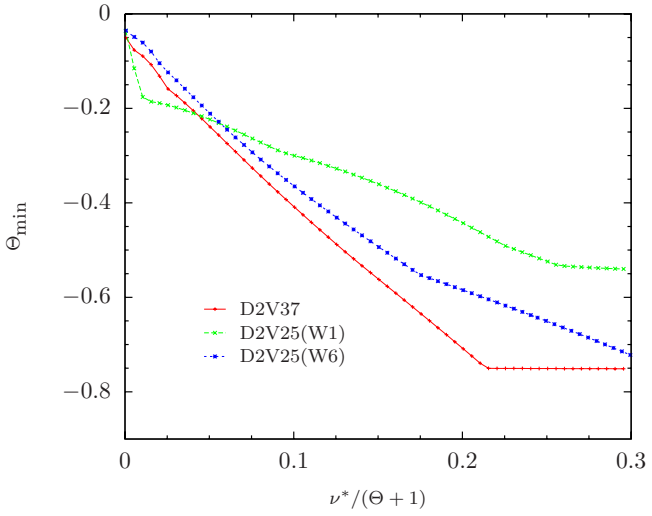

(b) $\Theta < 0$

FIG. 5. (Color online) Positive and negative maximum stable values for deviation of the temperature from T_o for $u^*=0.2$.

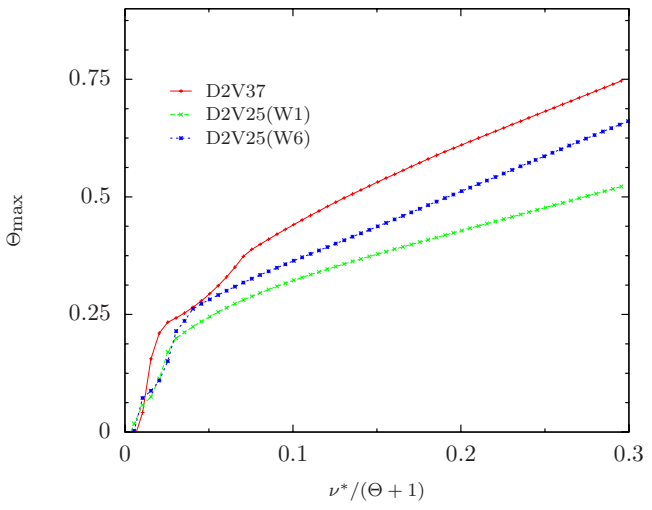

(a) $\Theta > 0$

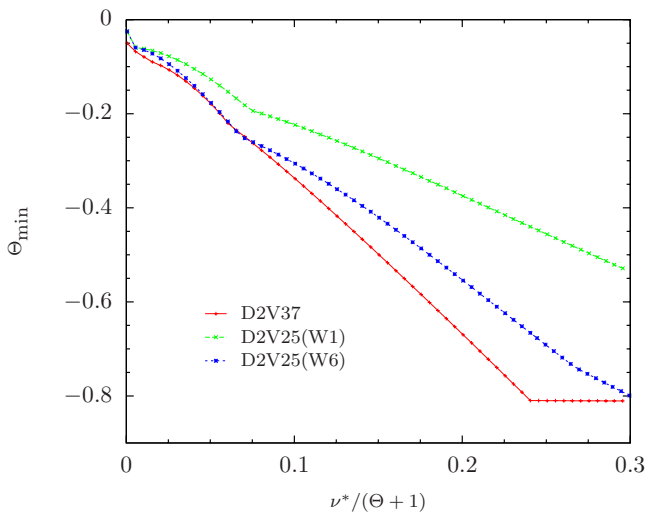

(b) $\Theta < 0$

FIG. 6. (Color online) Positive and negative maximum stable values for deviation of the temperature from T_o for $u^*=0.4$.

matic viscosity, instead of using the dimensionless relaxation time τ^* since in a great number of physical problems the parameter of interest is the Reynolds number.

Figure 3 shows a detailed stability map for the local velocity for these three models. It can be observed that the stability limits remain larger for higher order LB models even for very small viscosity values. In the case of the D2V37 athermal model, the maximum velocity predicted, in this analysis was $u^*=0.4$, corresponding to a dimensionless kinematic viscosity of $\nu^*=0.0007$.

2. Thermal models

The main purpose of this study is to understand the reasons why the LBE becomes unstable when the temperature deviations increase. To address this subject, the temperature deviations are expressed by

$$\Theta = \frac{T}{T_o} - 1. \tag{19}$$

The thermal LBE, D2V25(W1), D2V25(W2), and D2V37 presented by Philippi *et al.* [11], are investigated and compared with the thermal model of Chen *et al.* [9], since the latter model retrieves the correct macroscopic balance equations for the momentum and energy.

For the models considered in this analysis the dimensionless kinematic viscosity can be written as

$$\nu^* = \frac{(\Theta+1)}{a^2}\left(\tau^* - \frac{1}{2}\right) \tag{20}$$

and the Prandtl number is equal to 1.

Since the viscosity is dependent on the temperature the stability maps were drawn in terms of $\nu^*/(\Theta+1)$. Consider-

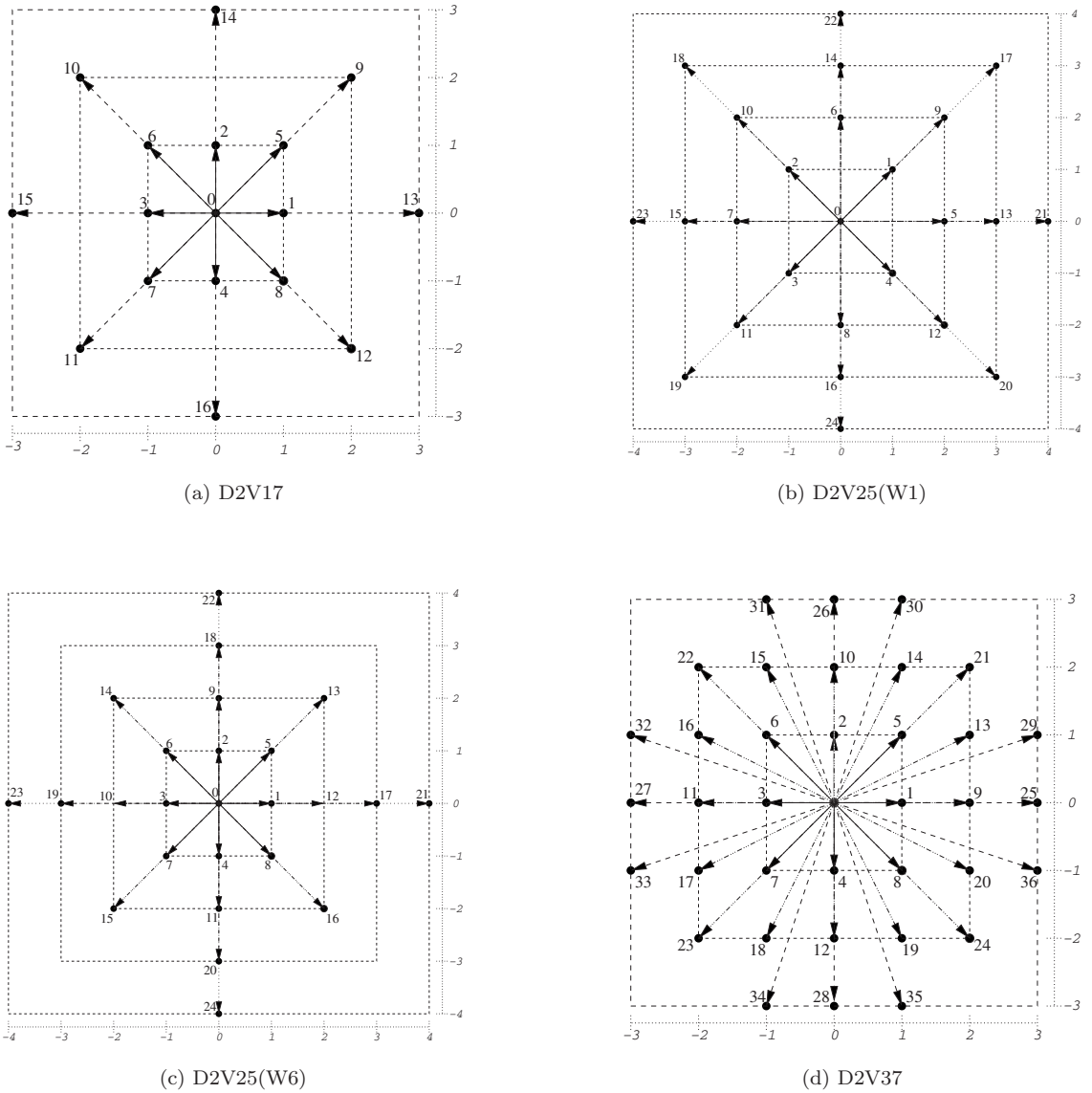

(a) D2V17

(b) D2V25(W1)

(c) D2V25(W6)

(d) D2V37

FIG. 7. Lattice vectors $\boldsymbol{c}_i$ for third and fourth order models.

ing that the model of Chen *et al.* has, in principle, no scale factor, the value of a for this model was set in such way that the macroscopic state with $\Theta=0$ is the most stable one.

Figure 4 shows both the (a) positive and (b) negative limits for Θ, considering a null local velocity. It can be observed that the model of Chen *et al.* gives no stable values for the temperature deviations, when $\nu^*/(\Theta+1)<0.2$. The results also show that the models proposed by Philippi *et al.* are stable over a large interval of temperatures even when the kinematic viscosity attains very low values. As in the previous section, the higher order D2V37 model has a broad stability range, followed by the D2V25(W6) LBE, although the D2V25(W1) LBE may appear to be more stable for low viscosity values, $\nu^*/(\Theta+1)<0.02$. It can also be noted that the curves are not symmetric with respect to the axis $\Theta=0$. This was to be expected since Θ is related to the internal energy through $e^*=(\Theta+1)/a^2$.

Figures 5 and 6 give the same Θ stability maps when the local velocity u^* increases, attaining the values $u^*=0.2$ and $u^*=0.4$. The Chen *et al.* model is not included since this model does not have any stability window in these stability maps when the local velocity $u^*\geq 0.2$.

As expected, an increase in the local velocity reduces the range of temperature deviations which results in a stable behavior.

The thermal LB models derived by Philippi *et al.* [11], are still stable over a large range of temperature deviations. Although this range decreases with u^* and disappears for very small values of $\nu^*/(\Theta+1)$ these results show that the D2V25 and D2V37 have very improved stability ranges when compared to past models.

Another important conclusion from this and the previous sections is that the main reason for LBE instability is a poor discrete representation of the continuous Boltzmann equation. In fact, although the present analysis is restricted to LBGK equations, in all the stability maps given in Figs. 4–6, stability is always increased when the LBE is derived in a systematic way from the continuous Boltzmann equation,

leading to enhanced higher-order representations of the continuous Boltzmann equation.

IV. CONCLUSION

The main purpose of this paper was to investigate the extent to which a temperature deviation can be supported by a thermal LBE, particularly when its order of approximation to the Boltzmann equation is increased. In this way, a linear stability analysis of several thermal and athermal models was performed.

Contrary to some conclusions that have been reported in LBE literature [14,18,20], our results show that the use of additional speeds improves the stability, when the LBE is derived in a systematic way, considering it as a polynomial approximation to the continuous Boltzmann equation. Also the quadrature weights and scaling factor must be chosen in such a way as to preserve the same moments as the MB distribution.

It has also been shown that for athermal models, the use of a higher order LBE increases the linear stability limits of the local velocity, $\boldsymbol{u}$. In particular, the use of more complete equilibrium distributions by the addition of suitable higher order Hermite polynomials gives a better stability to the LBE, although this does not affect the macroscopic behavior of its Knudsen first-order moments.

The large number of discrete velocities, which makes the present thermal LBE difficult to handle in computers in practical advection-diffusion problems, is a direct consequence of the adoption of a discrete collision-propagation scheme in deriving these models. The number of discrete velocities can be suitably reduced by using alternative finite-difference time and spatial discretization of the stream term in the Boltzmann equation and is the subject of a ongoing work being carried out by the authors.

In the same manner, although the present analysis was restricted to LBGK models, it can be easily extended to collision models that are beyond the BGK framework. An LBE with two relaxation times LBE that avoids the unitary Prandtl number restriction was systematically derived by the authors, [16], and will be the subject of a future paper on stability analysis.

ACKNOWLEDGMENTS

The authors are greatly indebted to CAPES (Coordenacao de Aperfeioamento de Pessoal de Nivel Superior), CNPq (Conselho Nacional de Desenvolvimento Cientifico e Tecnologico), Finep (Financiadora de Estudos e Projetos), and Petrobras (Petroleo Brasileiro SA).

APPENDIX: TWO-DIMENSIONAL LATTICES

The procedure described in Sec. II can be used to obtain the LBE as progressively enhanced representations of the continuous Boltzmann equation with the BGK collision model, when the order of the polynomial approximation to the MB equilibrium distribution is increased.

Seventeen discrete velocities were required for a full third-order model, resulting in the D2V17 LBE shown in Fig. 7(a) whose equilibrium distribution is given by

$$f_i^{\mathrm{eq},3} = \rho w_i \left[1 - \Theta + a^2 \boldsymbol{c}_i \cdot \boldsymbol{u} + \frac{a^4}{2}(\boldsymbol{c}_i \cdot \boldsymbol{u})^2 - \frac{a^2 u^2}{2} + \frac{a^2 c_i^2 \Theta}{2} + \frac{a^4 \Theta}{2} c_i^2 (\boldsymbol{c}_i \cdot \boldsymbol{u}) + \frac{a^6}{6}(\boldsymbol{c}_i \cdot \boldsymbol{u})^3 - 2\Theta a^2 (\boldsymbol{c}_i \cdot \boldsymbol{u}) - \frac{a^4 u^2}{2} \boldsymbol{c}_i \cdot \boldsymbol{u} \right], \tag{A1}$$

where the weights and the scaling factor a are shown in Table I.

TABLE I. Weights and scaling factor of D2V17 model.

i	w_i
0	$\frac{575+193\sqrt{193}}{8100}$
1–4	$\frac{3355-91\sqrt{193}}{18000}$
5–8	$\frac{655+17\sqrt{193}}{27000}$
9–12	$\frac{685-49\sqrt{193}}{54000}$
13–16	$\frac{1445-101\sqrt{193}}{162000}$
a	$\sqrt{\frac{5(25+\sqrt{193})}{72}}$

The models with fourth-order terms in the equilibrium distribution are the D2V25(W1), D2V25(W6), and the D2V37.

TABLE II. Weights and scaling factor of the D2V25 models.

i	D2V25(W1)	D2V25(W6)
0	$\frac{2592a^8-7380a^6+11165a^4-7950a^2+2148}{2592a^8}$	$\frac{16(6849-1135\sqrt{33})}{3(15-\sqrt{33})^4}$
1–4	$\frac{12a^4-13a^2+4}{32a^8}$	$\frac{64(2619-437\sqrt{33})}{15(15-\sqrt{33})^4}$
5–8	$\frac{-24a^6-89a^4-80a^2+24}{240a^8}$	$\frac{512(7-\sqrt{33})}{(15-\sqrt{33})^4}$
9–12	$\frac{-3a^4+10a^2-4}{320a^8}$	$\frac{8(159+47\sqrt{33})}{15(15-\sqrt{33})^4}$
13–16	$\frac{144a^6-574a^4+735a^2-264}{11340a^8}$	$\frac{2(17+\sqrt{33})}{(15-\sqrt{33})^4}$
17–20	$\frac{4a^4-15a^2+12}{12960a^8}$	$\frac{64(99-13\sqrt{33})}{105(15-\sqrt{33})^4}$
21–24	$\frac{-12a^6+49a^4-70a^2+36}{13440a^8}$	$\frac{4(-93+19\sqrt{33})}{105(15-\sqrt{33})^4}$
a	$\frac{1}{6}\sqrt{\frac{1}{2}\left(\frac{53(1081-18\sqrt{52413})^{1/3}+251-(1081-18\sqrt{52413})^{2/3}}{(1081-18\sqrt{52413})^{1/3}}\right)}$	$\frac{1}{2}\sqrt{\frac{1}{2}(15-\sqrt{33})}$

The 25-velocity lattices are shown in Figs. 7(b) and 7(c). These two LBE recover the complete Knudsen first-order advection-diffusion equations, without errors and their equilibrium distribution can be written as

$$f_i^{\mathrm{eq},4i} = f_i^{\mathrm{eq},3} + \rho w_i \left[\frac{a^4}{8}\Theta^2 c_i^4 - a^2\Theta^2 c_i^2 + a^2\Theta u^2 - \frac{a^4}{4}u^2 c_i^2\Theta - \frac{3a^4}{2}\Theta(\boldsymbol{u}\cdot\boldsymbol{c}_i)^2 + \frac{a^6}{4}\Theta(\boldsymbol{u}\cdot\boldsymbol{c}_i)^2 c_i^2 + \frac{a^4}{8}u^4 - \frac{a^6}{4}(\boldsymbol{u}\cdot\boldsymbol{c}_i)^2 u^2 - \frac{a^8}{192}u^4 c_i^2 + \frac{a^8}{24}u^2 c_i^2(\boldsymbol{u}\cdot\boldsymbol{c}_i)^2 \right]. \quad \text{(A2)}$$

The weights and the scaling factor for these models can be found in Table II.

Full fourth-order models required a set of 37 lattice vectors in two-dimensions, giving the D2V37 LBE, shown in Fig. 7(d) and its equilibrium distribution can be written as

$$f_i^{\mathrm{eq},4} = f_i^{\mathrm{eq},3} + \rho w_i \left[\frac{a^4u^4}{8} + a^2\Theta u^2 + \Theta^2 - \frac{a^6u^2}{4}(\boldsymbol{c}_i\cdot\boldsymbol{u})^2 - \frac{3a^4}{2}\Theta(\boldsymbol{c}_i\cdot\boldsymbol{u})^2 - a^2\Theta^2 c_i^2 - \frac{a^4}{4}\Theta u^2 c_i^2 + \frac{a^8}{24}(\boldsymbol{c}_i\cdot\boldsymbol{u})^4 + \frac{a^6}{4}\Theta(\boldsymbol{c}_i\cdot\boldsymbol{u})^2 c_i^2 + \frac{a^4}{8}\Theta^2 c_i^4 \right] \quad \text{(A3)}$$

with the weights and scaling factor given in Table III.

TABLE III. Weights and scaling factor of the D2V37 model.

i	w_i
0	$\frac{56266R^2-7^{2/3}(19991-338\sqrt{30})R+7^{4/3}(14323+6238\sqrt{30})}{264600R^2}$
1–4	$\frac{31206R^2-7^{2/3}(3201+466\sqrt{30})R-7^{4/3}(2427-706\sqrt{30})}{264600R^2}$
5–8	$\frac{29232R^2+7^{2/3}(3888+265\sqrt{30})R+7^{4/3}(216-1027\sqrt{30})}{529200R^2}$
9–12	$\frac{42R^2+7^{2/3}(33+2\sqrt{30})R-\sqrt[3]{7}(3+62\sqrt{30})}{3600R^2}$
13–20	$\frac{1638R^2+7^{2/3}(1647+4\sqrt{30})R-7^{4/3}(891+496\sqrt{30})}{264600R^2}$
21–24	$\frac{-126R^2+7^{2/3}(1161+194\sqrt{30})R+7^{4/3}(1107-242\sqrt{30})}{1058400R^2}$
25–28	$\frac{14R^2+7^{2/3}(131+10\sqrt{30})R+7^{4/3}(17-34\sqrt{30})}{264600R^2}$
29–36	$\frac{-168R^2+7^{2/3}(228+71\sqrt{30})R+7^{4/3}(516-29\sqrt{30})}{1058400R^2}$
a	$\frac{1}{6}\sqrt{49-\frac{17(7)^{2/3}}{R}+7^{1/3}R}$
R	$(67+36\sqrt{30})^{1/3}$

[1] G. R. McNamara and G. Zanetti, Phys. Rev. Lett. **61**, 2332 (1988).
[2] U. Frisch, B. Hasslacher, and Y. Pomeau, Phys. Rev. Lett. **56**, 1505 (1986).
[3] F. Higuera and J. Jiménez, Europhys. Lett. **9**, 663 (1989).
[4] S. Chen, H. Chen, D. Martinez, and W. Matthaeus, Phys. Rev. Lett. **67**, 3776 (1991).
[5] Y. H. Qian, D. d'Humières, and P. Lallemand, Europhys. Lett. **17**, 479 (1992).
[6] P. L. Bhatnagar, E. P. Gross, and M. Krook, Phys. Rev. **94**, 511 (1954).
[7] F. J. Alexander, S. Chen, and J. D. Sterling, Phys. Rev. E **47**, R2249 (1993).
[8] G. McNamara and B. Alder, Physica A **194**, 218 (1993).
[9] Y. Chen, H. Ohashi, and M. Akiyama, Phys. Rev. E **50**, 2776 (1994).
[10] X. He and L.-S. Luo, Phys. Rev. E **56**, 6811 (1997).
[11] P. C. Philippi, L. A. Hegele Jr., L. O. E. dos Santos, and R. Surmas, Phys. Rev. E **73**, 056702 (2006).
[12] X. Shan, X.-F. Yuan, and H. Chen, J. Fluid Mech. **550**, 413 (2006).
[13] D. N. Siebert, L. A. Hegele, Jr., R. Surmas, L. O. E. dos Santos, and P. C. Philippi, Int. J. Mod. Phys. C **18**, 546 (2007).
[14] S. Succi, *The Lattice Boltzmann Equation*, 1st ed. (Oxford University Press, New York, 2001), Chap. 14, pp. 246–247.
[15] D. d'Humières, Prog. Astronaut. Aeronaut. **159**, 450 (1992).
[16] P. C. Philippi, L. A. Hegele Jr., R. Surmas, D. N. Siebert, and L. O. E. dos Santos, Int. J. Mod. Phys. C **18**, 556 (2007).
[17] X. Shan and X. He, Phys. Rev. Lett. **80**, 65 (1998).
[18] P. Lallemand and L.-S. Luo, Phys. Rev. E **61**, 6546 (2000).
[19] J. D. Sterling and S. Chen, J. Comput. Phys. **123**, 196 (1996).
[20] P. Lallemand and L.-S. Luo, Phys. Rev. E **68**, 036706 (2003).